HJERTEFORUM
ORGAN FOR NORSK CARDIOLOGISK SELSKAP
SUPPL. 2 - 1996, VOLUME 9

Noninvasive computerized assessment of left ventricular function and systemic arterial properties.

Methodology and some clinical applications.

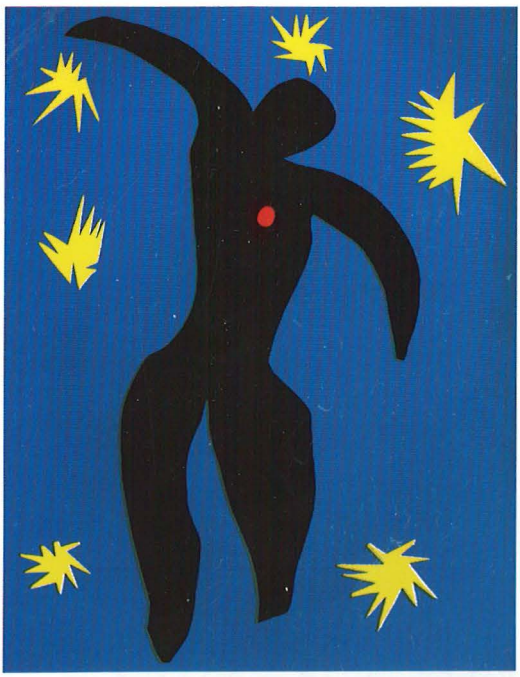

By

Svend Aakhus

University of Trondheim
Department of Medicine, Section of Cardiology
Trondheim - Norway

Noninvasive computerized assessment of left ventricular function and systemic arterial properties.

Methodology and some clinical applications.

By

Svend Aakhus

University of Trondheim
Department of Medicine, Section of Cardiology
Trondheim - Norway

Trondheim 1996
ISSN 0803-3668

Contents:

Acknowledgements:

The present work was carried out during my fellowship at the Section of Cardiology, Dept. of Medicine, Regional and University Hospital of Trondheim 1990 - 1994, and was financially supported by grants from the Norwegian Council on Cardiovascular Diseases (Oslo, Norway) and Vingmed Sound A/S (Horten, Norway). Support was also given by Hjerteforskningsfondet and Hoels legat (Regionsykehuset i Trondheim, Norway), Nathalia and Knut Juul Christiansens legat and Alexander Malthes legat (Oslo, Norway).

I am indebted to my mentors professor Liv Hatle and professor Terje Skjærpe for introducing me to Doppler echocardiography and clinical research, for enthusiastic support of the work, and for providing the excellent working facilities. Professor Bjørn A.J. Angelsen and Hans Torp, dr. techn., are acknowledged for their continuous interest in and support of the project. Dr. Knut Bjørnstad and cand. scient. Jørgen Mæhle were close co-workers during this work, and their contributions and friendship are greatly appreciated. Professor Kenneth M. Borow let me visit the Noninvasive Cardiac Imaging and Physiology Laboratory at the University of Chicago in 1990, where I was introduced to the combined use of external pulse tracing and echocardiography, and also found good friends. By courtesy of professor Ingemar Wallentin I also got the opportunity to visit the Dept. of Clinical Physiology at Sahlgrenska Sjukhuset, Gøteborg, where external pulse tracing is extensively used in cardiovascular diagnostics.

Further acknowledgements go to all co-authors, to colleagues at Dept. of Medicine and Dept. of Biomedical Engineering at the University of Trondheim, to the scientific nurses Torild Nergård and Marit Olstad Røe for their assistance with investigations, and to professor Rolf Rokseth for his thorough advices on manuscript preparation.

I am grateful for the technical support provided both by Vingmed Sound A/S (Horten, Norway) and Dept. of Biomedical Engineering, and for the professional assistance provided by the Medical Library and Information Center as well as the Audiovisual Dept., University of Trondheim.

The participating patients are acknowledged for their keen interest in the project. Finally, I thank my parents for their continuous support, and last but not least, I thank my wife Inger for her support and inspiration, and our kids Eirik and Simen for providing a refreshing distraction from this work.

List of papers:

I. Aakhus S, Torp H, Haugland T, Hatle L. Non-invasive estimates of aortic root pressures: external subclavian arterial pulse tracing calibrated by oscillometrically determined brachial arterial pressures. Clinical Physiology 1993;13:573-586.

II. Aakhus S, Soerlie C, Faanes A, Hauger SO, Bjoernstad K, Hatle L, Angelsen BAJ. Noninvasive computerized assessment of left ventricular performance and systemic hemodynamics by study of aortic root pressure and flow estimates in healthy men, and men with acute and healed myocardial infarction. American Journal of Cardiology 1993;72:260-267.

III. Aakhus S, Bjoernstad K, Jørstad S. Systemic cardiovascular response in hemodialysis without and with ultrafiltration with membranes of high and low biocompatibility. Blood Purification 1995;13:229-240.

IV. Aakhus S, Mæhle J, Bjoernstad K. A new method for echocardiographic computerized three-dimensional reconstruction of left ventricular endocardial surface: in vitro accuracy and clinical repeatability of volumes. Journal of the American Society of Echocardiography 1994;7:571-581.

V. Aakhus S, Bjørnstad K, Hatle L. Noninvasive study of left ventricular function and systemic haemodynamics during dipyridamole echocardiography stress test. Clinical Physiology 1994;14:581-594.

VI. Aakhus S, Bjørnstad K, Hatle L. Cardiovascular response in patients with and without myocardial ischaemia during dobutamine echocardiography stress test for coronary artery disease. Clinical Physiology 1995;15:249-263.

The papers will be referred to in the text by Roman numerals.

Introduction

Assessment of left ventricular performance and systemic hemodynamics is essential in patients with cardiovascular disease. Ultrasound techniques facilitate a noninvasive, efficient, and reliable evaluation of cardiac chambers, valves, and blood flow velocities, and have reduced the need for invasive procedures. Recently, techniques for three-dimensional reconstruction based on ultrasound data have also emerged. The present work originates from a desire to integrate and extend the use of noninvasive techniques for assessment of the performance of the left ventricle and the properties of the systemic arterial tree.

In routine assessment of global and regional left ventricular function, the properties of the systemic arterial tree are usually not accounted for. These properties are however of utmost importance since left ventricular performance are directly influenced by systemic arterial load [Urschel et al., 1968; Watanabe et al., 1992]. Systemic arterial pressure and flow data have mostly been used to evaluate the "steady" or mean flow properties of the systemic circulation, i.e. mean arterial pressure, cardiac output, and total peripheral resistance. Since the cardiovascular system operates in cycles i.e. is pulsatile, these parameters represent only a limited aspect of the systemic hemodynamics [Milnor, 1975]. The pulsatile properties of the systemic arteries can be assessed by analysis of aortic root pressure and flow data using analog models of the systemic circulation [Westerhof et al., 1971], or by estimating the hydraulic power requirements of the circulation [O'Rourke, 1967]. Invasive techniques have hitherto been required to obtain simultaneous recordings of aortic root pressure and flow, and the clinical applicability and relevance have therefore been limited to smaller patient groups.

Previous studies have indicated the similarity between an external tracing of the common carotid artery pulse and the central aortic pressure wave [Robinson, 1963; Martin et al., 1971; Van de Werf et al., 1975; Colan et al., 1985; Kelly et al., 1989b]. When the carotid artery pulse trace was calibrated with peak systolic and nadir diastolic brachial artery pressures obtained by the oscillometric technique, good estimates of central aortic systolic pressures were obtained [Colan et al., 1983; Colan et al., 1985; Kelly et al., 1989b]. Several investigators have used such a calibrated carotid artery pulse trace to represent aortic root pressure, and obtained noninvasive estimates of ventricular wall stress during ejection by combining the pressure data with echocardiographic measurements [Borow et al., 1988; Franklin et al., 1990]. The subclavian artery runs in the supraclavicular region, and the arterial pulse can usually be palpated closer to the central aorta than any other large artery. Since the pressure wave morphology changes gradually from the aortic root to the peripheral vessels [Nichols & O'Rourke, 1990], the subclavian artery pulse should in theory be well suited for indirect recording when the aim is to obtain a trace that represents the aortic root pressure.

Blood flow velocities and volume flow through the aortic annulus can be recorded by Doppler echocardiography [Ihlen et al., 1984; Skjærpe et al., 1985; Spencer et al., 1991]. By recording an external arterial pulse simultaneously with aortic annular flow by Doppler, estimates of instantane-

ous aortic root pressure and flow can be obtained. From aortic root pressure and flow data, both the "steady" and "pulsatile" characteristics of the cardiovascular system can be assessed [Yin, 1987; Milnor, 1989a; Nichols & O'Rourke, 1990].

In the present work, we were particularly interested in the left ventricular function and systemic hemodynamics in patients with coronary artery disease with or without myocardial infarction; and in the hemodynamic response during widely used interventions as hemodialysis and pharmacological cardiac stress tests. Concomitant with our work, reports from other investigators who used a similar approach emerged [Marcus et al., 1991; Kelly et al., 1992], and supported the rationale and potential of this methodology. The assessment of left ventricular function is, however, not complete without determination of the ventricular luminal volume. Conventional ultrasound methods for volume calculation rely on 1 or 2 echocardiographic imaging planes, and use the single- or biplane summation of disks method [Schiller et al., 1979]. These methods assume, however, that the ventricle has a symmetric geometry which is not the case in patients with regional myocardial disease (e.g. coronary artery disease). Three-dimensional reconstruction of the left ventricle may circumvent this important limitation, and can be based on ultrasound data [Pearlman, 1990]. In order to optimise the assessment of left ventricular function and systemic hemodynamics in patients with coronary artery disease, we introduced such a method in the present work.

On this background the aims of the present work can be stated.

Aims of study:

1. To evaluate whether the subclavian artery could be used as an indirect representation of the aortic root pressure waveform, and whether the subclavian artery pulse trace when calibrated with indirect brachial artery pressures represented the true aortic root pressure.
2. To develop a computer software designed for efficient calculation of parameters of left ventricular function and systemic "steady" and "pulsatile" hemodynamics based on Doppler echocardiograms and indirect aortic root pressures.
3. To test the accuracy of volumes determined by a new algorithm for three-dimensional reconstruction of cavity surfaces based on digital ultrasound data.
4. To assess left ventricular function and systemic hemodynamics with this methodology in:
   a) patients with acute and healed myocardial infarction,
   b) patients undergoing hemodialysis with dialysis membranes of different biocompatibility,
   c) patients undergoing pharmacological cardiac stress tests for coronary artery disease with dipyridamole or dobutamine.
5. To assess the repeatability and feasibility of this methodology in the clinical situation.

Subjects and methods:

All patients gave informed consent to participate in the studies during their hospital stay, either as regular ward patients or as out-patients referred for routine cardiac investigations. The healthy subjects were volunteers from the hospital staff, except in paper V where patients with normal coronary angiograms in spite of various chest pain syndromes were used as controls for patients with coronary artery disease. One patient was included both in paper II (group C) and paper V (group 3). One patient was referred twice (12 months apart), and the first assessment was used in paper II (group B) and the second in paper VI (group 2). Except for these two, no patient participated in more than one study. In the studies where either non-invasive techniques were evaluated against invasive methods [I], or coronary angiograms were used to classify patients [V,VI], the invasive procedures were part of the routine clinical evaluation and were not initiated by the study.

Instruments:

The studies in the present work were performed with identical equipment. The software was regularly upgraded for feasibility and user convenience, however, the basic calculations and estimation procedures were maintained. The ultrasound scanner (CFM 750, Vingmed Sound, Horten, Norway) was used with an annular array transducer of duplex type allowing both imaging (3.25 MHz) and flow velocity recordings (2.5 MHz). This scanner facilitates transfer of digital data from its replay memory via a data port (NB-DIO-24, National Instruments, Austin, TX, USA) to a computer (Macintosh II series, Apple Computers Inc., Cupertino, CA, USA) by use of specific software (EchoLink vs. 2.0-3.0, Vingmed Sound). The digitized electrocardiogram, phonocardiogram, and the pressure traces were transferred with the ultrasound data for storage and subsequent analysis in a general program for handling of digital ultrasound data (EchoDisp vs. 2.0 - 3.0, Vingmed Sound). This procedure ensured preservation of the quality of the data and the original frame-rate which ranged from 33 to 58 frames s^{-1} with a typical sector angle (i.e. between 45 and 90 degrees) and depth setting. A sector angle of 60 degrees with sector depth 16 cm was usually applied for apical imaging and provided 47 frames/s. This frame rate is by far superior to that of video recordings (25 to 30 frames s^{-1}). Ultrasound 2-dimensional image data were organized as cineloops on the computer. A cineloop comprises the sequentially recorded ultrasound images during 1 cardiac cycle, and facilitates a detailed analysis of cardiac dimensions and dynamic behaviour during the cardiac cycle. The digital data were stored on magneto-optical storage medium (Storage Dimensions, San Jose, CA, USA) comprising 1 gigabyte storage capacity per interchangeable disk.

A note about digital storage:

The present methodology relies on an efficient handling and storage of digital ultrasound and physiologic trace data. When data are transferred as digits from the scanner to the computer, a file is created. Such a file may occupy up to 3 megabytes of storage capacity. Since personal computers at present have limited data storage capacity, an external device must be used to manage the data obtained during clinical or research work. We have used a read and write magneto-optical system with inter-

changeable disks comprising 1000 megabytes (i.e. 1 gigabyte) of storage capacity. However, this technology is in our experience not very reliable and loss of data may occur. Therefore, we have used a digital tape system for backup of all recorded data. Although tape backup systems are slower than magneto-optical disks, they are reliable and allow complete restoration of data.

External arterial pulse tracing:

We used a standard external pulse transducer (Irex 120-0132, Irex Medical Systems, NJ, USA) which was connected via a 20 cm rigid plastic tube to a specially designed capillary funnel (Y-funnel E079E, Siemens-Elema AB, Solna, Sweden) with optimized dampening characteristics [Wikstrand et al., 1977]. The pulse transducer was connected to a custom built preamplifier (by courtesy of H.G. Torp, Dept. of Biomedical Engineering, University of Trondheim) with controls for gain and offset. The time constant of the pulse tracing system determines the rate of decay of transducer output [Johnson et al., 1971]. A low time constant (i.e. < 2 s) distorts the traced waveform [Johnson et al., 1971; Lewis et al, 1977]. We used a time constant of 4.7 s in order to ensure adequate reproduction of the pressure pulse. The preamplifier was connected to the ultrasound scanner where the analog trace signal was digitized for every 5 ms (i.e. rate of digitization: 200 Hz) and displayed. The pulse transducer was manually positioned over the right subclavian artery in the medial supraclavicular region, and the pulse was traced during a brief period of apnea, usually close to end of expiration in order to minimise baseline drift during respiration. The manometer used for measurement of brachial artery pressure was of oscillometric type (UA 751, Takeda Inc., Tokyo, Japan).

Doppler echocardiography:

Aortic annulus blood flow velocities were recorded from the apical transducer position with pulsed Doppler technique [Hatle & Angelsen, 1985]. From this position the ultrasound beam can usually be aligned close to the assumed direction of blood flow in the left ventricular outflow tract. Moreover, the outflow tract is usually well visualized on the two-dimensional echocardiograms and can therefore be used to guide the ultrasound beam and sample volume to the annular origo where the best estimate for the mean flow velocity is found [Rossvoll et al., 1991]. When an optimal velocity recording was obtained, as defined by a clean narrow band of peak velocities and a well defined valve closure click, the imaging was terminated in order to enhance the sampling frequency and improve the Doppler signal. We made no attempt to correct the angle deviation between the ultrasound beam and the assumed direction of blood flow. In most patients it is possible to maintain this angle within 20 degrees when recording from the apical position with the patient in left lateral position. Due to the cosine function of the Doppler equation, this ensures that the true blood flow velocities will be less than 6% underestimated. Volume flow was obtained by multiplying the annular blood flow velocity with the annular cross-sectional area. Since the aortic annulus is rigid and maintains its cross-sectional area during hemodynamic alterations [Christie et al., 1987], it is particularly suited for determinations of volume flow. The annular border is assumed to be circular and its cross-sectional area (A) can therefore be calculated directly from measurements of the internal diameter (d): $A = p\,(d/2)^2$. We measured this diameter, d, in systole between the insertion of the valve leaflets on a 2-dimensional parasternal long axis echocardiogram using the trailing-to-leading edge method [Skjærpe et al., 1985].

Preprocessing:

First the sampled data were evaluated on the computer screen in order to select cardiac cycles with optimal data. Then, the maximal velocities (outer envelope) of the aortic annular Doppler spectrum in systole were manually traced on the computer by use of a cursor. The maximal velocities were chosen rather than the mean velocities because they are more easily defined and less influenced by any position of the sample volume partly outside the vessel [Gisvold & Brubakk, 1982]. End-systole was defined at the initial signal of aortic valve closure click. When using an external artery pulse trace as a substitute for central aortic pressure a number of problems have to be solved. First, the arterial pulse is delayed in time relative to the aortic root pressure wave corresponding to the distance between aortic root and location for pulse tracing. Second, the external pulse tracing is influenced by respiration and skin and muscle movement. Following input of patient height, weight, systolic and diastolic brachial artery pressures, and aortic annular diameter, the software processed the data as follows: 1) any linear drift in pulse trace recording was corrected (see Appendix); 2) the pressure and flow velocity data from the selected beats were signal averaged to yield pressure and flow traces for an averaged cardiac cycle; 3) the averaged pressure trace was corrected for time delay with respect to the flow trace as schematically shown in Figure 1; and 4) the averaged flow velocity trace was transformed to a volume flow curve by multiplying each incremental flow velocity data point (every 5 ms) with the calculated aortic root cross sectional area.

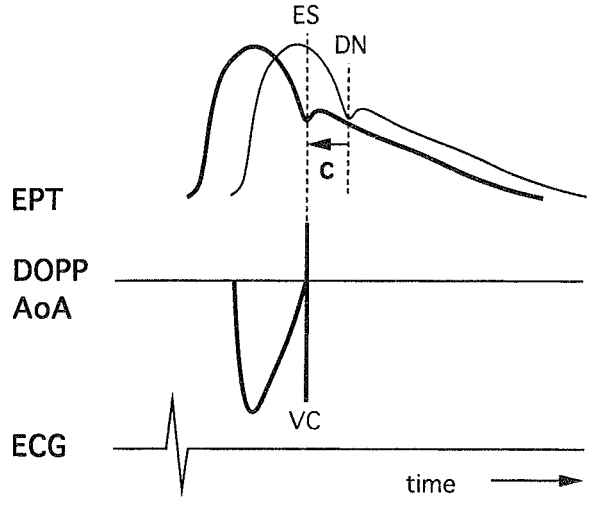

Figure 1. Correction of time delay (c) in the external subclavian artery pulse trace (EPT). End-systole on the recorded pressure trace (thin line) as defined by the nadir of the dicrotic notch (DN), was automatically aligned with end-systole (ES) on the averaged Doppler flow velocity recording in the aortic annulus (DOPP AoA) as defined by the valve closure click (VC). All recorded pressure data points were automatically corrected to produce the time corrected pulse trace (bold line), which was used with the recorded aortic annulus flow recording in subsequent calculations and estimations. The time delay was in most patients approximately 20 ms; here exaggerated for illustrative purpose. ECG is electrocardiogram.

Calculations:

Once the pulse trace and flow data were preprocessed, the pulse trace was calibrated by assigning the brachial artery systolic pressure to its peak and the diastolic pressure to its nadir [Colan et al., 1985; I]. Subsequent calculations (see Appendix; II) assume that pressure and flow data represent simultaneously recorded aortic root pressure and flow curves. From the pressure curve, aortic root mean systolic, end-systolic, mean-diastolic, end-diastolic, and mean arterial pressure were calculated. Estimates of stroke volume, cardiac output, and left ventricular ejection time were obtained from the flow curve.

Model of systemic circulation:

Peripheral resistance, arterial compliance, and characteristic impedance were estimated from the simultaneous estimates of aortic root pressure and flow by use of a three-element windkessel model [Westerhof et al., 1971]. In this model it is assumed that peripheral resistance is constant, flow out of the systemic arteries is proportional to the pressure drop, venous pressure is negligible, the pressure is equal in the entire systemic arterial tree, and arterial compliance is constant during the cardiac cycle. Clearly, these assumptions are to some extent violated in the intact circulation. Nevertheless, this model has proven useful in evaluation of systemic circulation in experimental and clinical studies [Elzinga & Westerhof, 1973; Sunagawa et al., 1985; Laskey et al., 1990]. Different mathematical procedures may be used for estimation of the 3 model parameters. The estimation procedure we have chosen [II, Angelsen et al., 1994] is schematically shown in Figure 2. The Nelder Mead Simplex algorithm was chosen due to its robustness for the initial parameter values [Dennis & Woods, 1987]. Mathematical aspects of this estimation procedure are described in the appendix of paper II.

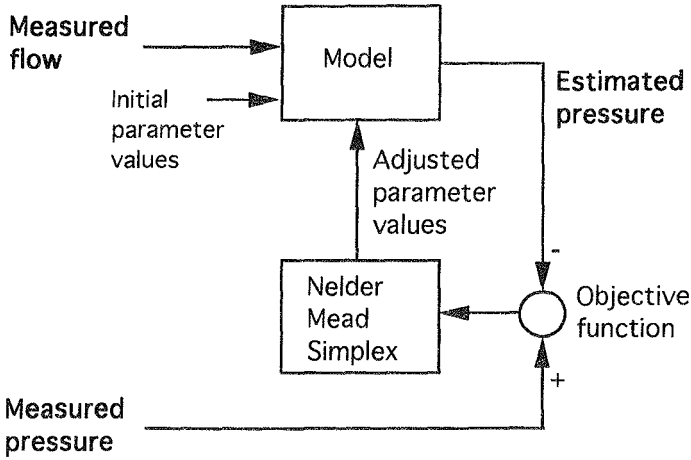

Figure 2. Estimation scheme for the parameters of the 3-element windkessel model. The measured aortic annulus flow is used as input to the mathematical model equations which for a given parameter set produce an estimate of the pressure curve at the inlet of the system (i.e. aortic root). The mean square difference between the estimated and the measured pressure curves is used as the objective function in a nonlinear optimization algorithm (Nelder Mead Simplex). This algorithm adjusts the parameter set, and the procedure is repeated until a minimum of the objective function is found.

External power:

Total external power was calculated as the product of the instantaneous values for aortic root pressure and flow throughout the cardiac cycle, steady external power was calculated [Nichols & O'Rourke, 1990] as the product of mean aortic root flow and pressure, and oscillatory external power was obtained as the difference between total and steady external power [Laskey et al., 1985].

Regional wall motion:

In the present work [V,VI], left ventricular regional wall motion was assessed by use of a 16 segment model of the left ventricle as recommended by the American Society of Echocardiography [Schiller et al., 1989]. When ultrasound imaging is adequate, this technique allows assessment of wall motion (i.e. myocardial wall motion and thickening) in all regions of the left ventricle. An index of left ventricular wall motion can then be calculated as the sum of segment scores over the number of segments assessed. We have previously reported an inter-observer agreement of 94% or better for outcome of echocardiography stress test when using this technique on ultrasound images of left ventricle displayed in cine-loop format [Bjoernstad et al., 1993a; Bjørnstad et al., 1995].

Summary of results:

Paper I:

In this study, we compared the subclavian artery pulse tracing with simultaneously obtained direct aortic root pressures in 26 patients (aged 39 - 74 years) with various cardiovascular disorders. The two waveforms agreed well with cross-correlation coefficients for systole and diastole of 0.98. The difference between the pulse trace and the direct pressure curve, when the former was calibrated with the peak-systolic and nadir-diastolic pressures of the latter, was on the average less than 1 mmHg for systole and diastole. At end-systole the mean difference was 5 mmHg. Indirect brachial artery peak-systolic pressures obtained by oscillometry were (mean±SD) 3±7 mmHg below the corresponding direct measurements, whereas indirect nadir-diastolic pressures were 8±4 mmHg above. The difference between the pulse trace and the direct pressure curve, when the pulse trace was calibrated with indirect brachial artery pressures, was at end-systole 6±6 mmHg and for mean arterial pressures 5±4 mmHg. Thus, the external subclavian arterial pulse tracing provides a noninvasive and clinically feasible access to the aortic root pressure waveform. With optimal calibration, good estimates of aortic root pressures throughout systole and diastole can be obtained, whereas end-systolic pressure tends to be slightly overestimated.

Paper II:

In this study, we combined echocardiographic imaging and Doppler velocity recordings with subclavian artery pulse trace calibrated by indirectly obtained brachial artery pressures to evaluate left ventricular function and systemic hemodynamics in 8 healthy subjects (group A), in 12 patients with recent myocardial infarction (group B), and in 8 with healed myocardial infarction and dilated left ventricle (group C). The noninvasively obtained aortic root pressure and flow data were used to estimate peripheral resistance, arterial compliance, and characteristic impedance (three-element windkessel model) of the systemic circulation. There were no significant group differences for either aortic root pressure estimates or heart rate. In group B and C, stroke index and cardiac index were lower and total peripheral resistance higher than in group A. There were no group differences in the model estimates of total arterial compliance, whereas the characteristic impedance was higher in group C than in A, indicating stiffer proximal arteries in group C. Both total and steady external power were lower in group B and C than in group A, whereas no group difference was found for % oscillatory power. The inter-observer repeatability of this methodology for recording was good for pressure estimates (coefficients of variation: 4 to 8%) and lower for the derived parameters (stroke index: 12%; cardiac index: 13%; windkessel model parameters: 11 to 20%; and external power: 13 to 17%). The repeatability for analysis was good with coefficients of variation between 1 and 9%.

Paper III:

In this study, Doppler echocardiography was combined with indirectly calibrated subclavian artery pulse trace to assess the systemic cardiovascular response during hemodialysis with membranes of different biocompatibility. Eight hemodialysis patients (aged 24 to 73 years) were treated with a low biocompatible (cuprophane) and a

high biocompatible (polyacrylonitrile) membrane in a randomized double-blind cross-over protocol using bicarbonate hemodialysis without ultrafiltration the first 60 minutes and with ultrafiltration the remaining treatment time. There was no significant difference in the cardiovascular response on the 2 membranes, neither during isolated hemodialysis nor when ultrafiltration was added. Mean arterial pressure increased 10% ($p<0.001$) during isolated hemodialysis and returned to baseline levels with ultrafiltration. Cardiac index decreased 22% ($p<0.001$) during ultrafiltration, due to the greater decrease in left ventricular stroke index (31%, $p<0.001$) than increase in heart rate (9%, $p<0.05$). Total peripheral resistance increased 10% ($p<0.05$) during isolated hemodialysis, and a further 20% ($p<0.01$) when ultrafiltration was added. Thus, profound cardiovascular alterations occurred during hemodialysis treatment but were not related to the biocompatibility of the membranes.

Paper IV:

In this study, we evaluated the in vitro accuracy and clinical repeatability of volumes derived by a new algorithm for three-dimensional reconstruction of cavity surfaces based on echocardiographic apical images obtained by probe rotation. The accuracy of the method was tested in latex phantoms (true volumes: 32 to 349 cm^3) with (n=9) or without (n=9) rotational symmetry around the midcavitary long axis. Repeatability of left ventricular volumes was assessed in subjects without (n=5) or with (n=10) myocardial disease. The influence on volume estimates by 1) angular deviation (±15 degrees) from the assumed position of the imaging planes; and 2) using 4 versus 3 imaging planes, were tested in 10 additional patients. Estimated phantom volumes, obtained from 4 and 3 image planes, were close to true volumes with a difference (mean±SD) of 0±2 and 2±3 cm^3 in symmetrical and 1±3 and 4±4 cm^3 in asymmetrical objects, respectively. Biplane and single plane volume estimates were less accurate. Inter- and intraobserver repeatability of left ventricular volumes determined by the three-dimensional method was good for analysis (coefficients of variation: 3.5 to 6.2%), and acceptable for recording (coefficients of variation: 7.4 to 10.9%). Angular deviation of imaging planes produced only small errors (mean±SD: 0.3±3.2%) in left ventricular cross-sectional area, which was equally well reproduced from 4 (error: 0.8±0.7%) and 3 (error: 1.2±1.6%) imaging planes. Hence, the present algorithm performs well with digital ultrasound data to reproduce volumes of symmetrical and deformed in vitro objects accurately. The repeatability of left ventricular volumes obtained with this method was good.

Paper V:

In this study, we assessed the systemic cardiovascular response during cardiac stress testing with dipyridamole (0.84 mg kg^{-1} iv.) in 10 subjects (aged 44 to 61 years) with normal coronary arteries (group 1), and in patients with coronary artery disease either without (group 2, n=6) or with (group 3, n=8) echocardiographic evidence for myocardial ischemia during the test. Left ventricular wall motion and dimensions, and aortic root pressure and flow were obtained by Doppler echocardiography combined with an indirectly calibrated subclavian artery pulse trace. Peripheral arterial resistance, total arterial compliance, and characteristic impedance were estimated from aortic root pressure and flow, by use of a three-element windkessel model of the systemic circulation. Left ventricular ejection fraction improved from baseline to peak stress in group 1 (mean±SD: 62±6 vs. 65±6%, $p=0.05$), whereas it was not signi-

ficantly changed in group 2 (58±10 vs. 56±6%), and decreased in group 3 (53±10 vs. 43±10%, $p<0.05$). Otherwise, the hemodynamic response was similar in the 3 groups: heart rate increased by ≥30% and cardiac index by ≥37%, whereas stroke index and arterial pressures were maintained at or slightly above baseline. Peripheral resistance decreased ≥22%, and total arterial compliance and aortic characteristic impedance were not significantly altered during test. The worsening of wall motion abnormality at peak stress in group 3 was not significantly related to the change in systemic hemodynamics. Thus, dipyridamole acted predominantly on the arterioles without significantly influencing the large systemic arteries. Myocardial ischemia during the test resulted in an impaired regional and global left ventricular function, but did not influence the systemic arterial response in these patients.

Paper VI:

In this study, we assessed the systemic cardiovascular response during dobutamine echocardiography stress test for coronary artery disease. Nine patients without (group 1, aged 48 to 72 years) and 9 with myocardial ischemia during test (group 2, aged 53 to 73 years), were investigated by use of Doppler echocardiography and an indirectly calibrated subclavian artery pulse trace. Peripheral resistance, total arterial compliance, and aortic characteristic impedance were estimated by use of a three-element windkessel model of the systemic circulation. During infusion of dobutamine up to 40 $\mu g\ kg^{-1}min^{-1}$, arterial pressure was maintained near baseline levels, whereas heart rate and cardiac index increased, and more so in group 1 (mean: 89 and 79%) than in group 2 (58 and 52%, $p<0.05$ vs. group 1). Peripheral resistance was decreased ≥32% at peak stress, whereas characteristic impedance was maintained at or above baseline in both groups, and total arterial compliance was not significantly altered. The cardiovascular response was not influenced by the wall motion abnormalities. Thus, in these patients the inotropic, chronotropic, and vasodilatory effects of dobutamine balanced the ischemic impairment of left ventricular function during the stress test.

General discussion:

Subclavian artery pulse trace:

The arterial pressure wave is altered as it runs from the aorta to the periphery [Nichols & O'Rourke, 1990]. The subclavian arterial pulse can usually be palpated closer to the central aorta than any other large artery, and is therefore in theory well suited for external tracing of a pulse representative for the aortic root pressure wave. Furthermore, tracing of the subclavian artery pressure pulse does not carry the risk of cerebral complications or activation of vascular reflexes as carotid artery pulse tracing potentially may do. We obtained acceptable subclavian artery pulse tracings in 73% of patients during the short time available during routine cardiac catheterization [I]. It is our experience that the pulse can be adequately traced in approximately 90% of adult patients during conventional Doppler echocardiographic examination. In children and very obese patients the subclavian artery pulse may occasionally be difficult to trace. Patients with neck vessel bruits were not included in the present work, since an arterial stenosis may alter the arterial pressure wave. Since the Doppler echocardiographic examination usually requires that the patient is in the slight left lateral position, we have routinely used the right subclavian artery for pulse tracing.

The results of paper I indicate that the subclavian artery pulse trace represents the aortic root pressure wave morphology well over a wide range of arterial pressures with cross-correlation coefficients close to unity. To our knowledge, this type of waveform analysis has not been used to compare carotid artery pulse tracings with aortic pressures. Therefore we do not know whether the subclavian artery pulse trace represents the aortic root pressure wave better than the carotid artery pulse trace. However, we and others [Colan et al., 1985] have the impression that the carotid pulse tracing deviates more from the aortic root pressure by having a rapid systolic rise which is not often seen in the subclavian artery pulse trace. When the subclavian artery pulse trace was calibrated with the direct peak systolic and nadir diastolic pressures, the average difference from the aortic root pressure curve was less than 1 mmHg in systole and diastole, however, at end-systole the difference was greater (mean±SD: 5±4 mmHg). This indicates that when the pulse trace is optimally calibrated it represents the direct aortic root pressures well throughout the cardiac cycle, with a small exception for end-systole. However, the direct pressure measurement system used in this study had a relatively low frequency response which may have caused a high frequency "overshoot" [Grossmann, 1986] and therefore a false low dicrotic notch and end-systolic pressure. Thus, the true difference between indirect and directly measured end-systolic pressure is probably less than indicated in this study. With the oscillometric technique, peak-systolic brachial artery pressure was close to the direct aortic root pressure, whereas nadir-diastolic pressure was overestimated by 8 mmHg. Consequently, mean arterial pressures were slightly over-estimated by the indirect method.

Oscillometry:

The oscillometric method for indirect blood pressure measurement utilises the oscillations in pulsating systemic arteries [Ramsey, 1979]. When a cuff is applied to the

upper arm and inflated to a pressure above the peak systolic brachial artery pressure blood flow through the artery is obstructed, and the amplitude of the oscillations is small. When the cuff pressure is gradually released, this amplitude increases suddenly when blood starts to flow through the vessel indicating the peak systolic pressure. The amplitude increases with further reduction of cuff pressure until a peak amplitude is reached. This peak amplitude corresponds to mean arterial pressure [Ramsey, 1979]. Following further reduction in cuff pressure, the amplitude declines to a steady level. The nadir diastolic pressure is defined to correspond to the transition zone between declining and stable amplitudes. The algorithm for determination of peak systolic and nadir diastolic pressures, may differ slightly between different manometer types [Johnson & Kerr, 1985]. The device we have used in the present work determines peak systolic and nadir diastolic pressures to correspond to the 1st and 5th phase of the Korotkoff sounds, respectively [B. Johnsen, Scan-Med A/S, Drammen, Norway, personal communication]. This may explain the systematic overestimation of aortic root end-diastolic pressure which has been slightly better estimated by oscillometric devices using a different algorithm [Borow & Newburger, 1982]. Although the estimates of aortic root pressures in the present work were slightly overestimated, the repeatability of measurements was good [II] and the relative change during interventions as well as the relative difference between groups of patients are likely to be appropriately characterized.

Significance of patient position:

The systolic and diastolic brachial artery pressures are assumed to represent peak systolic and nadir diastolic aortic root pressures. When the patient is in the left lateral position, however, the right arm will be elevated relative to the aortic root. The vertical difference between brachial artery and aortic root is on the average (mean±SD) 16±3 cm as measured in 19 representative patients with coronary artery disease [S. Aakhus, unpublished results]. Due to hydrostatic forces, the right brachial artery pressure will be reduced by 0.7 mmHg for every centimetre the artery is elevated above the aortic root (vertical height). Thus, by measuring the vertical height between the assumed position of the aortic root and brachial artery, the hydrostatic pressure difference can be calculated and used to correct the measured pressures. In the present work this was not done since repeat Doppler echocardiography was performed with the patient in a relatively constant position (i.e. the optimal patient position during recording of aortic annulus Doppler blood flow velocities is fairly constant). Furthermore, the average patient position is expected to be similar in groups of patients. Whereas, the recorded pressures therefore necessarily were slightly lower than true aortic root pressures, the relative difference between groups and the relative change during interventions are likely to be appropriately characterized.

Echocardiography:

The most important limitation of echocardiography is suboptimal image quality in the individual patient. When image quality is poor, the identification of endocardial borders may be difficult. When the available acoustic windows do not allow imaging over the cardiac apex, the image of the left ventricle will be foreshortened. Furthermore, movement of the heart during the cardiac and respiratory cycles influence the echocardiograms. These factors add errors to the determination of left ventricular volumes by echocardiography [Wallerson & Devereux, 1986]. In the present work, all ultrasound imaging and Doppler recording of blood flow velocities were performed with the patient in left lateral position, and

the recordings were obtained during a brief period of apnea close to end-expiration. Furthermore, in order to improve the ultrasonic access to the patient's cardiac apex we used a specially designed investigation table with a crescent shaped cut-off on the left side.

The pulsed Doppler recordings of blood flow velocities in the present work are assumed to be representative for aortic annular mean spatial velocity. The best estimate for this mean velocity is found by recording the velocities in the spatial center of annulus [Rossvoll et al., 1991] where we aimed to position the Doppler sample volume. We also aimed to maintain a small angle, i.e. less than 20 degrees, between the assumed direction of blood flow and the ultrasound beam. With this procedure a Doppler recording of aortic annular velocities usually has a narrow range of velocities, and the difference between mean and maximal velocities is small. In the present work we traced the maximal flow velocities ("outer envelope"). This technique leads to some overestimation of true aortic flow velocity. However, it provides, when used with the trailing-to-leading edge determined aortic annular area, very good agreement with invasively obtained stroke volumes [Dubin et al., 1990].

Data from at least 3 cardiac cycles were signal averaged, and estimates of volume flow were obtained by multiplying the aortic annular velocities by the annular cross-section area which was calculated from the annular diameter obtained from the parasternal long axis echocardiograms at the valve leaflets insertion [Ihlen et al., 1984] assuming a circular orifice. The measurement of annular diameter is critical since it is squared when the cross-sectional area is calculated. We have found that repeat measurements of aortic annular diameter have a variability (coefficient of variation) of 4.1 % [II]. Since the aortic annulus is regarded to be relatively constant during exercise and hemodynamic alterations [Stewart et al., 1985; Christie et al., 1987; Rassi et al., 1988], we used the area obtained at baseline for all repeat assessments during interventions [III,V,VI], thus reducing measurement variability. Patients with aortic stenosis (i.e. a pressure gradient over the aortic valve) have a disturbed aortic annular flow pattern, and were not included in the present work.

Choice of vascular model:

We used the three-element electric analog model of the systemic circulation as basis for estimation of systemic arterial properties. The reason was that this model have been well described, and has been useful in experimental and clinical studies [Westerhof et al., 1971; Liu et al., 1986; Laskey et al., 1990]. Furthermore, this model is simple and the limited number of parameters are interpretable in a physiologic context: the parameter resistance represents the peripheral arteriolar resistance, compliance represents the total arterial volume compliance i.e. the increment of volume produced by an increment of pressure in the system, and characteristic impedance represents the proximal arterial resistance and is related to the aortic stiffness and inversely to the aortic cross-sectional diameter [Milnor, 1989b]. More complicated models may give a more detailed description of the arterial properties [Deswysen et al., 1980], but the interpretation of their parameters may be difficult [Westerhof et al., 1969]. In addition, complicated models are less robust [Angelsen et al., 1994] and do more often fail to converge to a solution for the parameters, and will also require longer time for estimation of the model parameters. When using the three-element model, we found that the estimated pressure curve agreed well with the measured pressure curves in 28 subjects [II], thus indicating

the appropriateness of the model and its solution on clinically relevant data.

The present work does not directly test the validity of the hemodynamic parameters derived from the noninvasive estimates of aortic root pressure and flow (i.e. estimates of model parameters and external power). The validity of the noninvasive estimates of aortic root pressure [I; Marcus et al., 1994] and flow [Ihlen et al., 1984; Dubin et al., 1990; Coats, 1990, Spencer et al., 1991] is well documented. Other investigators have found that characteristic impedance and external power obtained by similar noninvasive techniques correlated well with invasive data [Kelly & Fitchett, 1992]. Recently, arterial compliance estimated from pressure and flow data (three-element windkessel model) obtained by calibrated subclavian pulse tracings and Doppler echocardiography in 8 patients, was found to agree well with invasively obtained values [Marcus et al., 1994], whereas characteristic impedance deviated more. Both studies are relatively small, and there are certain limitations in their invasive assessment of aortic root flow which relied on the combined use of thermodilution technique and electromagnetic flow recording. In spite of this, these studies support that adequate noninvasive recordings of aortic root pressure and flow are likely to provide a valid estimate of vascular model parameters.

The estimation procedure used in the present work [II,V,VI] utilized pressure and flow data from the entire cardiac cycle. It is possible to add criteria to the estimation procedure (weighting). We have tested how the model parameters were influenced by use of different limiting criteria for the estimation procedure, that is "forcing" the estimated pressure curve to replicate either of the following: the systolic part of the measured pressure curve; the diastolic part; the measured pulse pressure; the peak systolic pressure; or finally the nadir diastolic pressure. These differently weighted estimation procedures produced but minor changes in the parameter estimates (Table 1). This indicates that weighted estimation is not necessary in routine assessment of systemic arterial properties in patients. We also tested the feasibility of the previously

Table 1. Effect of weighted estimation on the solution of the 3-element windkessel model.

Weighting of estimation:	R (dyn s cm^{-5})	C (cm^3 $mmHg^{-1}$)	Zc (dyn s cm^{-5})
Systolic and diastolic	1214±291	1.36±0.30	53±24
Systolic	1215±294	1.36±0.32	53±23
Diastolic	1209±284	1.34±0.28	58±28
Pulse pressure	1214±291	1.40±0.35	53±24
Peak systolic	1214±292	1.32±0.32	54±24
Nadir diastolic	1211±292	1.42±0.31	56±25

Values are mean±SD of estimations performed on aortic root pressure and flow data from 5 patients with mild hypertension. R=peripheral resistance; C=total arterial compliance; Zc=characteristic impedance. No significant difference was found between the different estimation procedures (ANOVA on individual data, F-test).

often used method of fixed point iteration method to estimate the parameters [Slørdahl et al., 1994; Marcus et al., 1994], but this procedure failed to converge in 2 of the 5 patients and gave unlikely results for arterial compliance in 1 (7.36 cm^3 $mmHg^{-1}$).

The 3-element windkessel model assumes a linear pressure-volume relationship in the systemic circulation, i.e. that compliance is constant over the range of pressures [Liu et al., 1986]. This is an approximation [Bergel, 1961], and errors may be introduced when repeat studies are performed on patients where arterial blood pressure changes during the study. In papers V and VI, this model was used to assess arterial properties during influence of dipyridamole and dobutamine, respectively. Although these drugs had profound circulatory effects, mean arterial pressure was maintained relatively unchanged during the studies.

Three-dimensional echocardiography:

The algorithm used in this work for three-dimensional reconstruction of object surfaces from ultrasound image data [IV-VI] has previously been described [Mæhle et al., 1994]. The results of paper IV show that the algorithm performs excellently in terms of volume determination, when cavity borders are well defined on the ultrasound images, as in the latex phantoms. Moreover, good estimates of cavity volumes were provided by using as few as 3 apical imaging planes, and the repeatability was better for the three-dimensional method than for the conventional biplane or single plane methods. This is important because the 3 standard apical imaging planes (4-chamber, long axis 2-chamber, and long axis) are defined by anatomical landmarks [Schiller et al., 1979; Henry et al., 1980] and are part of the routine echocardiographic examination. Recording of 4 or more imaging planes requires on the other hand a completely new procedure for apical imaging [Angelsen et al., 1993], where guiding of the rotational angle is necessary. These results encouraged us to use the clinically more feasible method of 3 imaging planes for three-dimensional reconstruction and calculation of left ventricular volumes from ultrasound image data. This algorithm has later been tested by other investigators who in abstract form have reported a good correlation between left ventricular volumes by the three-dimensional method and by nuclear magnetic resonance imaging [Iwase et al., 1994], as well as between left ventricular stroke volumes by three-dimensional method and Doppler technique [Mele et al., 1994].

The spatial position of the 3 apical imaging planes may deviate from their assumed position (0, 61, and 102 degrees) and this will result in errors in the three-dimensional reconstruction. However, we found that the reconstructed cross-sectional area, and thus left ventricular cavity volume, was but little influenced by a deviation of ±15 degrees in any of the imaging planes [IV]. This supports the use of the 3 standard apical imaging planes for assessment of left ventricular volumes in the clinical situation. However, the accuracy could be improved by measuring the angulation of the imaging planes during the examination, and introduce them in the algorithm. This option has been implemented in the latest version of this software.

Repeatability of measurements:

Noninvasive techniques are, in contrast to the invasive ones, usually well suited for repeatability studies. The present methodology combines Doppler and imaging ultrasound with an indirectly calibrated external pulse tracing, and both recording and interpretation of data are subject to varia-

bility. In this work we have analyzed both the variability due to recording and that due to analysis. This has been treated in detail in paper II for hemodynamic parameters, and in paper IV for left ventricular volumes determined by three-dimensional reconstruction. We found that the variability due to recording was more than twice that of interpretation, and the variability of interpretation was similar between and within observers. Composite parameters (i.e. those derived from 2 or more other parameters) as stroke volume, cardiac output, peripheral resistance, arterial compliance, characteristic impedance, and external power parameters had the largest variability. The repeatability studies [II,IV] were performed within 1 hour to minimize the physiological variability that may be encountered over a longer observational period. The coefficients of repeatability (CR) given in Table 2 (adapted from paper II) indicate how large a recorded change in a parameter must be in an individual patient before it reflects a true change (with 95 % confidentiality).

Thus, in repeat assessments in a particular patient peripheral resistance must change more than 300 dyn s cm^{-5}, total arterial compliance more than 0.80 cm^3 $mmHg^{-1}$, and characteristic impedance more than 33 dyn s cm^{-5}, in order to indicate a true change, i.e. a change that cannot be explained by variability of the measurements. However, the sensitivity to detect a change in a group of patients is much better. For a group of 20 subjects undergoing repeat measurements, a change in the group means above 71 dyn s cm^{-5} for peripheral resistance, above 0.19 cm^3 $mmHg^{-1}$ for arterial compliance, and above 8 dyn s cm^{-5} for characteristic impedance, will represent a true change in the group mean with 95% confidentiality. For smaller groups the confidence limits will be

Table 2. Interobserver repeatability for recording of noninvasive parameters of systemic hemodynamics.

	mean	Δ	CR	t·SEM
Systolic pressure (mmHg)	105	1	12	2
End-systolic pressure (mmHg)*	90	1	12	3
Diastolic pressure (mmHg)	62	1	10	2
Mean arterial pressure (mmHg)*	80	2	8	2
Heart rate (b min^{-1})	61	2	6	1
Stroke index (cm^3 m^{-2})	41	1	10	2
Cardiac index (l min^{-1} m^{-2})	2.45	0.01	0.61	0.12
Peripheral resistance (dyn s cm^{-5})*	1366	28	300	71
Total arterial compliance (cm^3 $mmHg^{-1}$)*	2.03	0.10	0.80	0.19
Characteristic impedance (dyn s cm^{-5})*	100	1	33	8

Results from 2 immediately consecutive assessments in 20 subjects (n=18). Mean=mean of 2 assessments; Δ=mean difference between 2 assessments; CR=coefficient of repeatability; t·SEM=t from the t-distribution corresponding to 20 (* n=18) subjects multiplied with standard error of the differences (SEM). The 95% confidence limits for the mean is represented by mean±t·SEM.*

slightly larger, and for larger groups they will be smaller.

Clinical applications:

The properties of the arterial tree influence left ventricular performance [Urschel et al., 1968; Watanabe et al., 1992; Maruyama et al., 1993], and are known to be altered by aging [Nichols et al., 1985; Lang et al., 1994], hypertension [Nichols et al., 1986; O'Rourke, 1990], certain cardiovascular acting drugs [Pepine et al., 1979; Yaginuma et al., 1986], the presence of coronary artery disease [Nichols et al., 1977], atherosclerosis [Nakashima & Tanikawa, 1971], and congestive heart failure [Pepine et al., 1978; Laskey et al., 1985]. In the present work, systemic arterial properties were characterized by 3 parameters: peripheral resistance, total arterial compliance, and characteristic impedance. These parameters were estimated from aortic root pressure and flow data obtained noninvasively by the combined use of Doppler echocardiography and calibrated subclavian artery pulse tracing. The methodology was feasible in patients with acute and healed myocardial infarction [II], in repeat assessments of systemic hemodynamics during hemodialysis [III], and during cardiac stress tests with either dipyridamole [V] or dobutamine [VI]. This indicates that most stable patients with cardiovascular diseases can be assessed with this methodology at baseline and during interventions.

Whereas peripheral resistance was elevated both in patients with acute and those with healed myocardial infarction and dilated left ventricles [II], only the latter had significantly elevated characteristic impedance as compared to the apparently healthy subjects. Total arterial compliance trended towards lower values in patients with acute infarction and lowest in those with healed infarction. Characteristic impedance is related more to the stiffness and diameter of the proximal aorta [Milnor, 1989b], whereas total arterial compliance reflects the elasticity of the entire systemic arterial tree [Laskey et al., 1990]. The observed greater characteristic impedance in the patients with left ventricular dilatation may be due to an increased aortic wall stiffness or a smaller aortic diameter, or both, but the trend towards lower total arterial compliance in these patients suggests that the wall stiffness was most important.

Characteristic impedance has previously been assessed invasively in patients with congestive heart failure, however, the results are not entirely consistent [Pepine et al., 1978; Laskey et al., 1985], and may not be relevant for patients with coronary heart disease as those in the present paper II. A recent experimental study have indicated that an increase in characteristic impedance may precede the increase in peripheral resistance during development of congestive heart failure [Eaton et al., 1993]. Previous studies using different methodology have indicated that aortic distensibility is lower in patients with coronary artery disease than in normal subjects [Stefanadis et al., 1987], and that the distensibility decreases with the severity of coronary artery disease [Hirai et al., 1989]. The cause for these findings is, however, elusive. Arterial stiffness may be altered by neuroadrenerg activity [Fleisch et al., 1970; Pagani et al., 1975] which increases after myocardial infarction [Rouleau et al., 1991]. Atherosclerosis may increase arterial stiffness [Nakashima & Tanikawa, 1971], but is regarded to be a relatively slow process [Ross, 1986]. Further studies are needed to explain the mechanism for the altered characteristic impedance in these patients with left ventricular dilatation after myocardial infarction.

In paper III we assessed the influence of dialysis membrane biocompatibility on left ventricular function and systemic he-

modynamics during hemodialysis. Isolated hemodialysis increased peripheral resistance and mean arterial pressures, and when ultrafiltration was added the mean arterial pressure decreased due to decreased stroke volume and peripheral resistance. Left ventricular shortening decreased due to the greater reduction of end-diastolic dimension ("preload") than end-systolic dimension. The cardiovascular response was not different between treatments on the two dialysis membranes although their biocompatibility was markedly different. This indicates that a preference can not be put on membranes of high versus low biocompatibility with respect to the acute hemodynamic response during hemodialysis in relatively stable uremic patients.

In paper V we found that infusion of dipyridamole during stress echocardiography dilated the peripheral systemic arterioles but did not influence the larger systemic arteries. This is similar to the effects of other vasodilators as nitroprusside [Yin et al., 1983] and glyceryl trinitrate [Gundel et al., 1981; Yaginuma et al., 1986]. The reduced peripheral resistance was balanced by an increased cardiac output so that mean arterial pressure was maintained relatively unchanged during this test with high-dose intravenous dipyridamole. In some patients significant arterial hypotension may be encountered during test [Bjørnstad et al., 1995]. These patients do often have an impaired chronotropic response due to e.g. atrio-ventricular conduction abnormalities, and may not be able be increase their cardiac output appropriately during vasodilation.

Dobutamine has been extensively used in clinical work, both to improve inotropy in cardiac pump failure [Leier et al., 1979], to elicit myocardial ischemia during stress testing for coronary artery disease [Sawada et al., 1991], and to identify regions of ischemic but still viable myocardium [Cigarroa et al., 1993]. Dobutamine is supposed to have less chronotropic effects than dopamine [Leier et al., 1978], however, the hemodynamic effects of dobutamine have mainly been tested with low to intermediate doses and most often in patients with cardiac pump failure. In paper VI we tested the hemodynamic effects of graded infusions of dobutamine from low to high infusion rates (i.e. 40 $\mu g\ kg^{-1}\ min^{-1}$) in patients without evident cardiac pump failure. The results indicated that dobutamine had a complex influence on arterial properties. At low infusion rates (i.e. <15 $\mu g\ kg^{-1}\ min^{-1}$) dobutamine increased characteristic impedance (i.e. proximal arterial resistance) with little change in peripheral resistance, whereas higher infusion rates reduced peripheral resistance substantially and proximal resistance returned to baseline. The reason for this complex effect on arterial resistance may potentially be found in the differential adrenergic receptor distribution in the peripheral and proximal arterial system [Fleisch et al., 1970] in these patients. In patients with congestive heart failure, low to moderate infusion rates of dobutamine have been reported to decrease characteristic impedance and peripheral resistance concordantly [Binkley et al., 1990]. The discrepancy between this study and our results is not evident, but may be related to the greater neuroadrenerg activation in patients with congestive heart failure.

Papers V and VI also comprised patients who developed echocardiographic evidence for myocardial ischemia during test. The systemic arterial response during these tests were not related to the presence of ischemia. Left ventricular ejection fraction decreased in patients with ischemia during dipyridamole test whereas this parameter was difficult to assess during dobutamine test due to the vigorous cardiac activity at peak stress. Wall motion abnormalities precede both electrocardiographic changes and chest pain during development of regional myocardial ischemia [Battler et

al., 1980; Visser et al., 1986]. The stress echocardiographic tests are usually terminated promptly when new wall motion abnormalities are observed. Thus, myocardial ischemia is generally mild and brief, and the hemodynamic response must be interpreted within this context.

The patients with myocardial ischemia during dobutamine test had an impaired chronotropic response that only partly could be explained by differences in pretest beta-blockade. It has been reported that patients with congestive heart failure have a reduced chronotropic response during exercise, probably due to desensitization of beta-receptors [Colucci et al., 1989]. Whether this mechanism is present in patients with ischemic heart disease and a history of myocardial infarction has not yet been settled.

In paper IV a new algorithm for determination of cavity volumes based on digital ultrasound data was validated in vitro and the repeatability of left ventricular volumes was assessed. The algorithm reproduced the object volumes accurately. The results of paper IV also infer that three-dimensional reconstructions of the left ventricular endocardial surface can be performed accurately from only 3 apical imaging planes. Then the volume can be determined within few minutes after imaging has been completed. The most important limitation with this method refer to that of clinical echocardiography in general, namely dependency on appropriate image quality and position of probe over the true cardiac apex. Suboptimal recordings reduce the accuracy of the volume estimate. Although stroke volume can be calculated as the difference between end-diastolic and end-systolic left ventricular volumes, the variability of the two latter implies that the difference (i.e. stroke volume) may not be very reliable. In the present work stroke volumes were therefore obtained by Doppler echocardiography and not from left ventricular volume estimates.

The presented algorithm for three-dimensional reconstruction also allows quantitation of the area of endocardium with normal and abnormal motion by use of certain mathematical analysis techniques [Mæhle et al., 1994]. This analysis has not yet been fully validated and was not used in the present work, but holds great promise for quantitative assessment of the extent of abnormal regional wall motion in patients with ischemic heart disease at rest and during cardiac stress testing [Bjoernstad et al., 1993b].

External power:

Total external power (work per unit time) represents the total energy loss by transport of blood from the ventricle to the tissues. Steady external power represents the energy loss associated with blood transport during steady flow conditions, and oscillatory power represents the energy loss due to the arterial pulsations during blood transport [O'Rourke, 1967]. The ratio between oscillatory and total power, % oscillatory power, has been proposed as an indicator of the efficiency of the systemic circulation, i.e. how well the left ventricle is matched to the systemic arteries [O'Rourke, 1967]. This perception was based on evidence from animal experiments during gross hemodynamical alterations, where an increasing % oscillatory power was found to indicate a reduced cardiovascular efficiency in terms of blood transportation.

In the present work, the external power parameters were calculated from the noninvasive aortic root pressure and flow data. Oscillatory power was derived directly as the difference between total and steady external power [Laskey et al., 1985; Spencer et a., 1990] rather than by use of the more cumbersome method of Fourier analysis on pressure and flow waves [Milnor et al.,

1966]. However, these two approaches produce similar values for oscillatory power [Laskey et al., 1985].

We used the noninvasive estimates of external power to assess cardiovascular function in humans. In paper II it is shown that total, steady, and oscillatory powers were similarly decreased in patients with acute and healed myocardial infarction as compared to healthy subjects, most likely due to the combined effects of infarcted myocardium and the use of beta-blockers. In paper V it is shown that the vasodilator dipyridamole induced a balanced increase in the power parameters in healthy individuals, and in patients with and without myocardial ischemia during test. Paper VI shows that dobutamine increases oscillatory power relatively more than total power, thus increasing the % oscillatory power and decreasing ventricular-vascular efficiency. This finding may be related to the increased characteristic impedance observed during dobutamine infusions below 15 $\mu g\ kg^{-1}\ min^{-1}$. The sensitivity of the power parameters for myocardial ischemia appeared to be small in these patients. For example the patients with ischemia during cardiac stress tests with either dipyridamole [V] or dobutamine [VI] did not differ significantly from those without with respect to the power parameters or % oscillatory power. The external power parameters may thus be more pertinent to the systemic vessels than to the myocardium [Nichols & O'Rourke, 1990].

Perspectives:

The presented methodology can be applied by use of conventional equipment for echocardiography and external pulse trace recording which is available at most hospitals. It provides a non-invasive, feasible, cost-effective, and relatively fast access to important parameters of cardiac function and arterial properties. This work presents some aspects of the clinical potential for this type of analysis.

Conclusions:

The external subclavian artery pulse trace represented the aortic root pressure waveform well, and was feasible in the clinical situation. When this pulse trace was calibrated with brachial artery pressures measured by the oscillometric technique, it gave acceptable estimates of true aortic root pressures.

The specially designed computer software developed during this work provided an efficient calculation of parameters of left ventricular function, and of systemic "steady" and "pulsatile" hemodynamics.

The accuracy for volume determination of the presented algorithm for three-dimensional reconstruction of cavity surfaces was good.

By use of this methodology, it was found that: a) the state of the systemic arteries was different in patients with healed myocardial infarction and a dilated left ventricle versus those with recent infarction with normal ventricular size; b) the biocompatibility of dialysis membranes did not influence the systemic hemodynamic response during hemodialysis; c) stress echocardiography test with dipyridamole (0.84 mg kg^{-1}) reduced peripheral resistance whereas the large arteries were not significantly influenced. The systemic arterial response was not altered by ischemia during test. Stress echocardiography test with dobutamine elicited a complex vascular response. At low infusion rates (<15 μg kg^{-1} min^{-1}), proximal arterial stiffness tended to increase whereas peripheral resistance decreased. At higher infusion rates, both were decreased.

The inter-observer repeatability for hemodynamic parameters was good for analysis and acceptable for recording of data, and better for the pressure parameters than for the flow parameters. The repeatability of left ventricular volumes obtained by the three-dimensional algorithm was better than that of conventional echocardiographic methods.

References

Angelsen BAJ, Aakhus S, Rabben SI, Torp HG. Model-based estimation of vascular parameters: Evaluation of robustness and suitability of models. Echocardiography 1994;11:409-423.

Angelsen BAJ, Dørum S, Hoem J, Brubakk AO, Skjærpe T, Torp HG, et al. Annular array multiplanar TEE probe allowing 3D reconstruction of cineloops of the heart. In: Hanrath P, et al. (eds). Cardiovascular Imaging by Ultrasound. Netherlands: Kluwer Academic Publishers, 1993:287-296.

Battler A, Froelicher VF, Gallagher KP, Kemper WS, Ross J. Dissociation between regional myocardial dysfunction and ECG changes during ischemia in the conscious dog. Circulation 1980;62:735-744.

Binkley PF, Van Fossen DB, Nunziata E, Unverferth DV, Leier CV. Influence of positive inotropic therapy on pulsatile hydraulic load and ventricular-vascular coupling in congestive heart failure. J Am Coll Cardiol 1990;15:1127-1135.

Bergel DH. The static elastic properties of the arterial wall. J Physiol 1961;156:445-457.

Bjoernstad K, Aakhus S, Lundbom J, Bolz K, Rokseth R, Skjaerpe T, et al. Digital dipyridamole stress echocardiography in silent ischemia after coronary artery bypass grafting and/or after healing of acute myocardial infarction. Am J Cardiol 1993a;72: 640-646.

Bjoernstad K, Maehle J, Aakhus S. Quantitative computerized analysis of left ventricular wall motion. In: Domenicucci S, Roelandt J, Pezzano A, eds. Computerized echocardiography. Torino: Centro Scientifico Editore, 1993b:41-55.

Bjørnstad K, Aakhus S, Hatle L. Digital dipyridamole stress echocardiography for detection of coronary artery stenosis. Int J Cardiac Imaging 1995;11:163-170.

Borow KM, Newburger JW. Noninvasive estimation of central aortic pressure using the oscillometric method for analyzing systemic artery pulsatile blood flow: comparative study of indirect systolic, diastolic, and mean brachial artery pressure with simultaneous direct ascending aortic pressure measurements. Am Heart J 1982; 103:879-886.

Borow KM, Lang RM, Neumann A, Carroll JD, Rajfer SI. Physiologic mechanisms governing hemodynamic responses to positive inotropic therapy in patients with dilated cardiomyopathy. Circulation 1988;77: 625-637.

Christie J, Sheldahl LM, Tristani FE, Sagar KB, Ptacin MJ, Wann S. Determination of stroke volume and cardiac output during exercise: comparison of two-dimensional and Doppler echocardiography, Fick oximetry, and thermodilution. Circulation 1987;76: 539-547.

Cigarroa CG, de Filippi CR, Brickner ME, Alvarez LG, Wait MA, Grayburn PA. Dobutamine stress echocardiography identifies hibernating myocardium and predicts recovery of left ventricular function after coronary revascularization. Circulation 1993;88:430-436.

Coats AJS. Doppler ultrasonic measurement of cardiac output: Reproducibility and validation. Eur Heart J 1990;11(suppl I):49-61.

Colan SD, Fujii A, Borow KM, MacPherson D, Sanders SP. Noninvasive determination of systolic, diastolic and end-systolic blood pressure in neonates, infants and young children: comparison with central aortic pressure measurements. Am J Cardiol 1983;52:867-870.

Colan SD, Borow KM, Neumann A. Use of calibrated carotid pulse tracing for calculation of left ventricular pressure and wall stress throughout ejection. Am Heart J 1985;109:1306-1310.

Colucci WS, Ribeiro JP, Rocco MB, Quigg RJ, Creager MA, Marsh JD, et al. Impaired chronotropic response to exercise in patients with congestive heart failure. Role of postsynaptic ß-adrenergic desensitization. Circulation 1989;80:314-323.

Dennis JE Jr., Woods DJ. Optimization on microcomputers: the Nelder Mead simplex algorithm. In: Wouk A, ed. New computing environments: Microcomputers in large-scale computing. SIAM, 1987:116-122.

Deswysen B, Charlier AA, Gevers M. Quantitative evaluation of the systemic arterial bed by parameter estimation of a simple model. Med & Biol Eng & Comput 1980;18:153-166.

Dubin J, Wallerson DC, Cody RJ, Devereux RB. Comparative accuracy of Doppler echocardiographic methods for clinical stroke volume determination. Am Heart J 1990; 120:116-123.

Eaton GM, Cody RJ, Binkley PF. Increased aortic impedance precedes peripheral vasoconstriction at the early stage of ventricular failure in the paced canine model. Circulation 1993;88:2714-2721.

Elzinga G, Westerhof N. Pressure and flow generated by the left ventricle against different impedances. Circ Res 1973;32:178-186.

Fleisch JH, Maling HM, Brodie BB. Beta-receptor activity in aorta. Circ Res 1970; 26:151-162.

Franklin RCG, Wyse RKH, Graham TP, Gooch VM, Deanfield JE. Normal values for noninvasive estimation of left ventricular contractile state and afterload in children. Am J Cardiol 1990;65:505-510.

Gisvold SE, Brubakk AO. Measurement of instantaneous blood-flow velocity in the human aorta using pulsed Doppler ultrasound. Cardiovasc Res 1982;16:26-33.

Grossmann W. Cardiac catheterization and angiography. (3rd ed.) Philadelphia: Lea & Febiger, 1986.

Gundel W, Cherry G, Rajagopalan B, Tan L, Lee G, Schultz D. Aortic input impedance in man: acute response to vasodilator drugs. Circulation 1981;63:1305-1314.

Hatle L, Angelsen B. Doppler ultrasound in cardiology. Physical principles and clinical applications (2nd ed.) Philadelphia: Lea & Febiger, 1985:293-305.

Henry WL, DeMaria A, Gramiak R, King DL, Kisslo JA, Popp RL, et al. Report of the American Society of Echocardiography Comittee on nomenclature and standards in two-dimensional echocardiography. Circulation 1980;62:212-217.

Hirai T, Sasayama S, Kawasaki T, Yagi S. Stiffness of systemic arteries in patients with myocardial infarction. Circulation 1989; 80:78-86.

Ihlen H, Amlie JP, Dale J, Forfang K, Nitter-Hauge S, Otterstad JE, et al. Determination of cardiac output by Doppler echocardiography. Br Heart J 1984;51:54-60.

Iwase M, Kondo T, Hasegawa K, Kimura M, Fukui M, Matsuyama H, et al. Three-dimensional echocardiography and semiautomatic border detection to assess left ventricular volume and function. Circulation 1994;90:I-337.

Johnson JM, Siegel W, Blomquist G. Characteristics of transducers used for recording the apexcardiogram. J Appl Physiol 1971;31:796-800.

Johnson CJH, Kerr JH. Automatic blood pressure monitors. A clinical evaluation of five models in adults. Anaesthesia 1985; 40:471-478.

Kelly R, Karamonoglu M, Gibbs H, Avolio A, O'Rourke M. Noninvasive carotid pressure wave registration as an indicator of ascending aortic pressure. J Vasc Med Biol 1989b;1:241-247.

Kelly R, Fitchett D. Noninvasive determination of aortic input impedance and external left ventricular power output: a validation and repeatability study of a new technique. J Am Coll Cardiol 1992; 20:952-963.

Lang RM, Cholley BP, Korcarz C, Marcus RH, Shroff SG. Measurement of regional elastic properties of the human aorta: a new application of transosophageal echocar-

diography with automated border detection and calibrated subclavian pulse tracings. Circulation 1994;90:1875-1882.

Laskey WK, Kussmaul WG, Martin JL, Kleaveland JP, Hirshfeld JW, Shroff S. Characteristics of vascular hydraulic load in patients with heart failure. Circulation 1985;72:61-71.

Laskey WK, Parker G, Ferrari VA, Kussmaul WG, Noordergraaf A. Estimation of total systemic arterial compliance in humans. J Appl Physiol 1990;69:112-119.

Leier CV, Unverferth DV, Kates RE. The relationship between plasma dobutamine concentrations and cardiovascular responses in cardiac failure. Am J Medicine 1979; 66:238-242.

Leier CV, Heban PT, Huss P, Bush CA, Lewis RP. Comparative effects and regional hemodynamic effects of dopamine and dobutamine in patients with cardiomyopathic heart failure. Circulation 1978;58:466-475.

Lewis RP, Rittgers SE, Forester WF, Boudoulas H. A critical review of the systolic time intervals. Circulation 1977;56:146-158.

Liu Z, Brin KP, Yin FCP. Estimation of total arterial compliance: an improved method and evaluation of current methods. Am J Physiol 1986;251:588-600.

Marcus RH, Lang RM, Neumann A, Borow KM. A physiological approach to drug therapy in dilated cardiomyopathy. Echocardiography 1991;8:173-186.

Marcus RH, Korcarz C, McCray G, Neumann A, Murphy M, Borow K, et al. Noninvasive method for determination of arterial compliance using Doppler echocardiography and subclavian pulse tracings: validation and clinical application of a physiological model of the circulation. Circulation 1994;89:2688-2699.

Martin CE, Shaver JA, Thompson ME, Reddy PS, Leonard JJ. Direct correlation of external systolic time intervals with internal indices of left ventricular function in man. Circulation 1971;44:419-431.

Maruyama Y, Nishioka O, Nozaki E, Kinoshita H, Kyono H, Koiwa Y, et al. Effects of arterial distensibility on left ventricular ejection in the depressed contractile state. Cardiovasc Res 1993;27:182-187.

Mele D, Pratola C, Pedini I, Alboni P, Levine RA. Validation and application in patients of a new system for three-dimensional echocardiographic reconstruction of the left ventricle. Circulation 1994;90:I-337.

Milnor WR, Bergel DH, Bargainer JD. Hydraulic power associated with pulmonary blood flow and its relation to heart rate. Circ Res 1966;19:467-480.

Milnor WR. Arterial impedance as ventricular afterload. Circ Res 1975;36:565-570.

Milnor WR. Hemodynamics. Baltimore: Williams & Wilkins, 1989a.

Milnor WR. Hemodynamics. Baltimore: Williams & Wilkins, 1989b:193-196.

Mæhle J, Bjoernstad K, Aakhus S, Torp HG, Angelsen BAJ. Three-dimensional echocardiography for quantitative left ventricular wall motion analysis: a method for reconstruction of endocardial surface and evaluation of regional dysfunction. Echocardiography 1994;11:397-408.

Nakashima T, Tanikawa J. A study of human aortic distensibility with relation to atherosclerosis and aging. Angiology 1971; 22:477-490.

Nichols WW, Conti CR, Walker WE, Milnor WR. Input impedance of the systemic circulation in man. Circ Res 1977;40:451-458.

Nichols WW, O'Rourke MF, Avolio AP, Yaginuma T, Murgo JP, Pepine CJ, et al. Effects of age on ventricular-vascular coupling. Am J Cardiol 1985;55:1179-1184.

Nichols WW, O'Rourke MF, Avolio AP, Yaginuma T, Pepine CJ, Conti CR. Ventricular/vascular interaction in patients with mild systemic hypertension and normal peripheral resistance. Circulation 1986; 74:455-462.

Nichols WW, O'Rourke MF. McDonald«s blood flow in arteries. (3rd ed.) London: Edward Arnold, 1990.

O'Rourke MF. Steady and pulsatile energy losses in the systemic circulation under nor-

mal conditions and in simulated arterial disease. Cardiovasc Res 1967;1:313-326.

O'Rourke MF. Arterial stiffness, systolic blood pressure, and logical treatment of arterial hypertension. Hypertension 1990;15:339-347.

Pagani M, Schwartz PJ, Bishop VS, Malliani A. Reflex sympathetic changes in aortic diastolic pressure-diameter relationship. Am J Physiol 1975;229:286-290.

Pearlman AS. Measurement of left ventricular volume by three-dimensional echocardiography - present promise and potential problems. J Am Coll Cardiol 1993; 22:1538-1540.

Pepine CJ, Nichols WW, Conti CR. Aortic input impedance in heart failure. Circulation 1978;58:460-465.

Pepine CJ, Nichols WW, Curry RC, Conti CR. Aortic input impedance during nitroprusside infusion. J Clin Invest 1979;64:643-654.

Ramsey M III. Noninvasive automatic determination of mean arterial pressure. Med & Biol Eng & Comput 1979;17:11-18.

Rassi A, Crawford MH, Richards KL, Miller JF. Differing mechanisms of exercise flow augmentation at the mitral and aortic valves. Circulation 1988;77:543-551.

Robinson B. The carotid pulse II: relation of external recordings to carotid, aortic, and brachial pulses. Br Heart J 1963;25:61-68.

Ross R. The pathogenesis of atherosclerosis - an update. N Engl J Med 1986;314:488-499.

Rossvoll O, Samstad S, Torp HG, Linker DT, Skjærpe T, Angelsen BAJ, et al. The velocity distribution in the aortic anulus in normal subjects: a quantitative analysis of two-dimensional Doppler flow maps. J Am Soc Echocardiogr 1991;4:367-378.

Rouleau JL, Moyé LA, Champlain JA, Klein M, Bichet B, Packer M, et al. Activation of neurohormonal systems following acute myocardial infarction. Am J Cardiol 1991;68:80D-86D.

Sawada SG, Segar DS, Ryan T, Brown SE, Dohan AM, Williams R, et al. Echocardiographic detection of coronary artery disease during dobutamine infusion. Circulation 1991;83:1605-1614.

Schiller NB, Acquatella H, Ports TA, Drew D, Goerke J, Ringertz H, et al. Left ventricular volume from paired biplane two-dimensional echocardiography. Circulation 1979;60:547-555.

Schiller NB, Shah PM, Crawford M, deMaria A, Devereux R, Feigenbaum H, et al. Recommendations for quantitation of the left ventricle by two-dimensional echocardiography. J Am Soc Echocardiogr 1989; 2:358-367.

Skjærpe T, Hegrenæs L, Ihlen H. Cardiac output. In: Hatle L, Angelsen BA, ed. Doppler ultrasound in cardiology. 2 ed. Philadelphia: Lea & Febiger, 1985: 306-320.

Slørdahl SA, Kuecherer HF, Solbakken JE, Piene H, Angelsen BAJ, Schiller NB. Regurgitant volume in aortic regurgitation from a parameter estimation procedure. J Appl Physiol 1994;76:1378-1383.

Spencer KT, Lang RM, Neumann A, Borow KM, Shroff SG. Doppler and electromagnetic comparisons of instantaneous aortic flow characteristics in primates. Circ Res 1991;68:1369-1377.

Stefanadis C, Wooley CF, Bush CA, Kolibash AJ, Boudoulas H. Aortic distensibility abnormalities in coronary artery disease. Am J Cardiol 1987;59:1300-1304.

Stewart WJ, Jiang L, Mich R, Pandian N, Guerrero JL, Weyman AE. Variable effect of changes in flow rate through the aortic, pulmonary and mitral valves on valve area and flow velocity: impact on quantitative Doppler flow calculations. J Am Coll Cardiol 1985;6:653-662.

Sunagawa K, Maughan WL, Sagawa K. Stroke volume effect of changing arterial input impedance over selected frequency ranges. Am J Physiol 1985;248:477-484.

Urschel CW, Covell JV, Sonnenblick EH, Ross J, Braunwald E. Effects of decreased aortic compliance on performance of the left ventricle. Am J Physiol 1968;214:298-304.

Van De Werf F, Piessens J, Kesteloot H, De Geest H. A comparison of systolic time intervals derived from the central aortic pressure and from the external carotid pulse tracing. Circulation 1975;51:310-316.

Visser CA, David GK, Kan G, Romijn KH, Meltzer RS, Koolen JJ, et al. Two-dimensional echocardiography during percutaneous transluminal coronary angioplasty. Am Heart J 1986;111:1035-1041.

Wallerson DC, Devereux RB. Reproducibility of quantitative echocardiography: factors affecting variability of imaging and Doppler measurements. Echocardiography 1986;3:219-235.

Watanabe H, Ohtsuka S, Kakihana M, Sugishita Y. Decreased aortic compliance aggravates subendocardial ischemia in dogs with stenosed coronary artery. Cardiovasc Res 1992;26:1212-1218.

Westerhof N, Bosman F, De Vries CJ, Noordergraaf A. Analog studies of the human systemic arterial tree. J Biomechanics 1969;2:121-143.

Westerhof N, Elzinga G, Sipkema P. An artificial arterial system for pumping hearts. J Appl Physiol 1971;31:776-781.

Wikstrand J, Nilsson K, Wallentin I. Distortion of non-invasive cardiac pulse curves. A capillary-damped pick-up and a calibration unit for apex cardiograms and other pulse curves. Br Heart J 1977;39:995-1005.

Yaginuma T, Avolio A, O'Rourke M, Nichols W, Morgan JJ, Roy P, et al. Effect of glyceryl trinitrate on peripheral arteries alters left ventricular hydraulic load in man. Cardiovasc Res 1986;20:153-160.

Yin FCP, Guzman PA, Brin KP, Maughan WL, Brinker JA, Traill TA, et al. Effect of nitroprusside on hydraulic vascular loads on the right and left ventricle of patients with heart failure. Circulation 1983;67:1330-1339.

Yin FCP. Ventricular/vascular coupling. New York: Springer Verlag, 1987.

Appendix:

Some automated corrections and calculations in the software used in the present work:

Correction of linear drift in external pulse trace:

$$c_{adjusted}(t) = c(t) - \frac{c(t_{ed}) - c(0)}{t_{ed}} \cdot t$$

Mean arterial pressure (mmHg):

$$\bar{p} = \frac{1}{t_{ed}} \int_0^{t_{ed}} p(\tau)\,d\tau$$

Mean systolic pressure (mmHg):

$$\bar{p}_s = \frac{1}{t_{es}} \int_0^{t_{es}} p(\tau)\,d\tau$$

Doppler time velocity integral (cm):

$$v_{ti} = \int_0^{t_{es}} v(\tau)\,d\tau$$

Stroke volume (cm^3):

$$SV = \int_0^{t_{ed}} q(\tau)\,d\tau$$

Cardiac output (L/min):

$$CO = SV \cdot HR$$

Total peripheral resistance (dyn s cm^{-5}):

$$TPR = \frac{\bar{p}}{CO} \cdot 80$$

Total external power (mW):

$$TP = \frac{1}{t_{ed}} \int_0^{t_{ed}} p(\tau)q(\tau)\,d\tau$$

Steady external power (mW):

$$SP = \frac{1}{t_{ed}} \bar{p} \cdot SV$$

Oscillatory power (mW):

$$OP = TP - SP$$

Abbreviations: c(t); p(τ); q(τ) = pulse trace curve; pressure curve; and flow curve as functions of time, respectively; ed = end-diastole; es = end-systole; HR = heart rate.

Paper I.

Aakhus S, Torp H, Haugland T, Hatle L. Non-invasive estimates of aortic roo
pressures: external subclavian arterial pulse tracing calibrated by oscillometricall
determined brachial arterial pressures. Clinical Physiology 1993;13:573-586.

Clinical Physiology (1993) 13, 573–586

Non-invasive estimates of aortic root pressures: external subclavian arterial pulse tracing calibrated by oscillometrically determined brachial arterial pressures

S. Aakhus, H. Torp,* T. Haugland† & L. Hatle

Department of Medicine, Section of Cardiology, *Institute of Biomedical Engineering, and †Department of Radiology, University Hospital of Trondheim, Norway

(Received 30 October 1992; accepted 15 February 1993)

Summary. This investigation assessed the ability of a non-invasive method to reproduce aortic root pressure waveform and pressures. An external pulse tracing of the subclavian artery was obtained simultaneously with direct aortic root pressures during routine left heart catheterization in 26 patients (aged 39–74 years) with various cardiovascular disorders. Indirect brachial arterial peak-systolic and nadir-diastolic pressures were obtained with oscillometry. The direct and indirect peak-systolic and nadir-diastolic pressures, were separately used to calibrate the pulse tracing.

Adequate pulse tracing was obtained in 19 patients (73%). The waveforms agreed well with cross-correlation coefficients for systole and diastole of 0·98. The difference between the pulse trace and the direct pressure curve, when the first was calibrated with the peak-systolic and nadir-diastolic pressures of the latter on average was less than 1 mmHg for systole and diastole. At end-systole the mean difference was 5 mmHg.

Oscillometric brachial arterial peak-systolic pressures were (mean±SD) 3±7 mmHg below the corresponding direct measurements, while diastolic pressures were 8±4 mmHg above. The difference between the pulse trace and the direct pressure curve, when the pulse trace was calibrated with oscillometric pressures, was at end-systole 6±6 mmHg and for mean arterial pressures 5±4 mmHg.

Thus, the external subclavian arterial pulse tracing provides a non-invasive, clinically feasible access to the aortic root pressure waveform. With optimal calibration, good estimates of aortic root pressures throughout systole and diastole can be obtained, while end-systolic pressure tends to be slightly overestimated.

Key words: aortic root pressure, non-invasive method, calibrated external pulse trace, oscillometry.

Correspondence: Svend Aakhus MD, Department of Medicine, Section of Cardiology, University Hospital, 7006 Trondheim, Norway.

Introduction

Aortic root pressure waveforms can be used to characterize left ventricular performance and systemic arterial properties (O'Rourke *et al.*, 1987). Traditionally, these data have been obtained invasively, and a clinically more feasible approach is desirable.

Systolic, diastolic, and mean pressures in the ascending aorta can be estimated indirectly with oscillometric measurements on the brachial artery (Borow & Newburger, 1982). Both the carotid and axillary arterial pulse traces reproduce the main features of the central aortic pressure waveform (Robinson, 1963; Martin *et al.*, 1971; Van de Werf *et al.*, 1975; Colan *et al.*, 1984, 1985; Kelly & Karamanoglu *et al.*, 1989).

By calibrating the external carotid pulse tracing with oscillometric brachial arterial systolic and diastolic pressures, good estimates of the ascending aortic pressures during ejection and at end-systole have been obtained (Colan *et al.*, 1983, 1985). This method has been used to determine systemic vascular resistance (Stefadouros *et al.* 1973), and to assess left ventricular performance and wall stress in patients with impaired cardiac function (Borow *et al.*, 1983, 1985, 1988, 1989; Feldman *et al.*, 1986).

In the medial right supraclavicular region, closer to the ascending aorta the subclavian arterial pulse can be recorded. This pulse tracing should be more similar to the aortic root pressure waveform than a pulse that is traced more distantly. Therefore, the purposes of this investigation were (1) to assess the ability of the external subclavian pulse tracing to reproduce the aortic root pressure waveform, and (2) to compare pressures obtained from the subclavian arterial pulse tracing calibrated with oscillometric brachial arterial pressures, with the corresponding direct aortic root pressures.

Subjects

Patients referred to routine left sided cardiac catheterization were considered for the study. Patients with aortic valvular disease, arrhythmias at the time of investigation, or clinical signs of subclavian arterial disease (neck vessel murmurs or a pressure difference between the two upper arms $\geq$10 mmHg) were excluded. We also required that direct pressures were adequately recorded.

The study group comprised 23 males and 3 females aged 39–74 years (mean value: 62·9 years). All subjects gave their informed consent to participate in the investigation. Body surface area ranged from 1·48 to 2·20 m^2 (mean value: 1·92) and the upper arm circumference (measured 15 cm above the elbow joint) from 23·5 to 35·0 cm (mean value: 29·8 cm). Sixteen patients had previous myocardial infarction, six had prior coronary artery bypass grafting, three had hypertension, and three had congestive heart failure at the time of investigation. Eighteen patients used betablocking agents, 19 used long-acting nitrates, 17 used calcium-antagonists, six used diuretics, and one used ACE-inhibitor. Twenty-three patients used vasodilator therapy with either nitrates, calcium antagonists, ACE-inhibitors, or combinations of these.

The indications for coronary angiography were chest pain in 25 patients and cardiac evaluation before major surgery in one. One patient had a well-functioning prosthetic aortic valve, otherwise all patients had normal aortic valves. One patient had moderate mitral regurgitation. Coronary artery stenosis (more than 50% reduction of cross-sectional vessel diameter) in at least one vessel was documented in 24 patients on coronary angiography. Left ventricular contractility was normal in 14 patients reduced in nine, and could not be evaluated in three patients were ventriculography was not performed. End-diastolic pressure was elevated above 12 mmHg in five patients.

All patients had sinus rhythm and were hemodynamically stable without angina pectoris during the recordings.

Methods

All data were obtained with the patients in the supine position, and the protocol did not interfere with the routine catheterization procedure.

The external pulse tracing was recorded with a pulse transducer (Irex 120-0132, Irex Medical Systems, NJ, USA), connected via a 20 cm long and 0·4 cm wide plastic tube to a funnel with cross-sectional diameter 2·3 cm. The funnel was held in the medial supraclavicular region over the right subclavian artery, and the recordings were made during a short period of apnea.

An oscillometric microprocessor-controlled blood pressure manometer (UA 751, Takeda Medical Inc, Tokyo, Japan) was used with an adult-sized cuff positioned snugly on the patient's right upper arm. The cuff deflation rate was 3 mmHg s^{-1}. During deflation of the cuff, when blood starts to flow through the vessel, the amplitude of the vessel oscillations first increases, on further deflation it reaches a peak, before decreasing to a baseline when blood flow is unobstructed (Ramsey, 1979; Geddes, 1984). Systolic pressure is determined at the onset of increase in the amplitude of the oscillations, mean arterial at the peak amplitude, and diastolic pressure immediately before the baseline amplitude is reached. The pressures are determined by the UA 751 semi-automatically, independent of the observer, and can be stored for later print-out. We measured systolic and diastolic pressures with oscillometry at least twice immediately before and after pressure recordings, and used the average for calibration of the pulse tracing. If the measurements differed more than 10 mmHg, they were redone.

Routine catheterization of the aorta and left ventricle was performed via the femoral artery. A 7 end-hole pigtail catheter (527–750, Cordis Corp., FL, USA), 110 cm long, was positioned in the aortic root for direct pressure measurement and connected via a manifold to a strain gauge transducer (SensoNor 840, SensoNor, Horten, Norway) positioned at mid-chest level. This system had a natural frequency of 12·5 Hz and was slightly underdampened. The frequency response was considered adequate for recording of aortic pressures at normal resting heart rates (Grossmann, 1986).

The external pulse tracing and the direct aortic root catheter pressures were recorded simultaneously with a sample rate of 200 Hz and displayed in real time on a scanner

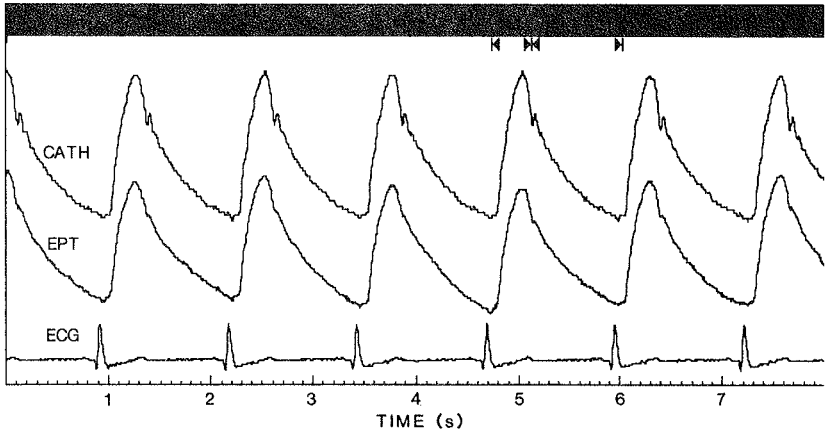

Fig. 1. External subclavian arterial pulse tracing (EPT) and direct aortic root pressure waveform (CATH) recorded simultaneously in a representative subject. The EPT is uncalibrated and scaled for comparison with CATH. Tabulators indicate the cardiac cycle shown in Fig. 2.

(CFM 750, Vingmed Sound, Horten, Norway). The time constant for amplification of the pulse signal was 4·7 s. The scanner was interfaced to a computer (Macintosh II-series, Apple Computer Inc, CA, USA) for transfer of the digitized pulse tracing and direct pressure curve. At least 5 cardiac cycles were recorded (Fig. 1).

To increase the number of comparisons, recordings were made both before and shortly after injection of 45 ml contrast medium (Hexabrix, Guerbet, France 320 mg I ml^{-1}) in the left ventricle (23 patients) or aorta (three patients). The injection rate was 18 ml s^{-1}. All recordings were made before the selective coronary angiography.

ANALYSIS

The criteria for an adequate pulse tracing were: (1) a reproducible beat-to-beat waveform, (2) a sharp end-diastolic deflection of curve before systolic ascent, (3) a defined end-systolic incisura, and (4) minimal baseline drift.

For each patient three cardiac cycles, not necessarily consecutive, comprising adequate pulse tracing and direct pressure curve, were selected for waveform analysis. The waveforms of the pulse tracing and the aortic root pressure were compared by calculation of the cross-correlation coefficient, r_{xy} (Horan & Flowers, 1968) for each selected beat. This coefficient provides a quantitative index for waveform similarity, independent of curve-calibration (see appendix). It varies from +1 for identical curves, to −1 for inversely identical curves, and it is zero when the two curves do not have any similarity. We determined r_{xy} separately for systole, diastole, and for the total cardiac cycle.

To further compare the pressure waveforms, the pulse trace was calibrated with the corresponding direct peak-systolic and nadir-diastolic pressures. The difference

between this 'optimally' calibrated pulse tracing and the direct pressure wave was determined throughout the cardiac cycle for every 5 ms. The average difference was determined separately for systole, for diastole, and for the total cardiac cycle.

To test the precision of the non-invasive method, we reselected at least three cardiac cycles from each recording in a new and independent analysis. The pulse tracing was now calibrated by assigning the oscillometrically determined systolic brachial arterial pressure to the peak of the pulse tracing, and the diastolic to its nadir (Stefadouros *et al.*, 1973; Colan *et al.*, 1985). End-systolic pressure was determined at the nadir of the incisura on the calibrated pulse tracing, and at the nadir of the dicrotic notch on the aortic root pressure curve (Fig. 2). Mean arterial pressure was determined as the integral of the calibrated pulse tracing and the aortic root pressure curve, respectively, both divided by cardiac cycle length.

REPRODUCIBILITY

The reproducibility of the oscillometrically-determined brachial arterial systolic and diastolic pressures was assessed by comparison of two consecutive manometer measurements made both before and after injection of contrast medium in each patient. The measurements were used without considering their outcome or potential use for calibration of the pulse tracing.

STATISTICS

Values are presented as mean ± standard deviation. The absolute differences (mmHg) between indirect and direct measurements were determined. A simple linear regression was performed with indirect measurements as predictor variables (x) and corresponding

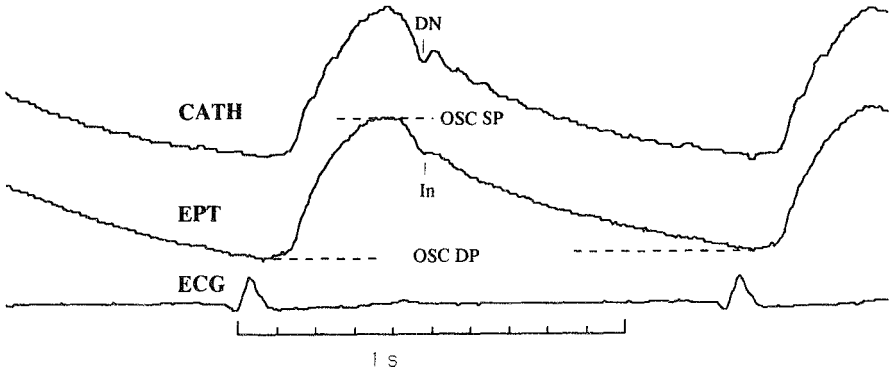

Fig. 2. The external pulse tracing (EPT) calibrated with oscillometrically determined systolic (OSC SP) and diastolic (OSC DP) brachial artery pressures to its peak and nadir, respectively. The end-systolic pressure is determined at the incisura (In) of the calibrated pulse tracing and at the nadir of the dicrotic notch (DN) of the direct aortic root pressure curve (CATH). Mean pressure was determined as the integral of each pressure curve divided by cardiac cycle length.

direct measurements as outcome variables (y). The precision of the non-invasive method was assessed by the 95% confidence interval for the predicted direct pressure corresponding to typical indirect measurements, namely the mean indirect pressure and pressures 20 and 40% above and below this value. The confidence interval is smallest at the mean indirect value, and slightly higher for higher and lower pressures. The coefficient of variation was determined as the standard deviation of the differences between the indirect and direct pressures over the mean of the measurements, and multiplied with 100. The absolute differences (mmHg) between the indirect and direct pressures were plotted against the direct pressures (Bland & Altman, 1986). Direct pressures measured before and after injection of contrast medium were compared using a paired two-tailed *t*-test with the level of significance set at 0·05.

Results

Aortic root pressures were adequately recorded in 26 patients either before (21 recordings) and/or after (25 recordings) injection of contrast medium. We obtained adequate external pulse tracings in 19 patients (18 recordings before and 18 after injection of contrast medium). Simultaneous recordings of pulse trace and aortic root pressure were thus adequately obtained in 73%.

Following injection of contrast medium, a slight increase in heart rate (54±8 to 57±9 beats min^{-1}, $P<0·01$) and peak-systolic pressure (128±23 to 134±26 mmHg, $P<0·05$) were observed, while no significant change in nadir-diastolic pressure occurred.

PRESSURE WAVEFORMS

Table 1 shows that the cross-correlation coefficient r_{xy}, for the pulse tracing and the direct aortic root pressure wave, was 0·98 for systole, diastole, and the total cardiac cycle. There was no difference in waveform-correlation of the patients with mean arterial pressures above the median (92 mmHg) and those with mean arterial pressures below. The pressure difference between the pulse tracing and the direct pressure wave when the first was calibrated with direct peak-systolic and nadir-diastolic pressures of the latter, was on the average less than 1 mmHg for both systole and diastole. At end-systole the average difference was 5±4 mmHg. This indicates that when the external subclavian pulse tracing is optimally calibrated, it reproduces the direct aortic root pressures well throughout systole and diastole, while end-systole tends to be slightly overestimated.

PRESSURE MEASUREMENTS AND ESTIMATES

Table 2 shows that the oscillometric measurements of brachial arterial systolic pressure were on the average 3 mmHg lower than the direct aortic root peak-systolic pressure. The differences were evenly distributed over the range of pressures (Fig. 3, upper panel). The regression equation for y, direct aortic root peak-systolic pressure and x,

Table 1. Waveform-comparison of the subclavian arterial pulse trace and direct aortic root pressure

	Systole	Diastole	Total cycle
Cross-correlation coefficient (r_{xy})	0·98±0·01 (0·95–1·00)	0·98±0·01 (0·93–1·00)	0·98±0·01 (0·96–1·00)
Pressure difference (mmHg)	0·7±2·2 (−3–10)	−0·2±4·3 (−12–13)	0·0±3·2 (−8–12)

Values are mean±SD, range in parenthesis, of 108 beat-to-beat comparisons in 19 patients. Pressure difference, the difference between the pulse trace and direct pressure waves, when the first was calibrated with the direct peak-systolic and nadir-diastolic pressures. The difference was determined for every 5 ms thoughout the cardiac cycle and averaged for systole, for diastole, and for the total cardiac cycle.

Table 2. Comparison of indirect and direct aortic root pressures

	Indirect	Direct		
Pressures	OSC BA	CATH	Difference	CV
Peak–systolic	127±23 (90–174)	131±24 (91–185)	−3·3±6·8 (−14–13)	5·3
Nadir–diastolic	75±10 (57–96)	67±10 (51–88)	7·5±4·1 (−2–15)	5·8
	EPT/OSC BA	CATH	Difference	CV
End–systolic	112±18 (83–149)	105±16 (79–140)	6·2±5·9 (−3–21)	5·4
Mean arterial	98±15 (71–128)	93±14 (70–124)	4·7±4·3 (−5–14)	4·5

Values are mean±SD, range in parenthesis. OSC BA, oscillometrically determined brachial arterial pressure (mmHg); EPT/OSC BA, pressures determined from the subclavian arterial pulse tracing calibrated with OSC BA (mmHg); CATH, direct aortic root pressures (mmHg); Difference, OSC BA-CATH (mmHg); CV, coefficient of variation (per cent).

indirect systolic pressure was $y=0{\cdot}999x+4{\cdot}2$, with $r=0{\cdot}96$ ($P=0{\cdot}0001$). For the mean indirect systolic pressure (127 mmHg) the standard error of the estimate was 6·6 mmHg and the 95% confidence interval for the predicted direct systolic pressure was 114–140 mmHg.

The oscillometric measurements of brachial arterial diastolic pressure were on the average 8 mmHg higher than the direct aortic root nadir-diastolic pressure. However, the differences were evenly distributed over the range of pressures (Fig. 3, lower panel). The regression equation was $y=0{\cdot}885x+1{\cdot}0$, with $r=0{\cdot}92$ ($P=0{\cdot}0001$). For the mean indirect diastolic pressure (75 mmHg) the standard error of the estimate was 4·0 mmHg and the 95% confidence interval for the predicted direct pressure was 67–83 mmHg.

The indirect estimates of end-systolic pressures were on the average 6 mmHg above the direct. The differences were evenly distributed over the pressure range (Fig. 4, upper

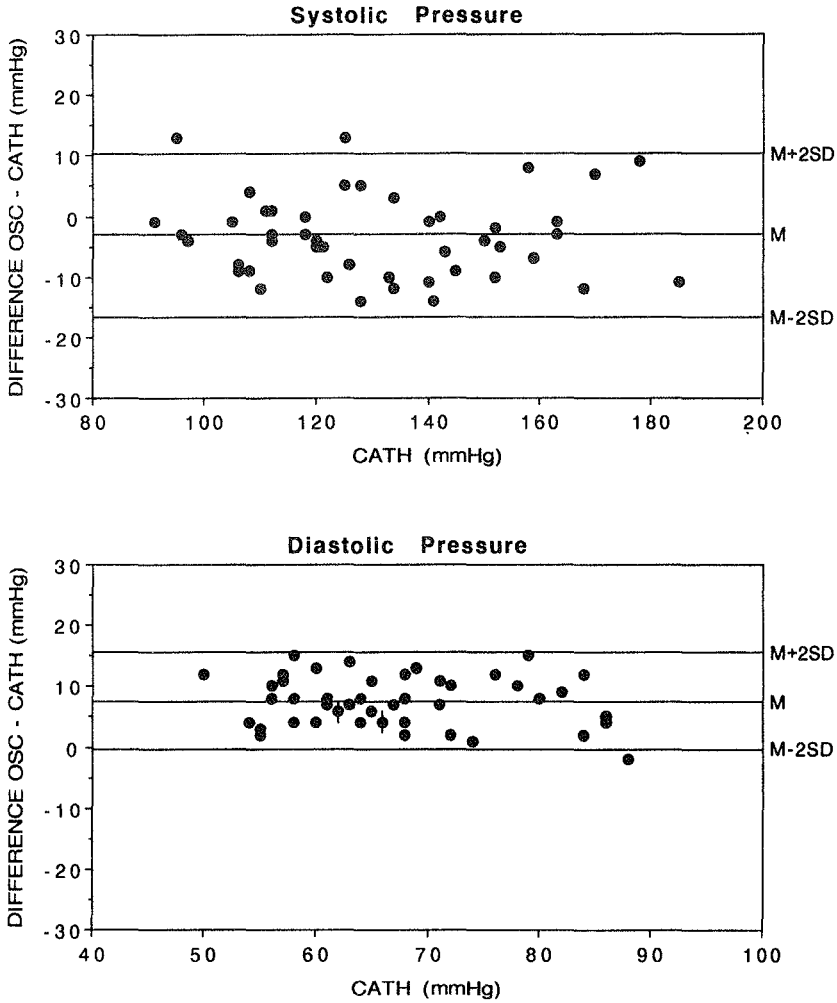

Fig. 3. The differences (mmHg) between oscillometrically determined brachial arterial pressures (OSC) and direct aortic root pressures (CATH) at the ordinate plotted against the direct pressures at the abscissa (46 comparisons in 26 patients). *Upper panel:* peak-systolic pressures. *Lower panel:* nadir-diastolic pressures. Duplicate set of values is indicated by a vertical short line. The horizontal lines show mean difference (M)±2SD.

panel). Eighty-one per cent of the non-invasive end-systolic pressure estimates was within 10 mmHg of the invasive measurement. The regression equation was $y=0{\cdot}841x+11{\cdot}5$, with $r=0{\cdot}94$ ($P=0{\cdot}0001$). For the mean indirect end-systolic pressure (112 mmHg) the standard error of the estimate was 5·4 mmHg and the 95% confidence interval for the predicted direct pressure was 101–123 mmHg.

The indirect estimates of mean arterial pressures were on the average 5 mmHg above the direct. The differences were slightly increased at the higher pressures as shown in

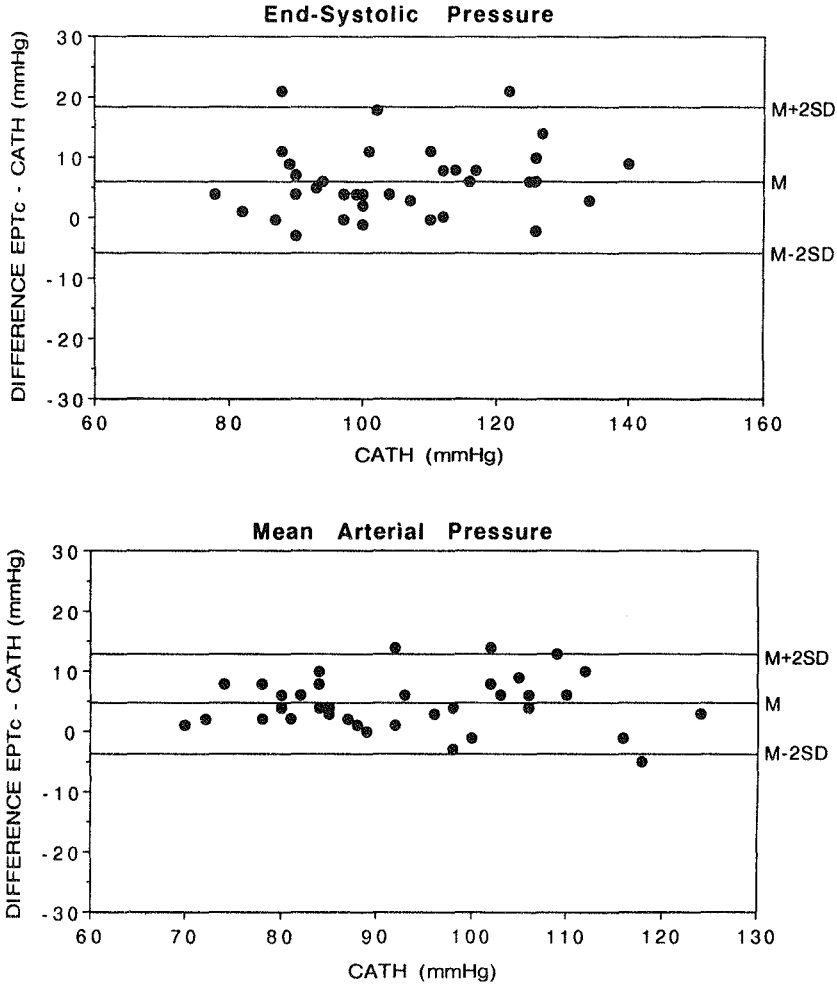

Fig. 4. The differences (mmHg) between pressures obtained from the oscillometrically calibrated subclavian arterial pulse tracing (EPTc) and direct aortic root pressures (CATH) at the ordinate plotted against the direct pressures at the abscissa (36 comparisons in 19 patients). *Upper panel:* end-systolic pressures. *Lower panel:* mean arterial pressures. The horizontal lines show mean difference (M)±2SD.

Fig. 4 (lower panel). However, 92% of the non-invasive mean pressure estimates was within 10 mmHg of the invasive measurement. The regression equation was $y=0{\cdot}910x+4{\cdot}2$, with $r=0{\cdot}95$ ($P=0{\cdot}0001$). For the mean indirect mean arterial pressure the standard error of the estimate was 4·3 mmHg and the 95% confidence interval for the predicted direct pressure 89–107 mmHg.

In general, for a typical indirect pressure estimate (i.e. the mean value), the corresponding direct pressure was within ±11% of this value, with 95% probability. This was also the case for indirect estimates 20 and 40% above the typical value. For indirect

estimates 20% below the typical value, the direct pressure will be within ±14% of the indirect. The coefficient of variation was lowest for the mean arterial pressure (4·5%) and highest for the nadir-diastolic (5·8%).

REPRODUCIBILITY

The relative difference between two consecutive oscillometric measurements (26 paired comparisons before and 25 after injection of contrast medium) was for systolic pressures 0±7 mmHg and for diastolic pressure 2±6 mmHg. The differences were evenly distributed over the range of pressures. For systolic pressures, 5 of the absolute pressure differences (9·8%) were larger than 10 mmHg, while four differences (7·8%) for diastolic pressures deviated that much.

Discussion

The study group comprised patients of different age, sex, body size, clinical condition, and with a wide range of blood pressures. In spite of the limited time available during the routine recording of aortic root pressures, we obtained an adequate external pulse tracing in 73% of the subjects. Thus, the calibrated external subclavian arterial pulse tracing seems to be a clinically feasible method. Furthermore, the pulse tracing reproduced the aortic root pressure waveform well with high cross-correlation coefficients for both systole and diastole. In our experience, the diastolic part of the arterial pulse, and in particular the end-diastolic deflection, may occasionally be difficult to trace, while the systolic part usually is obtained easily. This may explain why the cross-correlation for systole was slightly better than for diastole.

Our results demonstrate that once aortic root peak-systolic and nadir-diastolic pressures can be accurately estimated, the subclavian pulse tracing calibrated with these values provides good estimates of aortic root pressures throughout systole and diastole (Table 1), while end-systolic pressure still tends to be slightly overestimated. This may be due to waveform artefacts at end-systole (i.e. the incisura) and can be related to at least two factors. First, subcutaneous tissue may dampen high frequency components of the pulse wave (i.e. the incisura) and cause a false high indirect end-systolic pressure. Second, underdampening of the direct measurement-system may cause a slight undershoot of the dicrotic notch (Nichols *et al.*, 1990) and thus a false low direct end-systolic pressure. However, our data did not allow differentiation between these factors.

The oscillometric manometer used on the brachial artery gave reliable estimates of aortic root peak-systolic pressures over a wide range of pressures, while nadir-diastolic pressures were consistently over-estimated. The results are better than blood pressure measurements with the auscultatory method (Ragan & Bordley, 1941; Kotte *et al.*, 1943; Forsberg *et al.*, 1970), but for diastolic pressures not as good as those obtained with other oscillometric manometers (Ramsey, 1979; Borow & Newburger, 1982; Colan *et al.*, 1983). The slight underestimation of peak-systolic pressures counteracted the

relatively larger overestimation of nadir-diastolic pressures. Thus, over the wide range of pressures recorded in this study, end-systolic and mean arterial pressures were only slightly overestimated.

The precision of the non-invasive method was highest for mean arterial pressures and lowest for nadir-diastolic pressures, although the differences were small. For a typical indirect estimate of either systolic, diastolic, end-systolic, or mean arterial pressure, the corresponding direct pressure was within ±11% of the indirect, with 95% probability.

The indirect and direct waveforms correlated equally well at high and low pressures. Also, the difference between oscillometric and direct measurements of peak-systolic and nadir-diastolic pressures were constant over the range of pressures (Fig. 3) with small coefficients of variation. Thus, for practical purposes we consider the calibrated pulse tracing to be linearily related to the direct aortic root pressures.

Finally, even though systolic and diastolic pressures determined by oscillometry had an acceptable reproducibility, it is recommended that any set of consecutive measurements with more than 10 mmHg difference be repeated.

METHODOLOGICAL CONSIDERATIONS

The external pulse tracing must be recorded with equipment that meets certain specifications (Tavel, 1978). The length of the tube connecting the funnel to the transducer should be shorter than 28 cm to avoid significant resonance in the air column (Kesteloot *et al.*, 1969). The time-constant of the recording system should exceed at least 1 s to ensure adequate recording of the arterial waveform (Kesteloot *et al.*, 1969; Johnson *et al.*, 1971; Lewis *et al.*, 1977). We used a tubelength of 20 cm and a time-constant of 4·7 s. The frequency response of this type of transducers is usually adequate (flat to 30 Hz) (Johnson *et al.*, 1971; Lewis *et al.*, 1977).

Recently, a new external pulse transducer has been developed (Kelly & Hayward *et al.*, 1989). When used with the principle of applanation tonometry, the arterial pressure wave can be well reproduced. However, this method requires a more elaborate recording procedure than the transducer-system we used.

The oscillometric method for non-invasive measurement of systolic and diastolic brachial arterial pressures seems to be reliable and clinically feasible. However, during arrhythmias when significant beat-to-beat variations in blood pressure may occur, the measurements are not reliable. Our patients were all in sinus rhythm, so the accuracy during arrhythmias could not be assessed.

The oscillometric method requires that the arm with the cuff is kept relatively motionless during the measurement. In disoriented patients and small children, this may limit the use of the method. Oscillometry is further a somewhat slow procedure, usually 15–30 s is required for one measurement, and move during higher pressures and bradycardia. Rapid haemodynamic fluctuations may thus not be adequately documented with this method.

If the cuff is not at the level of the aortic root when the patient is in the left lateral position, the oscillometrically-determined pressures have to be corrected for the hydrostatic effect. This was not necessary in our study as the patients were supine with the cuff at aortic root level.

In aortic stenosis with a valvular gradient, the estimates of aortic root pressures do not represent left ventricular pressures during systole, and therefore, this method should not be used in assessment of left ventricular function.

CLINICAL IMPLICATIONS

The external tracing of the subclavian artery provides a non-invasive, repeatable, and clinically feasible access to the aortic root pressure waveform. When the pulse tracing is calibrated with non-invasively obtained systolic and diastolic brachial arterial pressures, good estimates of end-systolic and mean aortic root pressures can be obtained.

In patients with regular cardiac rhythm and normal aortic valves, this method can be combined with echocardiographic recordings of left ventricular dimensions and aortic root blood flow, and potentially be used for non-invasive assessment of left ventricular function and systemic arterial properties, in health and disease, and during pharmacological intervention.

Acknowledgment

This work was supported by a grant from the Norwegian Council on Cardiovascular Diseases.

References

BLAND J.M. & ALTMAN D.G. (1986) Statistical methods for assessing agreement between two methods of clinical measurement. *Lancet,* **i,** 307–310.

BOROW K.M. & NEWBURGER J.W. (1982) Noninvasive estimation of central aortic pressure using the oscillometric method for analyzing systemic artery pulsatile blood flow: Comparative study of indirect systolic, diastolic, and mean brachial artery pressure with simultaneous direct ascending aortic pressure measurements. *Am Heart J,* **103,** 879–886.

BOROW K.M., HENDERSON C., NEUMANN A., COLAN S., GRADY S., PAPISH S., GOORIN A. (1983) Assessment of left ventricular contractility in patients receiving Doxorubicin. *Ann Int Med,* **99,** 750–756.

BOROW K.M., COLAN S.D. & NEUMANN A. (1985) Altered left ventricular mechanics in patients with valvular aortic stenosis and coarctation of the aorta: Effects on systolic performance and late outcome. *Circulation,* **72,** 515–522.

BOROW K.M., LANG R.M., NEUMANN A., CARROL J.D. & RAJFER S.I. (1988) Physiologic mechanisms governing hemodynamic responses to positive inotropic therapy in patients with dilated cardiomyopathy. *Circulation,* **77,** 625–637.

BOROW K.M., NEUMANN A., ARENSMAN F.W. & YACOUB M.H. (1989) Cardiac and peripheral vascular responses to adrenoceptor stimulation and blockade after cardiac transplantation. *J Am Coll Cardiol,* **14,** 1229–1238.

COLAN S.D., FUJII A., BOROW K.M., MACPHERSON D. & SANDERS S.P. (1983) Noninvasive determination of systolic, diastolic and end-systolic blood pressure in neonates, infants and young children: Comparison with central aortic pressure measurements. *Am J Cardiol,* **52,** 867–870.

COLAN S.D., BOROW K.M., MACPHERSON D., SANDERS S.P. (1984) Use of the indirect axillary pulse tracing for noninvasive determination of ejection time, upstroke time, and left ventricular wall stress throughout ejection in infants and young children. *Am J Cardiol,* **53,** 1154–1158.

COLAN S.D., BOROW K.M. & NEUMANN A. (1985) Use of calibrated carotid pulse tracing for calculation of left ventricular pressure and wall stress throughout ejection. *Am Heart J,* **109,** 1306–1310.

FELDMAN T., BOROW K.M., SARNE D.H., NEUMANN A. & LANG R.M. (1986) Myocardial mechanics in hyperthyroidism: Importance of left ventricular loading conditions, heart rate and contractile state. *J Am Coll Cardiol,* **7,** 967–974.

FORSBERG S.Å., DE GUZMAN M. & BERLIND S. (1970) Validity of blood pressure measurement with cuff in the arm and forearm. *Acta Med Scand,* **188,** 389–396.

GEDDES L.A. (1984) *Cardiovascular devices and their applications* pp. 67–72. John Wiley & Sons, New York.

GROSSMANN W. (1986) Pressure measurement. In: *Cardiac catheterization and angiography* (ed. Grossmann W.), 3rd ed., pp. 118–134, Lea & Febiger, Philadelphia.

HORAN L.G. & FLOWERS N.C. (1968) The principle of waveform correlation in electrocardiographic research. *J Electrocardiology,* **1,** 43–50.

JOHNSON J.M., SIEGEL W. & BLOMQVIST G. (1971) Characteristics of transducers used for recording the apexcardiogram. *J Appl Physiol,* **31,** 796–800.

KELLY R., HAYWARD C., GANIS J., AVOLIO A. & O'ROURKE M. (1989) Noninvasive registration of the arterial pressure pulse waveform using high-fidelity applanation tonometry. *J Vasc Med Biol,* **1,** 142–149.

KELLY R., KARAMANOGLU M., GIBBS H., AVOLIO A. & O'ROURKE M. (1989) Noninvasive carotid pressure wave registration as an indicator of ascending aortic pressure. *J Vasc Med Biol,* **1,** 241–247.

KESTELOOT H., WILLEMS J. & VAN VOLLENHOVEN E. (1969) On the physical principles and methodology of mechanocardiography. *CTA Cardiologica,* **24,** 147–160.

KOTTE J.H., IGLAUER A. & JOHNSON M. (1943) Measurements of arterial blood pressure in the arm and leg: Comparison of sphygmomanometric and direct intra-arterial pressure with special attention to their relationship in aortic regurgitation. *Am Heart,* **28,** 476–490.

LEWIS R.P., RITTGERS S.E., FORESTER W.F. & BOUDOULAS H. (1977) A critical review of the systolic time intervals. *Circulation,* **56,** 146–158.

MARTIN C.E., SHAVER J.A., THOMPSON M.E., SUDHAKAR REDDY P. & LEONARD J.J. (1971) Direct correlation of external systolic time intervals with internal indices of left ventricular function in man. *Circulation,* **44,** 419–431.

NICHOLS W.W., O'ROURKE M.F. & MCDONALD R. (1990) McDonald's blood flow in arteries (3rd ed.), Edward Arnold, London.

O'ROURKE M.F., AVOLIO A.P. & NICHOLS W.W. (1987) Left ventricular-systemic arterial coupling in humans and strategies to improve coupling in disease states. In: *Ventricular/vascular coupling* (ed. Yin, F.C.P.), pp. 1–19. Springer Verlag, New York.

RAGAN C. & BORDLEY J. (1941) The accuracy of clinical measurements of arterial blood pressure. *Bull John Hopkins Hosp,* **69,** 504–528.

RAMSEY M. (1979) Noninvasive automatic determination of mean arterial pressure. *Med Biol Eng Comput,* **17,** 11–18.

ROBINSON B. (1963) The carotid pulse II: Relation of external recordings to carotid, aortic, and brachial pulses. *Br Heart J,* **25,** 61–68.

STEFADOUROS M.A., DOUGHERTY M.J., GROSSMANN W. & CRAIGE E. (1973) Determination of systemic vascular resistance by a noninvasive technic. *Circulation,* **47,** 101–107.

TAVEL M.E. (1978) Clinical phonocardiography and external pulse recording (3rd ed), pp. 26–28. Year Book Medical Publishers Inc., Chicago.

VAN DE WERF F., PIESSENS J., KESTELOOT H. & DE GEEST H. (1975) A comparison of systolic time intervals derived from the central aortic pressure and from the external carotid pulse tracing. *Circulation,* **51,** 310–316.

Appendix

The pressure waveforms used in this study were collected and stored digitally. The analogue to digital converter has eight-bit resolution, and the sampling rate was 200 Hz, giving a 5 ms temporal increment between the data samples. The digital waveform {x(k), k=0..N−1} from one heart cycle is related to the actual pressure waveform p(t) by:

$$x(k)=p(kT),\ k=0..N-1$$

Sample increment: T=5 ms

Delay after QRS: t=KT

Heart cycle time: NT

The cross-correlation coefficient r_{xy} between two waveforms {x(k), y(k), k=1..N} is defined as:

$$r_{xy}=\frac{\sum_{k=0}^{N-1}[x(k)-\bar{x}][y(k)-\bar{y}]}{\sqrt{\sum_{k=0}^{N-1}[x(k)-\bar{x}]^2\sum_{k=0}^{N-1}[y(k)-\bar{y}]^2}}$$

$$\bar{x}=\frac{1}{N}\sum_{k=0}^{N-1}x(k)$$

$$\bar{y}=\frac{1}{N}\sum_{k=0}^{N-1}y(k)$$

The correlation coefficient equals 1 if the two waveforms are identical and −1 if the waveforms are inverse, i.e. x(k)=−y(k).

Paper II.

Aakhus S, Soerlie C, Faanes A, Hauger SO, Bjoernstad K, Hatle L, Angelsen BAJ. Noninvasive computerized assessment of left ventricular performance and systemic hemodynamics by study of aortic root pressure an flow estimates in healthy men, and men with acute and healed myocardial infarction. American Journal of Cardiology 1993;72:260-267.

Noninvasive Computerized Assessment of Left Ventricular Performance and Systemic Hemodynamics by Study of Aortic Root Pressure and Flow Estimates in Healthy Men, and Men with Acute and Healed Myocardial Infarction

Svend Aakhus, MD, Carsten Soerlie, PhD, Audun Faanes, MSc, Svein O. Hauger, MSc, Knut Bjoernstad, MD, Liv Hatle, MD, and Bjoern A. J. Angelsen, dr.techn.

ortic root pressure and flow data can be used to sess left ventricular (LV) performance and prop- ties of the systemic arterial tree. The calibrated bclavian arterial pulse trace was combined with hocardiographic imaging and Doppler velocity cordings to obtain noninvasive estimates of aor- root pressure and flow in 8 healthy subjects roup A), 12 patients with recent myocardial in- rction (group B), and 8 with healed myocardial farction and a dilated left ventricle (group C). e pressure and flow data were transferred to a mputer and processed in specially designed ftware, including a new procedure for estima- n of 3-element windkessel model parameters. ere were no significant group differences for ei- er aortic root pressure estimates or heart rate. groups B and C, stroke and cardiac indexes ere lower and total peripheral resistance higher an in group A. There were no group differences the model estimates of total arterial compli- ce, whereas the characteristic impedance was eater in group C than in A, indicating a less com- ant aorta in C. Both LV total and steady power ere less in groups B and C than in A, whereas no oup difference was found for percent oscillatory wer. The reproducibility for recording was good r the aortic root pressure estimates, and lower r the derived parameters (stroke and cardiac in- xes, windkessel model parameters and LV pow-), whereas that for interpretation was generally od. This method provides a unique noninvasive cess to important parameters of LV function d the systemic circulation.

(Am J Cardiol 1993;72:260–267)

m the Department of Medicine, Section of Cardiology, and Depart- nt of Biomedical Engineering, University Hospital, Trondheim, rway. This work was supported by grants from the Norwegian Coun- on Cardiovascular Diseases, Oslo, Norway. Manuscript received tember 28, 1992; revised manuscript received February 25, 1993, accepted March 1.

Address for reprints: Svend Aakhus, MD, Department of Medicine, tion of Cardiology, University Hospital, 7006 Trondheim, Norway.

Left ventricular (LV) performance and systemic arterial properties can be assessed by analysis of aortic root pressure and flow data.[1,2] Invasive methods have usually been needed to obtain these data. However, the aortic root pressure waveform can be noninvasively reproduced by an external arterial pulse trace.[3–8] A carotid pulse tracing calibrated with brachial arterial pressures, obtained by oscillometry, provides reliable estimates of the aortic root pressures during ejection.[7,9] The external subclavian arterial pulse trace reproduces the aortic root pressure waveform both in systole and diastole.[10] Accurate estimates of aortic annulus blood flow can be obtained with echocardiographic imaging and Doppler velocity recordings.[11,12] Thus, noninvasive estimates of both aortic root pressure and flow can be obtained by a combined use of these methods.

The aim of this investigation was to study LV performance and systemic arterial properties noninvasively in healthy subjects, patients with acute myocardial infarction, and those with LV dilatation after myocardial infarction. We also assessed the interobserver reproducibility for both recording and interpretation of the data. The data were processed in specially designed computer software.

METHODS

Study subjects: In all, we studied 28 men. All subjects gave informed consent. Subjects with irregular cardiac rhythm, aortic valvular disease or neck vessel bruit were excluded from the study. Based on clinical examination, routine 12-lead electrocardiography, laboratory investigation and echocardiographic examination, subjects were separated into 3 groups. Group characteristics are listed in Table I.

Group A comprised 8 healthy men aged 24 to 62 years.

Group B comprised 12 men, aged 39 to 79 years, with acute myocardial infarction <20 days (range 4 to 19) before the study. Myocardial infarction was documented by ≥2 of the following criteria: (1) typical chest pain of >30-minute duration, (2) serial changes in the electrocardiogram typical of acute myocardial infarction, and (3) increase in serum cardiac enzymes to at least twice the normal value. The myocardial infarction was anterior in 11 patients and inferior in 1 by electro-

olume index was within the normal range in all pa-
ents.[13] LV ejection fraction was ≤50% in all but 3 pa-
ents, and all had LV wall motion abnormalities. Two
atients had more than trivial mitral regurgitation. All
atients received β-blocking agents, and 3 received ad-
itional vasodilator therapy.

Group C comprised 8 men, aged 38 to 74 years, with
yocardial infarction >3 months (range 3 to 120) before
ie study. Six patients had anterior and 2 inferior wall
ifarctions. The left ventricle was dilated, with end-dia-
olic volume indexes ≥80 cm^3/m^2. LV ejection fraction
as ≤50% in all patients, and all had LV wall motion
normalities. Three patients had more than trivial mi-
al regurgitation. Beta blockers were received by all but
patient, and 6 had additional vasodilator therapy.

No study subject had pulmonary congestion on aus-
ultation at rest. Medication was continued during the
ivestigation for all patients.

Data recording: Subjects rested on a bench for ≥10
inutes before they were examined in a slightly left lat-
ral decubitus position.

An ultrasound scanner (CFM 750, Vingmed Sound,
lorten, Norway) with a duplex probe was used for
chocardiographic imaging (frequency 3.25 MHz) and
oppler velocity recording (frequency 2.5 MHz), and
or display of the pulse tracing. The scanner was inter-
aced to a computer (Macintosh II series, Apple Com-
uter, Inc., Cupertino, California) for transfer of digital
ltrasound data.

The aortic annulus was imaged on 3 consecutive par-
sternal long-axis echocardiograms, and the diameter
as measured at the base of the aortic valve leaflets with
ie trailing-to-leading-edge method.[11] The average di-
meter was used in calculations of the aortic annulus
ross-sectional area, assuming a circular orifice. The left
entricle was imaged in 3 standard apical views (4- and
-chamber, and long-axis) that were transferred as cine-
oops to the computer. LV end-diastolic and end-systolic

TABLE 1 Patient Group Characteristics

	Group A	Group B	Group C
No. of pts./sex	8/M	12/M	8/M
Age (years)	41 ± 14 (24–62)	63 ± 12 (39–79)*	57 ± 14 (38–74)*
Body surface area (m^2)	1.89 ± 0.09	1.87 ± 0.15	1.88 ± 0.10
LV ejection fraction (%)	61 ± 6 (53–70)	46 ± 11 (24–67)*	42 ± 6 (32–47)*
LV end-diastolic volume index (cm^3/m^2)	55 ± 10 (43–70)	60 ± 9 (44 – 74)	96 ± 18 (80–133)*†

*p <0.05 versus group A; †p <0.05 versus group B.
Numbers are mean ± SD; range in parentheses.
LV = left ventricular.

volumes were determined by the biplane method of discs,[14] and ejection fraction was calculated as end-diastolic – end systolic/end-diastolic volume.

An external pulse transducer (Irex 120-0132, Irex Medical Systems, Ramsey, New Jersey) was connected through a preamplifier to the scanner. Pulse tracing of the right subclavian artery was obtained during a short period of apnea, usually close to end-expiration. The criteria for an adequate pulse tracing were as follows: (1) reproducible beat-to-beat waveform, (2) sharp deflection of the curve at the beginning of pulse ascent, and (3) minimal baseline drift. The analog signals were converted to digital at a rate of 200/s.

Aortic annulus blood flow velocities were recorded with pulsed Doppler from the apical position. The ultrasound beam was aligned as close as possible to the central blood flow direction, as identified by the orientation of the LV outflow tract and a well-defined Doppler signal with a narrow range of velocities. The sample volume was positioned at the aortic annular level, as defined by the valve closure click.

At least 5 cardiac cycles with simultaneously recorded pulse tracing, Doppler velocities and a 1-lead electrocardiogram were then transferred to the computer for off-line analysis.

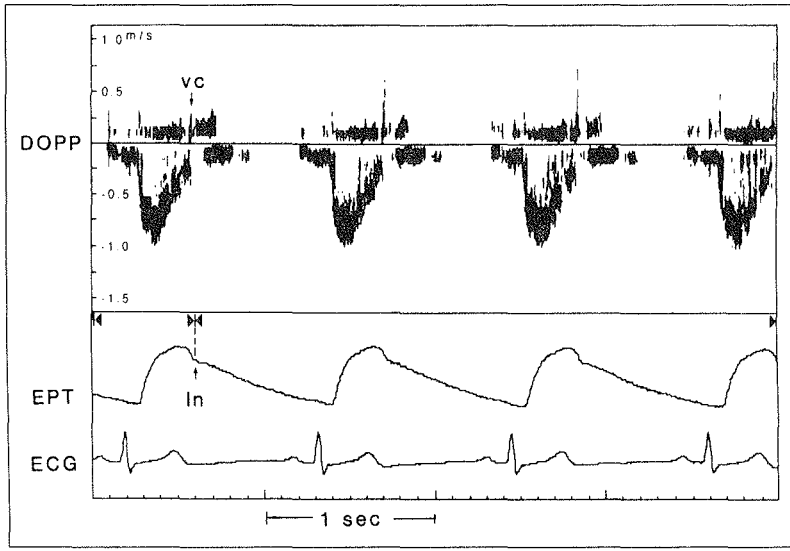

IGURE 1. External pulse racing (EPT) of right subcla-ian artery *(bottom)* record-d simultaneously with ulsed-wave Doppler (DOPP) ignals of blood flow veloci-ies in aortic annulus *(top).* nd-systole is defined at be-inning of aortic valve clo-ure click (VC) on Doppler ecording. Incisura (In) of ulse tracing occurs later han valve click (approxi-nately 20 ms), correspond-ng to pulse transmission ime from aortic root to sub-lavian artery. ECG = elec-rocardiogram.

in immediate succession, duplicate brachial arterial blood pressures were obtained with a semiautomatic oscillometric manometer (UA 751, Takeda Medical Inc., Tokyo) and an adult-size cuff on the patient's upper right arm; the average pressure was used in subsequent calculations. If pressure measurements differed >10 mm Hg, they were repeated.

Computer analysis: At least 3 cardiac cycles with adequate pulse tracing and Doppler signals were selected for analysis (Figure 1). The pulse tracing was calibrated with the oscillometrically determined systolic and diastolic brachial arterial pressures,[7] and the end-systolic incisura was defined by the investigator. The Doppler time-velocity integral was determined on the computer by manual tracing of the Doppler recording at the peak velocities during systole and at the zero line in diastole. End-systole was defined at the beginning of the aortic valve closure click on the Doppler recording.

The calibrated pulse tracing and Doppler velocity trace were then processed in specially designed computer software developed by the investigators. This software operates with a general program for handling digital ultrasound data (EchoDisp 5.0, Vingmed Sound). The data were low-pass filtered at 50 Hz with a sixth-order Butterworth filter and signal averaged. The calibrated pulse tracing was automatically corrected for pulse transmission time from the aortic root to the subclavian artery by aligning the pulse trace incisura with end-systole on the Doppler recording. The cardiovascular parameters were then determined without further observer interaction.

From the calibrated pulse tracing, mean systolic pressure was determined as the pressure integral over systole, end-systolic pressure was determined at the incisura, and mean arterial pressure as the pressure integral over the total cardiac cycle.

Instantaneous volume flow was obtained as the product of the Doppler time-velocity integral and aortic annular cross-sectional area. An example of signal-averaged pressure and flow estimates is shown in Figure 2.

LV ejection time was determined from the beginning of blood flow to the valve closure click on the Doppler velocity trace and corrected for heart rate by dividing with the square root of cardiac cycle length.[15] Stroke volume was determined as the integral of the volume flow curve, and cardiac output was obtained as the product of stroke volume and heart rate. Corresponding indexes were calculated by dividing with body surface area.[16] Total peripheral resistance was obtained as the mean arterial pressure over cardiac output, multiplied by 80 for unit conversion.[17]

The parameters of the 3-element windkessel model[18] of the systemic arterial tree (Figure 3) were estimated by using a refined mathematic procedure (see Appendix). Briefly, all pressure and flow data points throughout the cardiac cycle were used in the estimation, and the difference between the calibrated pulse tracing and model-estimated pressure curve was minimized with a nonlinear algorithm. In this model, peripheral resistance represents peripheral arteriolar resistance, and arterial compliance represents total compliance of the systemic arterial tree, whereas characteristic impedance represents proximal arterial (i.e., aortic) compliance.

LV external total power, steady power and oscillatory power were determined from the estimates of instantaneous aortic root pressure and flow,[12] and percent os-

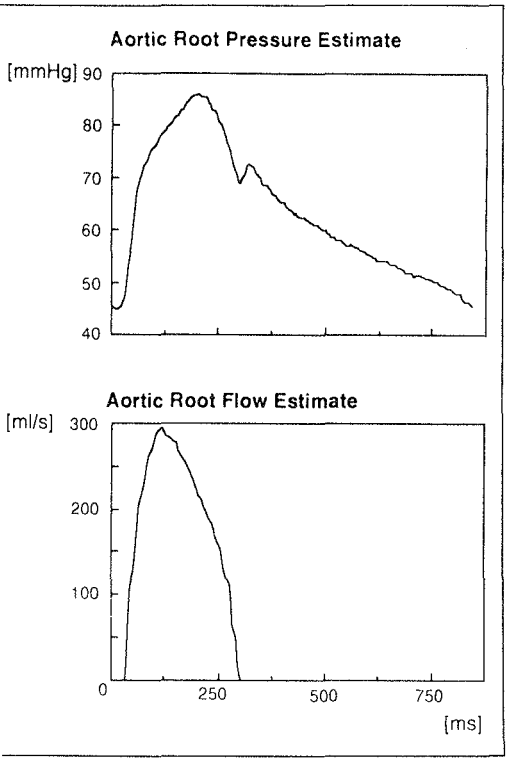

FIGURE 2. Computer-processed and signal-averaged estimates of aortic root pressure *(top)* and flow *(bottom)*, derived from 5 consecutive cardiac cycles comprising simultaneously recorded external pulse tracing and aortic annulus blood flow velocities (Doppler). Pressure curve was calibrated with systolic and diastolic brachial artery pressures (oscillometric method) and corrected for pulse transmission time by aligning end-systolic pulse trace incisura with valve closure click signal on Doppler recording. Instantaneous volume flow was obtained as product of blood flow velocities and annulus cross-sectional area.

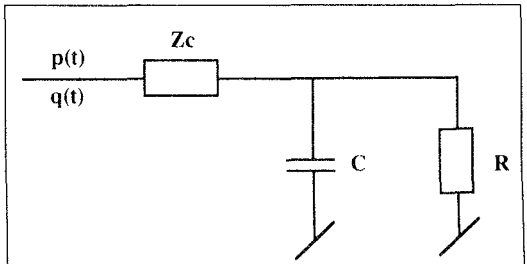

FIGURE 3. Electric equivalent of 3-element windkessel model of systemic arterial tree. Input variables are aortic root pressure (p[t]) and flow (q[t]) as functions of time. Parameters estimated from model are peripheral resistance (R), total arterial compliance (C) and characteristic impedance (Zc). See Appendix for details regarding estimation procedure.

TABLE II Group Results for Standard Hemodynamics

Variable	Group A	Group B	Group C
Systolic pressure (mm Hg)	110 ± 15	100 ± 17	114 ± 21
Mean systolic pressure (mm Hg)	92 ± 13	86 ± 14	95 ± 17
End-systolic pressure (mm Hg)	94 ± 15	88 ± 16	99 ± 17
Diastolic pressure (mm Hg)	64 ± 11	59 ± 10	65 ± 10
Mean arterial pressure (mm Hg)	85 ± 13	77 ± 13	85 ± 14
Heart rate (beats/min)	63 ± 11	59 ± 9	56 ± 13
Aortic annulus diameter (cm)	2.41 ± 0.16	2.15 ± 0.13*	2.13 ± 0.13*
Doppler time-velocity integral (cm)	21 ± 3	20 ± 3	21 ± 2
LV ejection time, rate-corrected ($ms^{1/2}$)	301 ± 20	299 ± 19	295 ± 32
Stroke index (cm^3/m^2)	50 ± 11	39 ± 6*	39 ± 4*
Cardiac index ($L/min/m^2$)	3.1 ± 0.6	2.2 ± 0.3*	2.1 ± 0.4*
Total peripheral resistance (dynes s cm^{-5})	1,202 ± 213	1,502 ± 278*	1,710 ± 276*

*$p < 0.05$ versus group A.
Values are group means ± SD.
LV = left ventricular.

TABLE III Group Results for Noninvasive Estimates of Three-Element Windkessel Model Parameters and Left Ventricular (LV) External Power

Variable	Group A	Group B	Group C
Peripheral resistance (dynes s cm^{-5})	1,124 ± 200	1,411 ± 273*	1,599 ± 249*
Arterial compliance (cm^3/mm Hg)	2.10 ± 0.59	1.80 ± 0.39	1.69 ± 0.66
Characteristic impedance (dynes s cm^{-5})	79 ± 25	92 ± 23	114 ± 37*
LV total power (mW)	1,303 ± 373	873 ± 294*	938 ± 283*
LV steady power (mW)	1,102 ± 330	732 ± 259*	767 ± 239*
LV oscillatory power (mW)	202 ± 53	141 ± 48*	171 ± 56
Percent oscillatory power (%)	16 ± 3	17 ± 3	18 ± 4

*$p < 0.05$ versus group A.
Values are group means ± SD.

latory power was calculated as oscillatory/total power 100. LV total power represents the energy loss during nsport of blood from the left ventricle to the tissues, l can be expressed as the sum of the steady and os- latory powers, where the former represents energy s at mean pressure and flow, and the latter represents ergy loss in arterial pulsations.

Reproducibility: The reproducibility study com- sed 20 subjects (group A: 6 subjects; B: 12; and C: Two investigators participated in the study. One in- stigator recorded the external pulse tracing and bra- al arterial blood pressures, and the other performed nocardiography. Immediately after this, the 2 investi- ors changed tasks and repeated the recordings with- t knowledge of the results obtained by the other. The cordings were completed within 1 hour. Thus, 40 ex- inations were performed in 20 subjects. For assess- nt of reproducibility of the recording technique (in- examiner reproducibility), the 40 examinations were alyzed blindly by 1 investigator. For assessment of re- oducibility of interpretation (interanalyzer repro- cibility), either the first or second examination for ch of the 20 patients was randomly selected for blind- analysis by both investigators.

Statistical analysis: All group characteristics are esented as mean ± SD. Comparisons between the oups were performed with 1-factor analysis of vari- ce (Fisher test) and nonparametric 2-tailed Mann- hitney U test, both with the level of significance set 0.05. The mean absolute interexaminer and interana- zer differences were determined with SDs. The coeffi- nt of repeatability was determined as 1.96 times the D of the differences between the investigators; it indicates the upper limit for 95% of the differences.[19] The coefficient of variation was determined for each parameter as the SD for the differences between the investigators over the mean of their results. Agreement between the 2 investigators' recordings was further assessed by plotting the differences between the 2 against their average for each parameter.[19]

RESULTS

Group characteristics (Tables II and III): There were no significant group differences for either aortic root pressure estimates, heart rate, time-velocity integral or LV ejection time. The aortic annulus diameter was smaller in groups B and C than in A. Stroke and cardiac indexes were both significantly less in groups B and C than in A. Total peripheral resistance, as determined from mean arterial pressure and cardiac output, was greater in groups B and C than in A. Similar group differences were found for the estimated peripheral resistance of the windkessel model (Table III and Figure 4). There were no significant group differences in the model estimates of total arterial compliance, whereas the characteristic impedance of group C was significantly greater than that of A. LV total and steady power were less in both groups B and C than in A. Oscillatory power was less in group B than in A. However, there was no difference between the groups in oscillatory power in relation to total power (percent oscillatory power). The pulse transmission time from the aortic root to the subclavian artery was equal in the 3 groups (range 15 to 35 ms for all subjects). The statistical significance of group differences was equally confirmed by the parametric and nonparametric tests.

TABLE IV Reproducibility of Noninvasive Cardiovascular Parameters

Variable	Interexaminer		Interanalyzer	
	CR	CV	CR	CV
Systolic pressure (mm Hg)	12	5.7	—	—
Mean systolic pressure (mm Hg)*	8	4.4	2	1.1
End-systolic pressure (mm Hg)*	12	6.7	2	1.1
Diastolic pressure (mm Hg)	10	8.1	—	—
Mean arterial pressure (mm Hg)*	8	5.0	2	1.3
Heart rate (beats/min)	6	5.0	0	0.0
Aortic annulus diameter (cm)	0.18	4.1	—	—
Doppler time-velocity integral (cm)	4	10.3	2	4.8
LV ejection time (ms)	14	2.3	16	2.6
Stroke index (cm^3/m^2)	10	12.2	2	2.3
Cardiac index ($L/min/m^2$)	0.61	12.7	0.18	3.5
Total peripheral resistance (dynes s cm^{-5})	310	10.8	90	3.3
Peripheral resistance (dynes s cm^{-5})*	300	11.2	82	3.2
Arterial compliance (cm^3/mm Hg)*	0.8	20.2	0.25	5.9
Characteristic impedance (dynes s cm^{-5})*	33	17.1	16	9.0
Total power (mW)*	259	13.3	73	3.5
Steady power (mW)*	223	13.8	63	3.6
Oscillatory power (mW)*	57	16.9	20	5.8
Percent oscillatory power (%)*	4	11.4	2	5.9

Interexaminer reproducibility determined from 2 investigators' independent examinations of 20 subjects (*n = 18). Interanalyzer reproducibility determined from 2 investigators' independent interpretations of 20 examinations (*n = 18).
CR = coefficient of repeatability; CV = coefficient of variation (%); LV = left ventricular.

Reproducibility (Table IV): In 2 subjects, the pulse trace quality was suboptimal. Thus, for parameters based on the calibrated pulse trace, the reproducibility study comprised 18 subjects. For recording, the best reproducibility was found for the aortic root pressure estimates, heart rate, aortic annulus diameter and LV ejection time. Reproducibility for recording was less good for the Doppler time-velocity integral and thus not so good for the derived parameters (stroke and cardiac indexes, windkessel model parameters and LV power estimates) where the coefficient of variation was ≥10%. The differences between the examiners were evenly distributed over the range of measurements as shown for windkessel parameters in Figure 5.

The reproducibility for interpretation (interanalyzer reproducibility) was generally better than that of recording, with a coefficient of variation ≤9%.

DISCUSSION

This study shows that aortic root pressure and flow estimates can be obtained noninvasively in the acute and chronic stage of myocardial infarction. Thus, important parameters of LV function and systemic arterial properties, otherwise only obtainable by invasive procedures, can be assessed rapidly without discomfort or risk, and there is no need for sedatives during the examination.

We compared cardiovascular parameters of patients with recent and healed myocardial infarction with those of normal subjects. The compromised myocardium and the general use of β-blocking agents of patients in groups B and C were probably the reasons for the reduced stroke and cardiac indexes, and the increased peripheral resistance.

Windkessel model parameters: The windkessel model provides a simplified but valuable description of the systemic arterial tree.[18,20,21] The appropriateness of the model can be assessed by its ability to predict input measurements. However, for perfect agreement between the measured and model-generated pressures, a more detailed description of the systemic arterial tree than that of the 3-element windkessel model is necessary. Despite this, we found good agreement between the calibrated pulse trace and the model-generated pressure curve in most study subjects (Figure 6). Furthermore, the estimation of the windkessel models is simpler and faster,

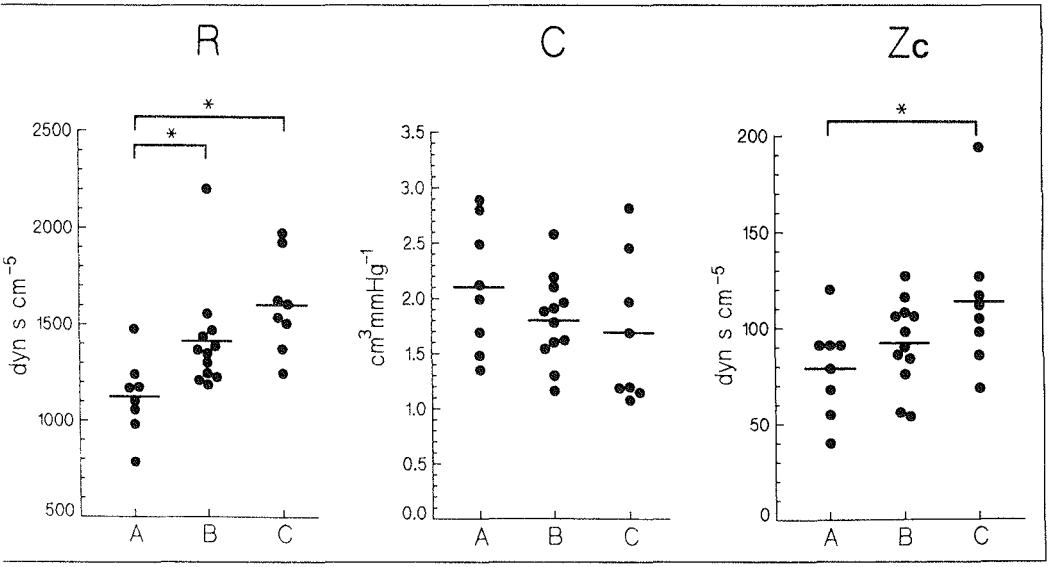

GURE 4. Plots of individual data for peripheral resistance (R), total arterial compliance (C) and characteristic impedance (c) in groups A, B and C. *Horizontal lines* represent group means, and *asterisks* denote significant differences between *oss-bar connected* groups with p <0.05.

l also less sensitive to measurement noise than that more complicated models; thus, it may be more fea- le for clinical use.

By using a windkessel model, we identified greater ipheral resistance in groups B and C than in A, and ater characteristic impedance in C. This indicates that h groups B and C had increased peripheral arteriolar e, whereas only C had increased aortic stiffness. Be- ıse patients in group C were not older than those in this cannot be explained by differences in age. The)lanation may be found in differences in sympathetic ·vous system activity[22] between groups B and C. The fer aorta in group C patients represents an increased istance to LV ejection and may adversely affect LV ·formance.

Left ventricular external power: The external power)ends both on LV performance and systemic arterial)perties. Therefore, the lower LV power in groups B l C were related to the reduced cardiac performance e to myocardial infarction and β-blocking agents. In)up C, the reduced cardiac performance more than ınterbalanced the increased characteristic impedance t otherwise would have increased LV external power. nilar results have been obtained from invasive data in ients with coronary artery disease.[23] Because percent :illatory power depends mainly on the aortic proper- s, one would expect it to be higher in patients with eater characteristic impedance; however, we found no)up differences for this parameter.

Comparison with invasive studies: Our estimates characteristic impedance in healthy subjects compare ll with results obtained with Fourier analysis of inva- e pressure and flow data.[24,25] Lower values have been tained in younger subjects,[26] in accordance with the ding that characteristic impedance increases with age.[27] r estimates of total arterial compliance in healthy sub- ts agree with those of investigators using the same ndkessel model on invasive data,[28] whereas lower val- s were obtained with the 2-element model.[29] This is not rprising, because the 2-element model has been shown produce consistently lower estimates for total arterial mpliance than does the 3-element model.[28]

Methodologic considerations: The measured brachi- arterial systolic and diastolic pressures were used to ibrate the subclavian arterial pulse trace. As the arte- l pressure pulse travels from the central aorta to the ripheral vessels, the waveform changes so that peak stolic pressure increases and nadir diastolic pressure creases.[30] By assuming that mean arterial pressure can expressed as the sum of diastolic pressure and one rd of pulse pressure, it can be shown that a 10% error either peak systolic or nadir diastolic pressure will ıse approximately a 4 or 7% error, respectively, in the imates of total peripheral resistance. A 10% error in ean arterial pressure produces a 10% error in the arte- l compliance estimate. With oscillometric measure- ents of brachial artery blood pressure, smaller devia- ns from aortic root pressures can be expected,[9,31] and e errors in model estimates may thus be smaller than se values.

Because all subjects were examined in a slightly left eral position, we did not correct for the hydrostatic ef- fect of the vertical difference between the cuff and aortic root. However, this can be performed by adding 0.7 mm Hg to the measured pressure for each centimeter the cuff is positioned above the aortic root.

The aortic annulus diameter is a critical measurement in the determination of volume flow because it is squared during calculations. A 10% error in the diameter will produce a 21% error in the flow estimates, and equivalent errors will occur in the parameters derived from the flow estimates. However, when the method is used for repeated studies, and the same annulus diameter can be used for each assessment, the variability of the derived parameters will be significantly reduced; then, the Doppler aortic annulus flow becomes the most critical recording. The velocity profile at the aortic annulus is slightly skewed with greater velocities toward the septum.[32] Therefore, Doppler recording in this region can lead to overestimation of blood flow. However, by positioning the sample volume in the center of

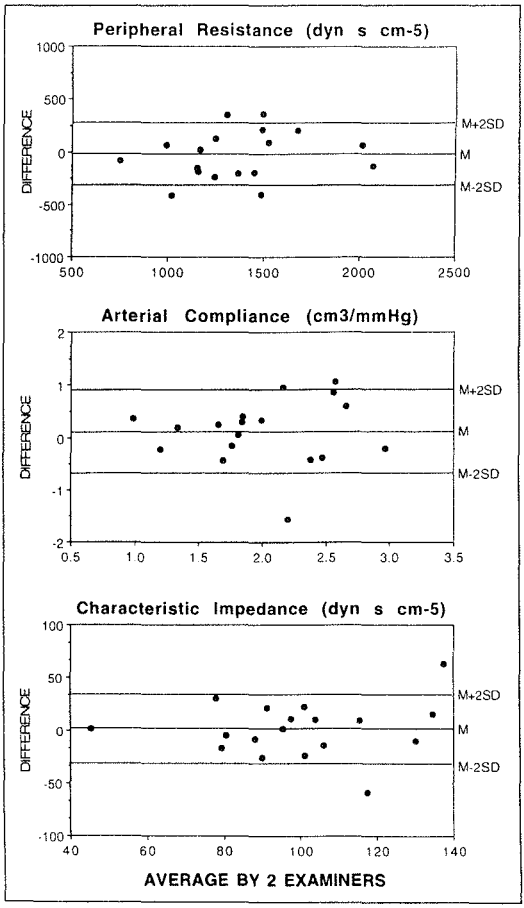

FIGURE 5. Interexaminer reproducibility for 3-element windkessel parameters. Parameters were obtained from 2 independent and consecutive noninvasive examinations of 18 subjects by 2 investigators. Absolute differences between 2 examiners *(ordinates)* are plotted against average values *(abscissas). Horizontal lines* indicate mean difference (M) ± 2 SD.

annulus, and the ultrasound beam in the direction of LV outflow, good estimates of mean velocities can be obtained.[32]

The estimates of windkessel model parameters and LV external power had a relatively low reproducibility for recording. For example, when characteristic impedance and arterial compliance are assessed in 1 subject by 2 investigators, differences ≤33 dynes s cm^{-5} and ≤0.8 cm^3/mm Hg, respectively, can be due to the variability in recording (Table IV). Thus, for repeated assessments of these parameters in a given subject, recordings should preferably be obtained by the same investigator. The reproducibility was generally good for analysis. Therefore, analysis of the pressure and flow data can be performed by different investigators.

Finally, the presented method relies on a regular cardiac rhythm. The averaged pressure and flow data cannot represent the beat-to-beat variation of pressure and flow that is frequently observed during arrhythmias. Furthermore, the oscillometric method of blood pressure measurement is less reliable during arrhythmias.

Clinical implications: This study presents a noninvasive method that is clinically feasible in most patients with regular heart rhythm and normal aortic valves. Important parameters of LV function and systemic arterial properties, which are otherwise only obtainable by invasive procedures, can rapidly be determined. However, special attention should be given to obtain correct measurements of aortic annulus diameter and blood flow velocities. The method is suitable for noninvasive monitoring of patients with various acute and chronic cardiovascular disorders including ischemic heart disease, congestive heart failure, cardiomyopathies and hypertension. Hemodynamic alterations during surgery, dialysis or treatment with pharmacologic agents can be detected early and defined.

APPENDIX

Estimation of the parameters of the three-element windkessel model: The electric equivalent of the model is shown in Figure 3.

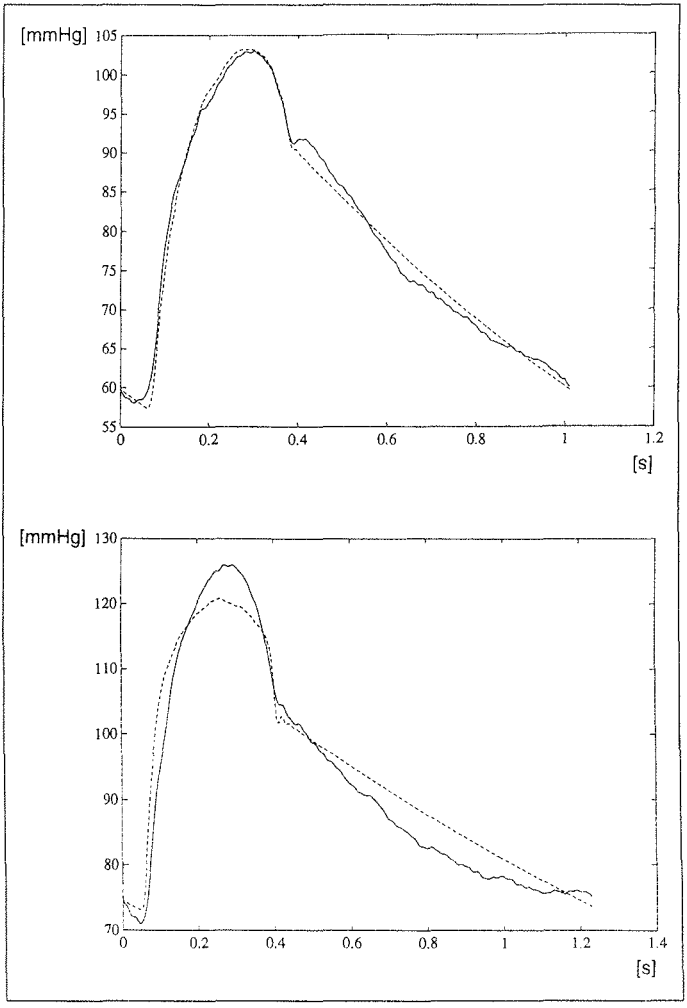

FIGURE 6. Comparison of calibrated subclavian artery pulse trace *(continuous lines)* and corresponding pressure curve generated from parameters of 3-element windkessel model *(dashed lines)* in 2 subjects. *Top panel* shows subject with best agreement between measured and generated pressure curves, whereas *bottom panel* shows subject with lowest agreement. In most cases, we found good agreement between calibrated pulse trace and model-generated pressure curve. As both cases show, measured pressure curve often deviates from exponential diastolic decay of model.

he model equations are:

$$\frac{dp_a(t)}{dt} = -\frac{1}{RC}p_a(t) + \frac{1}{C}q(t)$$

$$p(t) = p_a(t) + Z_c q(t)$$

re R is the peripheral resistance, C is the total arte- compliance, and Z_c is the aortic characteristic im- ance. p(t) is aortic pressure, and q(t) is aortic flow, as functions of time (t). p_a is the pressure reduc- over R and C.

he general solution to these equations is:

$$= e^{-(t-t_0)/T}\left\{p_a(t_0) + \frac{1}{C}\int_{t_0}^{t} e^{-(t_0-\tau)/T} q(\tau)\, d\tau\right\} + Z_c q(t) \quad (1)$$

re $T = RC$.

Letting $t = t_0 = 0$ at end-diastole, we obtain:

$$p(t) = e^{-t/T}\left\{P_d + \frac{1}{C}\int_0^t e^{\tau/t} q(\tau)\, d\tau\right\} + Z_c q(t) \quad (2)$$

re we note that $p(0) = p_a(0) = P_d$, because $q(0) = 0$. 3y finding the discrete form of the differential equa- , we can get a set of equations that are linear in their meters.

f we assume that q(t) is constant for the interval $_{k+1}\}$, we can solve the integral of the general solu- (equation 1) and get:

$$p_{k+1} = \alpha p_k + \left\{\frac{T}{C}(1-\alpha) - \alpha Z_c\right\} q_k + Z_c q_{k+1} \quad (3)$$

re $\alpha = e^{-\frac{h}{T}}$, and $h = t_{k+1} - t_k$.

Using least-squares method on this system, we get nates for R, C, and Z_c.

The parameter estimates are further refined by using onlinear optimization algorithm, the Nelder-Meade plex algorithm. The estimation scheme is defined as ows: (1) The parameters being estimated are R and The initial estimates were calculated using the least- ares method on equation 3. (2) The aortic character- impedance is calculated by using the principle of erial balance:

$$Z_c = \frac{\int_{RR} p(\tau)\, d\tau}{\int_S q(\tau)\, d\tau} - R$$

ere RR denotes the total cardiac cycle and S the sys- . (3) The estimated pressure curve is determined n the general solution of the 3-element windkessel del as a function of the measurements P_d and q(t), the parameters R, C and Z_c, given by equation 2. Finally, the error of the estimated pressure is calcu- d as the quadratic sum of the differences between asured and estimated pressures, and minimized by ng the Nelder-Meade simplex algorithm.

normal conditions and in simulated arterial disease. *Cardiovasc Res* 1967;1:313–326.

2. Milnor WR. Arterial impedance as ventricular afterload. *Circ Res* 1975;36: 565–570.

3. Robinson B. The carotid pulse II: relation of external recordings to carotid, aortic, and brachial pulses. *Br Heart J* 1963;25:61–68.

4. Martin CE, Shaver JA, Thompson ME, Reddy PS, Leonard JJ. Direct correlation of external systolic time intervals with internal indices of left ventricular function in man. *Circulation* 1971;44:419–431.

5. Van De Werf F, Piessens J, Kesteloot H, De Geest H. A comparison of systolic time intervals derived from the central aortic pressure and from the external carotid pulse tracing. *Circulation* 1975;51:310–316.

6. Colan SD, Borow KM, MacPherson D, Sanders SP. Use of the indirect axillary pulse tracing for noninvasive determination of ejection time, upstroke time, and left ventricular wall stress throughout ejection in infants and young children. *Am J Cardiol* 1984;53:1154–1158.

7. Colan SD, Borow KM, Neumann A. Use of the calibrated carotid pulse tracing for calculation of left ventricular pressure and wall stress throughout ejection. *Am Heart J* 1985;109:1306–1310.

8. Kelly R, Karamanoglu M, Gibbs H, Avolio A, O'Rourke M. Noninvasive carotid pressure wave registration as an indicator of ascending aortic pressure. *J Vasc Med Biol* 1989;1:241–247.

9. Colan SD, Fujii A, Borow KM, MacPherson D, Sanders SP. Noninvasive determination of systolic, diastolic and end-systolic blood pressure in neonates, infants and young children: comparison with central aortic pressure measurements. *Am J Cardiol* 1983;52:867–870.

10. Aakhus S, Torp H, Haugland T, Hatle L. Noninvasive estimates of aortic root pressures: External subclavian arterial pulse tracing calibrated by oscillometrically determined brachial arterial pressures. *Clin Physiol* (in press).

11. Skjaerpe T, Hegrenaes L, Ihlen H. Cardiac output. In: Hatle L, Angelsen BA, eds. Doppler Ultrasound in Cardiology. Philadelphia: Lea & Febiger, 1985:306–320.

12. Spencer KT, Lang RM, Neumann A, Borow KM, Shroff SG. Doppler and electromagnetic comparisons of instantaneous aortic flow characteristics in primates. *Circ Res* 1991;68:1369–1377.

13. Erbel R, Schweizer P, Herm G, Mayer J, Effert S. Apical 2-dimensional echocardiography: Normal values for single and bi-plane determination of left ventricular volume and ejection fraction. *Dtsch Med Wochenschr* 1982;107:1872–1877.

14. Schiller NB, Shah PM, Crawford M, deMaria A, Devereux R, Feigenbaum H, Gutgesell H, Reichek N, Sahn D, Schnittger I, Silverman NH, Tajik AJ. Recommendations for quantitation of the left ventricle by two-dimensional echocardiography. *J Am Soc Echocardiogr* 1989;2:358–367.

15. Tavel ME. Clinical Phonocardiography and External Pulse Recording. Chicago: Year Book Medical Publishers, 1978:50.

16. Du Bois D, Du Bois E. A formula to estimate the approximate surface area if height and weight be known. *Arch Intern Med* 1916;17:863–871.

17. Stefadouros MA, Dougherty MJ, Grossman W, Craige E. Determination of systemic vascular resistance by a noninvasive technic. *Circulation* 1973;47:101–107.

18. Westerhof N, Elzinga G, Sipkema P. An artificial arterial system for pumping hearts. *J Appl Physiol* 1971;31:776–781.

19. Bland JM, Altman DG. Statistical methods for assessing agreement between two methods of clinical measurement. *Lancet* 1986:1:307–310.

20. Burkhoff D, Alexander J, Schipke J. Assessment of windkessel as a model of aortic input impedance. *Am J Physiol* 1988;255:742–753.

21. Laskey WK, Parker G, Ferrari VA, Kussmaul WG, Noordergraaf A. Estimation of total systemic arterial compliance in humans. *J Appl Physiol* 1990;69:112–119.

22. Cohn JN. Nervous system control mechanisms in heart failure. *Acta Med Scand* 1986:219:15–20.

23. Nichols WW, Conti CR, Walker WE, Milnor WR. Input impedance of the systemic circulation in man. *Circ Res* 1977;40:451–458.

24. Laskey WK, Kussmaul WG, Martin JL, Kleaveland JP, Hirshfeld JW, Shroff S. Characteristics of vascular hydraulic load in patients with heart failure. *Circulation* 1985;72:61–71.

25. Ting CT, Brin KP, Lin SJ, Wang SP, Chang MS, Chiang BN, Yin FCP. Arterial hemodynamics in human hypertension. *J Clin Invest* 1986;78:1462–1471.

26. Murgo JP, Westerhof N, Giolma JP, Altobelli SA. Effects of exercise on aortic input impedance and pressure wave forms in normal humans. *Circ Res* 1981; 48:334–343.

27. Nichols WW, O'Rourke MF, Avolio AP, Yaginuma T, Murgo JP, Pepine CJ, Conti CR. Effects of age on ventricular-vascular coupling. *Am J Cardiol* 1985;55: 1179–1184.

28. Laskey WK, Parker G, Ferrari VA, Kussmaul WG, Noordergraaf A. Estimation of total systemic arterial compliance in humans. *J Appl Physiol* 1990;69:112–119.

29. Simon AC, Safar ME, Levenson JA, London GM, Levy BI, Chau NP. An evaluation of large arteries compliance in man. *Am J Physiol* 1979;237:550–554.

30. Nichols WW, O'Rourke MF. McDonald's Blood Flow in Arteries. 3rd ed. London: Edward Arnold, 1990:216–250.

31. Borow KM, Newburger JW. Noninvasive estimation of central aortic pressure using the oscillometric method for analyzing systemic artery pulsatile blood flow: comparative study of indirect systolic, diastolic, and mean brachial artery pressure with simultaneous direct ascending aortic pressure measurements. *Am Heart J* 1982;103:879–886.

32. Rossvoll O, Samstad S, Torp HG, Linker DT, Skjaerpe T, Angelsen BAJ, Hatle L. The velocity distribution in the aortic anulus in normal subjects: a quantitative analysis of two-dimensional Doppler flow maps. *J Am Soc Echocardiogr* 1991;4: 367–378.

Paper III.

Aakhus S, Bjoernstad K, Jørstad S. Systemic cardiovascular response in hemodialysis without and with ultrafiltration with membranes of high and low biocompatibility. Blood Purification 1995;13:229-240.

. Henderson, McGaw Park, Ill.

print
lisher: S. Karger AG, Basel
ted in Switzerland

Original Paper

Blood Purif 1995;13:229–240

Svend Aakhus[a]
Knut Bjoernstad[a]
Størker Jørstad[b]

Sections of
[a] Cardiology and
[b] Nephrology, Department of Medicine, University Hospital of Trondheim, Norway

Systemic Cardiovascular Response in Hemodialysis without and with Ultrafiltration with Membranes of High and Low Biocompatibility

Key Words
Hemodialysis
Membrane biocompatibility
Ultrafiltration
Systemic hemodynamics
Echocardiography
Noninvasive method

Abstract

In order to test whether dialyzer membrane biocompatibility influences systemic cardiovascular function, we treated 8 hemodialysis patients (4 men and 4 women, aged 24–73 years) with a low-biocompatible (cuprophane) and a high-biocompatible (polyacrylonitrile) membrane in a randomized double-blind crossover protocol using bicarbonate hemodialysis without ultrafiltration for the first 60 min and with ultrafiltration for the remaining treatment time. Left ventricular function and systemic hemodynamics were assessed noninvasively at baseline and during treatment by Doppler echocardiography combined with external subclavian artery pulse trace calibrated with oscillometrically measured brachial artery blood pressures. There was no significant difference in the cardiovascular response to the 2 membranes, neither during isolated hemodialysis nor when ultrafiltration was added. Mean arterial pressure increased 10% ($p < 0.001$) during isolated hemodialysis and returned to baseline levels with ultrafiltration. The cardiac index decreased 22% ($p < 0.001$) during ultrafiltration, due to the greater decrease in left ventricular stroke index (30%, $p < 0.001$) than increase in heart rate (9%, $p < 0.05$). Total peripheral resistance increased 10% ($p < 0.05$) during isolated hemodialysis and a further 19% ($p < 0.01$) when ultrafiltration was added. Hence, profound cardiovascular alterations were observed during hemodialysis treatment; however, these changes were not related to the biocompatibility of the membranes.

Accepted:
May 27, 1994

Svend Aakhus, MD
Medical Department B
Section of Cardiology
Rikshospitalet, The National Hospital

0253–5068/95/
0135–0229$8.00/0

Table 1. Patient characteristics

Patient	Age years	Sex	Primary disease	SBP/DBP
1	24	F	oxaluria	105/60
2	42	M	polycystic kidney disease	139/83
3	49	F	chronic glomerulonephritis	163/99
4	62	M	retroperitoneal fibrosis	181/72
5	64	M	renal carcinoma	111/56
6	67	F	diabetes	175/64
7	73	M	chronic glomerulonephritis	147/74
8	73	F	rheumatoid arthritis	169/78

SBP/DBP = Systolic/diastolic blood pressure at baseline of first treatment (mm Hg).

Introduction

Hemodynamic instability is a major prob-
n in hemodialysis treatment and has a mul-
actorial etiology [1–4]. The biocompatibili-
of the dialyzer membrane has an important
pact on circulatory parameters during he-
odialysis, and membranes with low biocom-
tibility are associated with leukopenia [5–
, thrombocytopenia [9], activation of the
mplement system [5–9], and hypoxemia [7,
]. Whether membrane biocompatibility
so influences hemodynamics during hemo-
alysis has not been settled [1–3, 11–12].
evious studies indicate that membranes
th low biocompatibility are associated with
evated pulmonary vascular resistance [7]
d may induce hemodynamic instability in
tically ill patients [13] whereas stable he-
odialysis patients seem to be less influenced
14, 15]. However, the hemodynamic in-
ence of bioincompatibility during hemodi-
sis may be confounded by the concomitant
culatory responses to volume depletion (i.e.
rafiltration) [16, 17] and dialysis buffer
mposition [18].

The present noninvasive study was de-
ned to assess the effects of membrane bio-compatibility on left ventricular function and systemic hemodynamics during a bicarbonate hemodialysis protocol that allowed separation of dialysis without and with ultrafiltration.

Methods

Study Subjects

Eight patients (4 men and 4 women), aged 24–73 years on regular hemodialysis with 3 treatments per week, gave informed consent to participate in the study. None had clinically significant valvular heart disease, neck vessel bruit or severely impaired left ventricular function (ejection fraction below 40%), and all were in sinus rhythm. Two patients had coronary artery disease, identified on stress echocardiography, and 1 had diabetes. Table 1 gives additional patient data. Three patients (subjects 1, 2 and 3) were in hemodialysis due to allograft rejection. Calcium antagonists were taken by 4 patients, nitrates by 2, loop diuretics by 2, ACE inhibitor by 1 and β-blocker by 1. Medication was continued throughout the study.

Dialysis Protocol

Each patient was treated with both a low biocompatible cuprophane membrane (AM–65H-SD; Asahi Medical Co., Ltd., Tokyo, Japan) and a high biocompatible polyacrylonitrile membrane [Filtral 12 (AN69HF); Hospal, Nürnberg, Germany] in a randomized, double-blinded crossover protocol. The patients were randomized to first treatment with either a cupro-

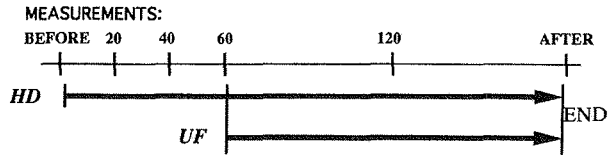

Fig. 1. Treatment protocol. Figures indicate total treatment time in minutes. Hemodialysis (HD) was performed throughout the treatment, whereas ultrafiltration (UF) was started after 60 min of hemodialysis and continued to the end of treatment (END). The total treatment time averaged for both membranes was 4.2 h. Data were obtained before the start of hemodialysis, then at 20, 40 and 60 minutes after the start of hemodialysis, and after 60 min of combined hemodialysis and ultrafiltration, and finally immediately after the end of treatment.

ane or polyacrylonitrile membrane, and the mem-ane identity was hidden from the patient and investi-tors by a covering. Randomization and blinding were rformed by personnel not participating in the data quisition. The 2 treatments were given within 2 eks, and on the same weekday intentionally matched blood flow rate, ultrafiltration rate and treatment ne. The dialyzer membranes had a similar surface ea and priming volume. All treatments were given on olume-guided machine allowing separation of hemo-lysis without and with ultrafiltration (Miro-clav; alyse-Technik, Ettlingen, Germany). Hemodialysis thout ultrafiltration (isolated hemodialysis) was per-med during the first hour of treatment and ultrafil-tion added thereafter. Bicarbonate buffer with a tem-rature of 37.0 °C was used during all procedures with otassium concentration of 2.0 mmol/l in 7 patients d 3.5 mmol/l in 1. Chloride was 106.5 mmol/l in the v-potassium and 108.0 mmol/l in the high-potassium ffer. Other constituents of the buffers were equal: lium 139 mmol/l, calcium 1.75 mmol/l, magnesium mmol/l, bicarbonate 33.2 mmol/l and acetate mmol/l. Vascular access was via an arteriovenous ula on the forearm in 15 of the treatments and a cen-l venous catheter in 1. Any intradialytic hypotension s to be treated with head-down tilting of the chair d infusion of 100 cm^3 10% saline.

Data Acquisition

Baseline hemodynamic data were recorded imme-tely before the extracorporeal circulation was estab-lished and the patient was connected to the dialyzer, then the recordings were repeated 20, 40, 60 and 120 min after the start of treatment and finally immediately before emptying of the dialyzer (fig. 1).

Arterial blood samples for routine analysis of hematocrit, white blood cell count (Coulter Counter; Coulter Corporate Communications, Hialeah, Fla., USA), serum sodium and bicarbonate (Greiner 450; Greiner Instruments AG, Langenthal, Switzerland) and blood gas (IL1302; Instrumentation Laboratories, Milano, Italy) were obtained simultaneously with hemodynamic data, except the 40-min measurement. Total protein, albumin, creatinine, urea (Greiner 450) and osmolality (Micro-osmometer; Labex AB, Helsingborg, Sweden) were measured immediately before and after treatment.

Noninvasive Assessment of Cardiovascular Function

At each measurement point, the patients were examined in the left lateral decubitus position after horizontal resting for at least 5 min. The setup has been described in detail elsewhere [19] and comprises the combined use of an ultrasound scanner (CFM 750; Vingmed Sound, Horten, Norway) with a duplex probe for echocardiographic imaging (3.25 MHz) and Doppler flow velocity recording (2.5 MHz), external tracing of the subclavian artery pulse and oscillometric measurement of the brachial artery pressures. The scanner was interfaced to a computer (Macintosh II series; Apple Computers, Cupertino, Calif., USA) for transfer

ligital ultrasound data and pulse tracing. The analog nals were converted to digits at 200 Hz.

Midventricular short-axis images of the left ventri- were recorded from the parasternal position and nsferred as cineloops (47 frames/s) to the computer. cineloop comprises sequential ultrasound images orded during 1 cardiac cycle. Left ventricular endo- dial borders were manually traced on the computer end-diastole (peak of R wave) and end-systole (last me before opening of mitral valve). The area within s short-axis (i.e. cross-sectional) endocardial trace s automatically determined, and the average left ntricular inner diameter was obtained as the diame- of the circle with the same area. Left ventricular ctional shortening was determined as the difference ween end-diastolic and end-systolic internal diame- s as a percent of the former [20].

Aortic annulus diameter was measured at the aortic ve leaflet insertion with the trailing-to-leading-edge thod. The average of 3 repeated measurements tained at baseline was used for calculation of annu- cross-sectional area, assuming a circular and con- nt orifice [21]. Aortic annulus blood flow velocities re recorded with pulsed Doppler sonography from apical position, and the ultrasound beam was gned with central blood flow direction and sample lume positioned at the aortic annular level. The sub- vian arterial pulse was noninvasively traced with an ernal pulse transducer (Irex 120–0132; Irex Medical stems, Ramsey, N.J., USA), coupled to a capillary mped funnel (Siemens-Elema AB, Solna, Sweden) ich was manually positioned in the right supracla- ular region. For all examinations, Doppler echocar- graphy was performed by one investigator and the ernal pulse tracing by another. At least 5 cardiac les with simultaneously recorded pulse tracing, ppler flow velocities and a lead III electrocardio- m were then transferred to the computer for analy- Brachial artery blood pressures were obtained with oscillometric manometer (UA 751; Takeda Medical ., Tokyo, Japan), and the average of 2 consecutive asurements, with less than 10 mm Hg difference d obtained with the Doppler flow velocity recording, s used in subsequent calculations.

At least 3 cardiac cycles with adequate subclavian ery pulse tracing and Doppler signals were selected analysis. The pulse tracing was calibrated with the illometrically determined systolic and diastolic bra- al artery pressures in order to obtain estimates for tic root pressure [22]. The Doppler time-velocity egral was determined on the computer by manual cing of peak velocities during systole and at the zero e in diastole, and end-systole was defined at the aor-

Table 2. Treatment characteristics

	CUP	PAN
Treatment time, h	4.3±0.7	4.1±0.8
Ultrafiltrate, liters	2.6±0.8	2.9±0.7
QB, ml/min	224±39	236±26
Weight loss, kg	2.2±0.7	2.1±0.7

Values are means ± SD. CUP = Cuprophane; PAN = polyacrylonitrile; QB = blood flow rate. There was no significant difference of CUP versus PAN.

tic valve closure click. The calibrated pulse tracing and Doppler flow velocity trace were then processed in specially designed computer software where mean arterial pressure was estimated from the calibrated pulse trace, and aortic root volume flow determined as the product of the aortic annular Doppler time-velocity integral and cross-sectional area. Stroke volume was determined as the integral of the volume flow curve over the cardiac cycle, and cardiac output was calculated as the product of stroke volume and heart rate. Corresponding indexes were calculated by dividing with body surface area. Total peripheral resistance was obtained as mean arterial pressure over cardiac output. Rate-corrected left ventricular velocity of circumferential fiber shortening is regarded to be a preload-insensitive index of left ventricular contractility [23] and was determined as the product of the square root of cardiac cycle length and fractional shortening, divided by left ventricular ejection time.

Statistical Analysis

Continuous variables are presented as means ± SD (means ± SEM in figures). For each parameter the change from baseline was assessed with a paired 2-sided t test. Analysis of variance for repeated measurements (2-factor) was used to assess the independent influence of membrane ('between-factor') and treatment time ('within-factor'). A multivariate approach was used for complete data sets and a univariate one for incomplete data. The level of significance was set at 5%. Analysis of variance was carried out separately for hemodialysis without and with ultrafiltration. Standard statistical software (Statview 512/SuperAnova; Abacus Concepts, Berkeley, Calif., USA) was used for computations on a personal computer (Macintosh II series).

Table 3. Laboratory data

		Before	After
pH	CUP	7.40±0.02	7.46±0.03[a]
	PAN	7.40±0.03	7.47±0.02[a]
Base excess, mmol/l	CUP	0±1	5±1[a]
	PAN	0±2	6±1[a]
$PaCO_2$, kPa	CUP	5.1±0.4	5.4±0.4
	PAN	5.1±0.5	5.4±0.4
Bicarbonate, mmol/l	CUP	25±1	29±1[a]
	PAN	25±2	30±1[a]
PaO_2, kPa	CUP	13±1	13±4
	PAN	12±4	12±3
O_2 saturation, %	CUP	98±1	97±2
	PAN	96±4	97±1
Albumin, g/l	CUP	35±5	38±4[a]
	PAN	34±5	37±5
Total protein, g/l	CUP	66±6	77±7[a]
	PAN	65±6	76±6[a]
Hematocrit, %	CUP	31±5	35±6[a]
	PAN	31±3	35±5[a]
White blood cell count, $\times 10^9$/l	CUP	7.5±2.6	8.7±3.4
	PAN	8.8±3.8	7.7±3.4
Urea, mmol/l	CUP	22±4	8±2[a]
	PAN	21±4	7±2[a]
Creatinine, µmol/l	CUP	744±238	372±148[a]
	PAN	773±193	337±82[a]
Osmolality, mosm/kg	CUP	308±5	295±9[a]
	PAN	302±9	299±7
Sodium, mmol/l	CUP	135±6	139±4
	PAN	136±4	139±2

Values are means ± SD. CUP = Cuprophane; PAN = polyacrylonitrile; [a] $p < 0.05$, before versus after dialysis treatment. There was no significant difference of CUP versus PAN.

Results

On echocardiographic screening, 4 patients had thickening of one or more of the rtic cusps, neither with hemodynamic sigicance. One patient had a small amount of pericardial fluid. Treatment characteristics are given in table 2. There was no significant difference between the 2 membranes with respect to treatment time, ultrafiltration, blood flow rate or weight loss during treatment. Laboratory data are given in table 3. There

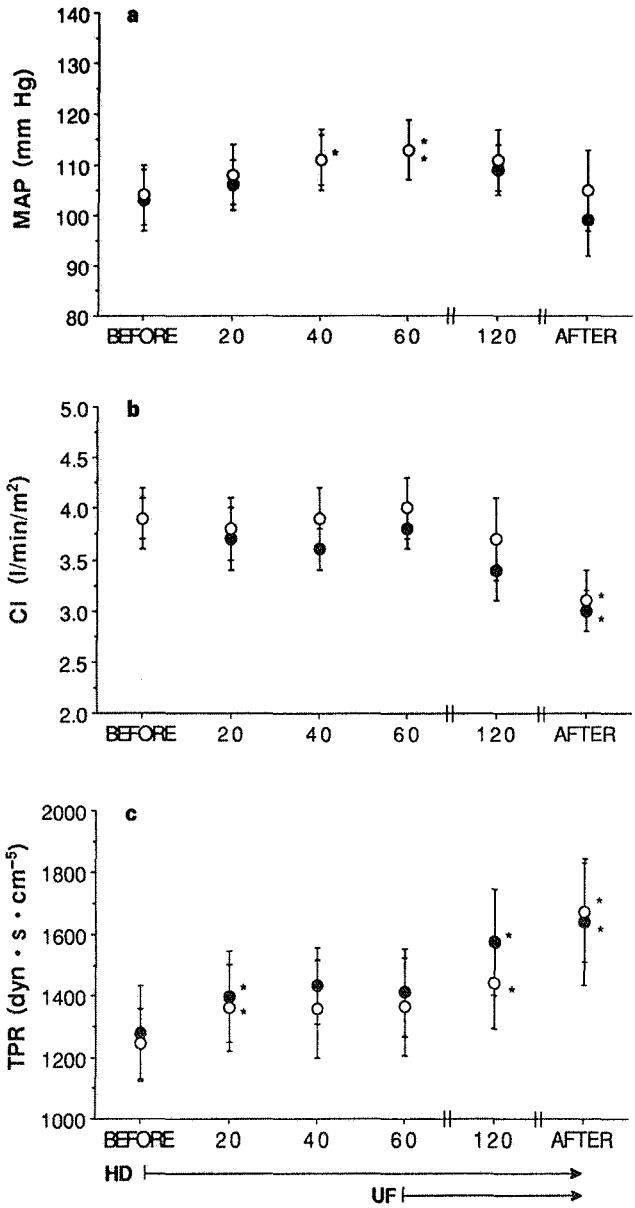

Fig. 2. Cardiovascular function ring treatment. Mean arterial essure (MAP, **a**), cardiac index I, **b**), and total peripheral resis- nce (TPR, **c**) during treatment th cuprophane (●) and polyacry- nitrile dialyzer membranes (○). gures at abscissas indicate total eatment time in minutes. HD = emodialysis; UF = ultrafiltration. rcles represent mean values, bars e 1 SEM. * $p < 0.05$ versus be- re. See also table 5.

as no statistically significant difference be- ween the membranes with respect to blood rameters before treatment. After treatment ere was a minor difference in pH ($p <$ 05), whereas the other parameters were similar. However, 20 minutes after the start of hemodialysis, white blood cell counts were significantly reduced on treatment with the cuprophane membrane (mean ± SD: 2.9 ± 1.2 × 10^9/l vs. baseline: 7.5 ± 2.6 × 10^9/l,

Table 4. Systemic hemodynamics

		Before	60 min	After
Mean arterial pressure, mm Hg	CUP	103±17	113±16[a]	99±21[b, c]
	PAN	104±17	113±18[a]	105±22
Heart rate, beats/min	CUP	69±9	69±12	77±19[a]
	PAN	72±12	72±15	76±15
Stroke index, cm^3/m^2	CUP	57±14	57±13	40±12[a, b]
	PAN	55±12	58±20	41±12[a, b]
Cardiac index, $l/min/m^2$	CUP	3.9±0.8	3.8±0.5	3.0±0.7[a, b]
	PAN	3.9±0.7	4.0±1.0	3.1±1.0[a, b]
Total peripheral resistance, $dyn \cdot s \cdot cm^{-5}$	CUP	1,277±439	1,410±408	1,639±578[a]
	PAN	1,244±324	1,364±448	1,670±453[a, b]
LV fractional shortening, %	CUP	34±8	33±7	30±11
	PAN	35±9	35±11	27±11[a]
LV Vcf_c, circles/s	CUP	0.90±0.24	0.91±0.24	0.90±0.36
	PAN	0.94±0.27	0.93±0.33	0.80±0.33[a]

Values are means ± SD. Before, 60 min and after refer to dialysis treatment (see text). CUP = Cuprophane; PAN = polyacrylonitrile; [a] $p < 0.05$ versus before; [b] $p < 0.05$ versus 60 min; [c] $p < 0.05$, CUP versus PAN; LV = left ventricular; Vcf_c = velocity of circumferential fiber shortening, rate corrected.

< 0.01), whereas it did not change on polyacrylonitrile.

Systemic Hemodynamics

There was no statistically significant difference between treatments with cuprophane and polyacrylonitrile membranes with respect to mean arterial pressure, heart rate, stroke index, cardiac index, total peripheral resistance, left ventricular fractional shortening or rate-corrected velocity of fiber shortening, either during isolated hemodialysis nor when ultrafiltration was added (table 5).

On both membranes, mean arterial pressure increased significantly during isolated hemodialysis (average increase: 10%) and declined to baseline values during ultrafiltration (fig. 2, tables 4 and 5). One patient experienced hypotension (i.e. mean arterial pressure was reduced 25 mm Hg or more) on both membranes, and 1 had hypotension on cuprophane only. All hypotensive episodes commenced after approximately 2 h of ultrafiltration and were characterized by reduced stroke volume and peripheral resistance and but little increase in heart rate. The cardiac index (fig. 2) was maintained in the upper normal range during isolated hemodialysis but decreased significantly during ultrafiltration (average decrease: 22%) due to the relatively greater reduction in left ventricular stroke index (average reduction: 30%) than increase in heart rate (average increase: 9%; fig. 3). One patient changed vascular access from fistula to central venous catheter from first to second treatment; however, the cardiac index at baseline was similar: 4.0 and 3.7 $l/min/m^2$, respectively. On both membranes, total peripheral

Table 5. Analysis of variance
le: p values

Dependent variable	HD		HD + UF	
	MBR	TT	MBR	TT
Mean arterial pressure	0.950	0.0001	0.530	0.014
Heart rate	0.630	0.170	0.720	0.023
Stroke index	0.960	0.190	0.880	0.0001
Cardiac index	0.660	0.130	0.810	0.0001
Total peripheral resistance	0.810	0.010	0.950	0.001
LV fractional shortening	0.920	0.100	0.990	0.005
LV Vcf_c	0.970	0.290	0.910	0.021

Two-factor analysis of variance (general linear model for repeated measurements) for assessment of independent influence of membrane (MBR) as between-factor and treatment time (TT) as within-factor. Separate analyses of variance were performed for isolated hemodialysis (HD) and for hemodialysis with ultrafiltration (HD + UF). LV = Left ventricular; Vcf_c = velocity of circumferential fiber shortening, rate corrected.

sistance increased 10% during isolated he-
odialysis and by a further 19% when ultra-
tration was added (fig. 2, table 4). Left ven-
cular fractional shortening (fig. 3) was not
anged during isolated hemodialysis but de-
eased significantly during added ultrafiltra-
n due to the greater magnitude of decrease
m 60 min to the end of treatment in left
ntricular end-diastolic dimensions (average
crease 14%; cuprophane: 55 ± 5 to 48 ±
nm and polyacrylonitrile: 57 ± 5 to 49 ±
nm), than in end-systolic dimensions (aver-
e decrease 7%; cuprophane: 37 ± 4 to 34 ±
nm and polyacrylonitrile: 38 ± 8 to 36 ±
nm). Rate-corrected velocity of circumfer-
tial fiber shortening was not changed dur-
isolated hemodialysis but increased dur-
the first hour of added ultrafiltration to
ak at 120 min treatment time: 1.04 ± 0.27
cles/s on polyacrylonitrile and 0.99 ± 0.33
cles/s on cuprophane (average increase
m baseline: 10.0%, $p < 0.05$) and declined
values at or slightly below baseline at the
d of treatment.

Discussion

Echocardiography is a well-established method for noninvasive assessment of left ventricular geometry and function, and is particularly suitable for repeated assessments in dialysis patients since it avoids the potential adverse effects of invasive measurements: thromboembolism, infection and arrhythmia. Furthermore, the investigation is comfortable for the patients with little risk for stress responses and no need for sedation.

Membrane Biocompatibility

The present investigation was focused on the systemic cardiovascular response during hemodialysis and ultrafiltration on cuprophane and polyacrylonitrile membranes which were selected for their particularly different biocompatibility. The treatment time and efficiency were similar on the 2 membranes. The different biocompatibility of the membranes was documented by the substantially reduced white blood cell counts after 20 min of hemodialysis with the cuprophane

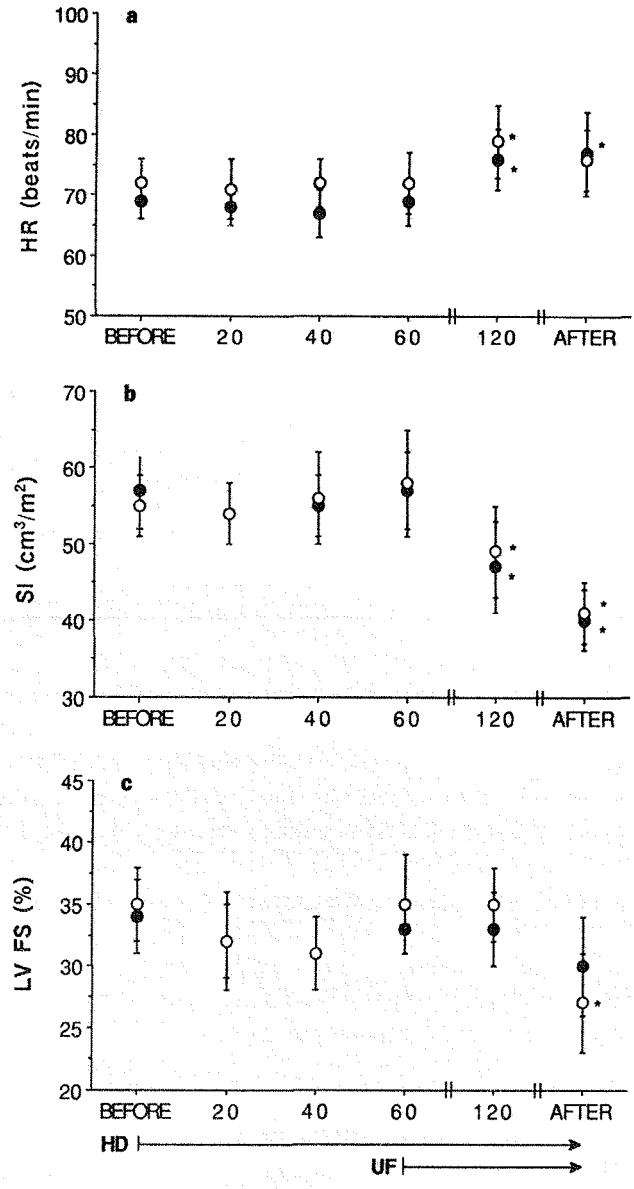

Fig. 3. Cardiovascular function ring treatment. Heart rate (HR, left ventricular stroke index (SI, and left ventricular fractional rtening (LV FS, **c**) during treatnt with cuprophane (●) and pocrylonitrile dialyzer membranes . Figures at abscissas indicate al treatment time in minutes. breviations as in figure 2.

embrane. However, the systemic hemodymic response was not significantly different the 2 membranes during isolated hemodisis nor when ultrafiltration was added. A evious study has reported a similar lack of influence by membrane bioincompatibility on systemic hemodynamics during isolated hemodialysis with acetate buffer [7], and other investigators have also reported that the change in arterial blood pressure during bicar-

ɔnate hemodialysis was not related to mem-ane biocompatibility [15]. However, a re-nt study of hemodynamics during hemofil-ation in patients with combined renal and epatic failure showed that membranes of low ocompatibility were associated with a more onounced depression of cardiac output and erfusion pressure [13]. Thus, although our sults and those of others indicate that the ocompatibility of the dialyzer membrane oes not significantly influence systemic he-odynamics during hemodialysis in hemody-amically stable patients, further investiga-ons are needed to evaluate the implications unstable patients.

Isolated Hemodialysis

The increase in peripheral resistance dur-g isolated hemodialysis was present after 0 min of treatment and maintained un-anged until ultrafiltration was added. Mean terial pressure increased concordantly, nce heart rate and stroke volume were un-anged. This pattern occurred concordantly n both membranes and may be due to reflex rculatory adjustments which occur during lood filling of the dialyzer [16]. The cardiac ndex was in the upper normal range before nd during isolated hemodialysis due to the yperdynamic circulatory state associated ith arteriovenous fistula flow and anemia in ese patients with end-stage renal disease.

Hemodialysis with Ultrafiltration

Ultrafiltration reduces circulatory volume nd left ventricular filling (preload) and pro-uces a Frank-Starling effect [17] which will ecrease stroke volume in spite of maintained ontractility. Vasoconstriction increases in re-ponse to depletion of circulatory volume and pports the perfusion pressure during ultra-tration. This response is better maintained ith bicarbonate than acetate buffers [18]. In e present study, the decrease in stroke vol-ume during hemodialysis with ultrafiltration was of greater magnitude than the reflex increase in heart rate and peripheral resistance. Thus, the slightly elevated arterial pressure at the end of isolated hemodialysis declined to baseline levels during ultrafiltration. Left ventricular end-diastolic dimensions decreased more than end-systolic ones during ultrafiltration, presumably due to the greater magnitude of change in preload than in afterload. Left ventricular rate corrected velocity of circumferential fiber shortening is regarded to be an index of left ventricular contractility insensitive to changes in preload and inversely related to afterload [23]. The slight increase in fiber shortening after 1 h of ultrafiltration was of equal magnitude on both membranes and may be related to the increase in serum ionized calcium reported during hemodialysis with buffers containing calcium at or above 1.75 mmol/l [24, 25], as in the present study. At the end of treatment, fiber shortening was decreased to or slightly below baseline levels for cuprophane and polyacrylonitrile treatments, respectively. Analysis of variance showed that there was no significant difference between the membranes with respect to fiber shortening during hemodialysis without or with ultrafiltration.

Intradialytic Hypotension

Patient No. 4 experienced hypotension on both membranes after approximately 2 h of hemodialysis with ultrafiltration (i.e. after 3 h of total treatment) due to decreased stroke volume which was not balanced by adequate vasoconstriction and heart rate response. Patient No. 2 also had hypotension on cuprophane after 3 h of total treatment with a similar hemodynamic derangement. Thus, these patients may have had impaired autonomic nervous system response leading to a hemodynamic instability [26]. Since all the hypotensive episodes occurred after 2 h of ultrafiltra-

on, they are likely related to depletion of cir-
ulatory volume and not to bioincompatibili-
y where effects present rapidly after estab-
shment of contact between blood and mem-
rane [8].

Methodological Considerations

By using each patient as his own control in
his crossover study, the influence of random
ariability on the parameters was reduced, as
lso indicated by the similar hemodynamics
t the two baselines. Still, with the limited
umber of study subjects we cannot exclude
mall differences in the hemodynamic profile
f the membranes. However, our analysis sug-
ests that such a difference must be small and
unlikely in these patients. The results
hould be directly relevant to the clinical situ-
tion where medication generally is main-
ined during treatments. By keeping the ex-
miners' tasks constant during the study,
nterobserver variability was eliminated. The
recision of oscillometric blood pressure mea-
surements is reduced during arrhythmias; however, all patients were in sinus rhythm during all treatments.

Conclusion

This noninvasive study of systemic cardiovascular response during dialysis indicates that left ventricular function and systemic hemodynamics are not significantly influenced by the dialyzer membrane biocompatibility during bicarbonate hemodialysis with or without ultrafiltration.

Acknowledgements

This study was supported by a grant from the Norwegian Council on Cardiovascular Diseases, Oslo, Norway. The authors gratefully acknowledge the kind assistance from the staff at the Hemodialysis Unit at the University Hospital, Trondheim. Part of this work was presented at the 11th Annual Meeting of the International Society of Blood Purification, 1993.

References

Henderson LW: Symptomatic hypotension during hemodialysis. Kidney Int 1980;17:571–576.

Campese VM: Cardiovascular instability during hemodialysis. Kidney Int 1988;33(suppl 24):S186-S190.

Daugirdas JT: Dialysis hypotension: A hemodynamic analysis. Kidney Int 1991;39:233–246.

Zuchelli P, Santoro A: Dialysis-induced hypotension: A fresh look at pathophysiology. Blood Purif 1993; 11:85–98.

Craddock PR, Fehr J, Dalmasso AP, Brigham KL, Jacob HS: Hemodialysis leukopenia: Pulmonary vascular leukostasis resulting from complement activation by dialyzer cellophane membranes. J Clin Invest 1977;59:879–888.

6 Ivanovich P, Chenoweth DE, Schmidt R, Klinkmann H, Boxer LA, Jacob HS, Hammerschmidt DE: Symptoms and activation of granulocytes and complement with two dialysis membranes. Kidney Int 1983;24:758–763.

7 Schohn DC, Jahn HA, Eber M, Hauptmann G: Biocompatibility and hemodynamic studies during polycarbonate versus cuprophane membrane dialysis. Blood Purif 1986;4:102–111.

8 Chenoweth DE, Cheung AK, Henderson LW: Anaphylatoxin formation during hemodialysis: Effects of different dialyzer membranes. Kidney Int 1983;24:764–769.

9 Hakim RM, Schafer AI: Hemodialysis-associated platelet activation and thrombocytopenia. Am J Med 1985; 78:575–580.

10 Aurigemma NM, Feldman NT, Gottlieb M, Ingram RH, Lazarus JM, Lowrie EG: Arterial oxygenation during hemodialysis. N Engl J Med 1977;297:871–873.

11 Hakim RM: Clinical sequelae of complement activation in hemodialysis. Clin Nephrol 1986;26(suppl 1): S9-S12.

12 Henderson LW, Koch KM, Dinarello CA, Shaldon S: Hemodialysis hypotension: The interleukin hypothesis. Blood Purif 1983;1:3–8.

13 Davenport A, Davison AM, Will EJ: Membrane biocompatibility: Effects on cardiovascular stability in patients on hemofiltration. Kidney Int 1993;43(suppl 41):S230-S234.

Quereda C, Orofino L, Marcen R, Sabater J, Matesanz R, Ortuno J: Influence of dialysate and membrane biocompatibility on hemodynamic stability in hemodialysis. Int J Artif Organs 1988;11:259–264.
Skroeder NR, Jacobson SH, Lins LE, Kjellstrand CM: Biocompatibility of dialysis membranes is of no importance for objective or subjective symptoms during or after hemodialysis. Trans Am Soc Artif Intern Organs 1990;36:M637-M639.
Hampl H, Paeprer H, Unger V, Fischer C, Resa I, Kessel M: Hemodynamic changes during hemodialysis, sequential ultrafiltration, and hemofiltration. Kidney Int 1980;18: S83-S88.
Nixon JV, Mitchell JH, McPhaul JJ, Henrich WL: Effect of hemodialysis on left ventricular function: Dissociation of changes in filling volume and in contractile state. J Clin Invest 1983;71:377–384.
Vagge R, Cavatorta F, Queirolo C, Rosseli P, Gentile A, Bertulla A: Hemodynamic changes during acetate dialysis, bicarbonate dialysis and hemofiltration. Blood Purif 1988;6: 43–50.
19 Aakhus S, Soerlie C, Faanes A, Hauger SO, Bjoernstad K, Hatle L, Angelsen BAJ: Noninvasive computerized assessment of left ventricular performance and systemic hemodynamics by study of aortic root pressure and flow estimates in healthy men, and men with acute and healed myocardial infarction. Am J Cardiol 1993;72:260–267.
20 Schiller NB, Shah PM, Crawford M, deMaria A, Devereux R, Feigenbaum H, Gutgesell H, Reichek N, Sahn D, Schnittger I, Silverman NH, Tajik AJ: Recommendations for quantitation of the left ventricle by two-dimensional echocardiography. J Am Soc Echocardiogr 1989;2: 358–367.
21 Christie J, Sheldahl LM, Tristani FE, Sagar KB, Ptacin MJ, Wann S: Determination of stroke volume and cardiac output during exercise: Comparison of two-dimensional and Doppler echocardiography, Fick oximetry, and thermodilution. Circulation 1987;76:539–547.
22 Aakhus S, Torp H, Haugland T, Hatle L: Noninvasive estimates of aortic root pressures: External subclavian arterial pulse tracing calibrated by oscillometrically determined brachial arterial pressures. Clin Physiol 1993;13:573–586.
23 Colan SD, Borow KM, Neumann A: Left ventricular end-systolic wall stress-velocity of fiber shortening relation: A load-independent index of myocardial contractility. J Am Coll Cardiol 1984;4:715–724.
24 Henrich WL, Hunt JM, Nixon JV: Increased ionized calcium and left ventricular contractility during hemodialysis. N Engl J Med 1984;310: 19–23.
25 Lang RM, Fellner SK, Neumann A, Bushinsky DA, Borow KM: Left ventricular contractility varies directly with blood ionized calcium. Ann Intern Med 1988;108:524–529.
26 Velez RL, Woodard TD, Henrich WL: Acetate and bicarbonate hemodialysis in patients with and without autonomic dysfunction. Kidney Int 1984;26:59–65

Paper IV.

Aakhus S, Mæhle J, Bjoernstad K. A new method for echocardiographic computerized three-dimensional reconstruction of left ventricular endocardial surface: in vitro accuracy and clinical repeatability of volumes. Journal of the American Society of Echocardiography 1994;7:571-581.

A New Method for Echocardiographic Computerized Three-dimensional Reconstruction of Left Ventricular Endocardial Surface: In Vitro Accuracy and Clinical Repeatability of Volumes

Svend Aakhus, MD, Jørgen Mæhle, MSc, and Knut Bjoernstad, MD, *Trondheim, Norway*

This study evaluates the in vitro accuracy and clinical repeatability of volumes derived by a new algorithm for three-dimensional reconstruction of cavity surfaces based on echocardiographic apical images obtained by probe rotation. The accuracy of the method was tested in latex phantoms (true volumes, 32 to 349 cm³) with (n = 9) or without (n = 9) rotational symmetry around the midcavitary long axis. Repeatability of left ventricular volumes was assessed in subjects without (n = 5) or with (n = 10) myocardial disease. Estimated phantom volumes obtained from four (three) imaging planes were close to true volumes with a mean difference ± SD of 0 ± 2 (2 ± 3) cm³ in symmetric and 1 ± 3 (4 ± 4) cm³ in asymmetric objects. Biplane and single-plane volume estimates were less accurate. Interobserver and intraobserver repeatability of three-dimensional left ventricular volumes was good for analysis (coefficients of variation: 3.5% to 6.2%) and was lower for recording (coefficients of variation: 7.4% to 10.9%). Hence the present algorithm reproduces volumes of symmetric and deformed in vitro objects accurately over a wide range of size and shape, and it produces repeatable left ventricular volumes in the clinical situation. (J AM SOC ECHOCARDIOGR 1994;7:571-81.)

dimensions are important for prognosis in vith heart disease. Serial assessment of left r dimensions and geometry is conventionrmed by two-dimensional (2D) echocar- with the use of apical four-chamber and (two-chamber) imaging planes to obtain cular volume by the biplane disk summaod.[1] Because this method is limited by geoumptions of ventricular shape and is not rate when the ventricle is regionally disthods for measurement of left ventricular volume by three-dimensional (3D) echocardiography have gained increasing attention.[2] Cavity volumes can be derived from 3D reconstructions of the left ventricle based on defined endocardial borders on multiple 2D echocardiograms.[3-16] Different methods for image acquisition and processing have been reported, with either the parasternal position for short axis imaging[3-8] or the apical position for long axis imaging, obtained by parallel probe displacement[9] or rotation.[10,11,17] The spatial position of transducer and imaging planes can accurately be registered by use of mechanical arms[4,12] or acoustic systems,[8,13-15] which, however, cannot be used in all clinical situations.[2]

It is recognized that 3D echocardiography produces more accurate and repeatable left ventricular volume estimates than does conventional 2D imaging.[8,16] However, 3D echocardiography is not regarded as feasible in the everyday clinical practice because of the complexity of image acquisition and data processing. We have developed a new algorithm for 3D reconstruction of cavity surfaces[18] based on apical imaging planes obtained by probe rotation.

epartment of Medicine, Section of Cardiology, and ment of Biomedical Engineering, University of

y grants from the Norwegian Council on Cardiovas- s (Oslo, Norway) and Norwegian Technical Research NF).

ests: Svend Aakhus, MD, Department of Medicine, ardiology, University Hospital, N-7006 Trondheim,

94/$3.00 + 0 27/1/57579

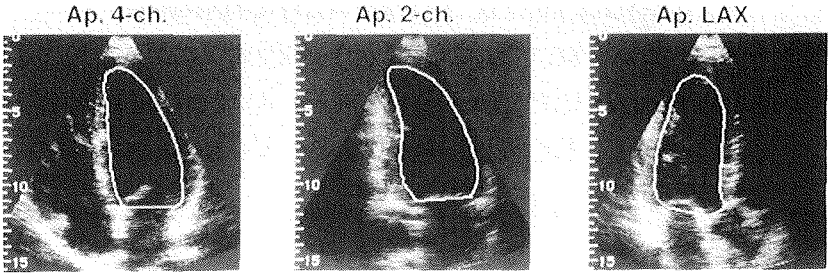

Figure 1 Two-dimensional ultrasound images of left ventricle in end-diastole obtained from apical position. *From left to right:* apical four-chamber, long-axis (two-chamber), and long-axis imaging planes. Endocardial traces are shown as *white continuous lines.* Numbers indicate distance from transducer in centimeters.

Table 1 Interobserver variability for three-dimensional estimates of left ventricular volumes, recording

	Average by two observers	Recording 1-2	CR	CV (%)
LV EDV (cm^3)	125 (83, 246)	−7 ± 9 (−50, 16)	18	7.4
LV ESV (cm^3)	70 (30, 203)	0 ± 8 (−39, 23)	16	10.9
LV SV (cm^3)	55 (36, 74)	−6 ± 6 (−25, 8)	12	11.8
LV EF (%)	47 (17, 64)	−3 ± 4 (−13, 16)	8	8.7

Mean values (± SD), range in parentheses, of two independent observers' recordings in 15 subjects.
LV, Left ventricular; *EDV,* end-diastolic volumes; *ESV,* end-systolic volume; *SV,* stroke volume; *EF,* ejection fraction; *CR,* coefficient of repeatability; *CV* coefficient of variation.

This algorithm was designed to be fast and simple to use and to be operable with commercially available ultrasound and computer equipment. The algorithm accepts any number of imaging planes from 3 to 12, and in this study we assessed the accuracy of volume estimation in vitro by using three or four imaging planes and the clinical repeatability by using apical imaging planes identified by anatomic landmarks.

METHODS

In Vitro Accuracy

An ultrasound scanner (Vingmed 750, Vingmed Sound, Horten, Norway) with a 3.25 MHz annular array transducer was used for all ultrasound imaging. Nine thin-walled latex balloons were filled with 20% ethanol solution to obtain objects with a clinically relevant range of cardiac volumes (i.e., 32 to 349 cm^3) and with rotational symmetry around the midcavitary long axis. Ultrasound imaging was performed with the phantoms immersed in this solution, where ultrasound velocity is 1540 m/sec and similar to that in blood and soft tissue. The probe was mounted in a hull with angle guide around the circumference. Four long-axis ultrasonic images were obtained by subsequent probe rotation in increments of 45 degrees around the midcavitary long axis (0, 45, 90, and 135 degrees). The imaging planes were adjusted to avoid foreshortening without altering the angle of rotation. The images were transferred as digital scanline data (Echolink 3.0, Vingmed Sound) to a computer (Macintosh series II, Apple Computers, Cupertino, Calif.) for analysis in specially designed software operating under a general program for handling of digital ultrasound data (EchoDisp 3.0, Vingmed Sound). Subsequently the phantoms were deformed by application of adhesive tape to obtain rotational asymmetry around the long axis comparable to that of regionally diseased left ventricles. The imaging procedure was then repeated, thus a total of 18 phantoms were studied. The thin phantom wall border was defined at peak ultrasound back scatter intensity (i.e., at midline of the wall echoes) and was manually traced on the computer on all four images, allowing a short "mitral-plane" at basis. Cavity volume was then determined by use of the algorithm for 3D reconstruction as described below first by use of all four border traces and subsequently by use of three border traces (i.e., 0, 90, and 135 degrees). Conventional biplane and single-plane volumes were obtained by the disk summation method

the 0 and 90 degree images and the 0 degree
ge only, respectively. With this procedure the in
accuracy of the methods could be compared
out redrawing the wall contours. The procedure
repeated in a blinded fashion at least 4 weeks
, and the average volume estimate was calculated
omparison with true volume. True volumes were
rmined as the difference between total and dry
ıtom weight divided by 0.96 to correct for the
ion density.

ical Repeatability of Left Ventricular
ımes by 3D

en subjects, 13 men and two women who ranged
ge from 28 to 75 years and had a representative
e of cardiac dimensions (Table 1), gave informed
ent to participate in the study. Five subjects were
hy, seven had previous myocardial infarction,
hree had dilated left ventricles caused by conges-
cardiomyopathy (two patients) or coronary ar-
disease (one patient). All patients were in sinus
ım; one had first-degree atrioventricular block,
one had left bundle branch block. Medication
continued through the investigation. All subjects
examined in the left lateral decubitus position
at least 5 minutes supine rest, and all had read-
echocardiograms, although they were not spe-
lly selected for echogenicity. Ultrasound images
obtained independently and in immediate and
om succession by two experienced investigators
g apical access to the four-chamber, long-axis
-chamber), and long-axis imaging planes (Fig-
1), which were identified by anatomic land-
s.[1,19] The four-chamber plane was assigned 0
ees, and the angular deviations of long axis (two-
ıber) and long axis from this plane were assumed
: 62 and 101 degrees counterclockwise, respec-
y.[20] For each imaging plane sequential images
one cardiac cycle (cineloop) were sampled, usu-
t 47 frames/sec, during held end-expiration and
ferred as digital scanline data to the computer.
lectrocardiogram (lead III) was recorded with
ıltrasound data. The two assessments of each
ct were completed within 1 hour.
ıe duplicate set of images from each subject (two
dings) was analyzed in a blinded fashion by two
ɔendent observers on two occasions more than
ays apart. On the computer endocardial border
ition was optimized by adequate contrast set-
and the endocardial borders of all three imaging
es were manually traced in end-diastole (defined
e R-peak on the electrocardiogram) and end-
ıle (defined at the frame before mitral valve open-

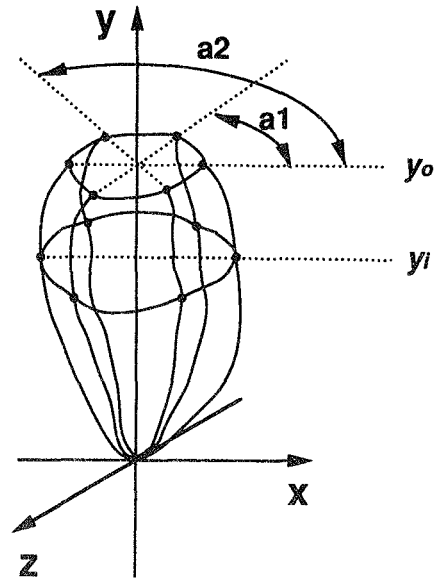

Figure 2 Principle for three-dimensional reconstruction of left ventricular endocardial surface from multiple apical long axis ultrasound images. Endocardial border trace from each image (three traces shown) are reassembled in Cartesian xyz–system according to their relative angles (a1, a2), common position of apex in origo, and common mitral plane midpoint. Mitral valve annulus is determined by (1) finding the plane $y = ax + bz + y_o$ as best fit to border trace endpoints (least squares method), (2) projecting these endpoints into this plane, and (3) reconstructing annulus by cubic spline interpolation on these projected points. Multiple planes in parallel with mitral plane, y_o, are then positioned between apex and mitral midpoint. At each plane, y_i, a closed curve is generated by cubic spline interpolation through points of intersection between plane and apical border traces. Endocardial surface is then reconstructed from the cubic spline interpolated multiple apical and cross-sectional borders (see text).

ing). Endocardium was traced at the echogenic transition zone between left ventricular cavity and myocardial wall, excluding the papillary muscles and including the left ventricular outflow tract up to the aortic valve in the long-axis plane (Figure 1). Mitral valve plane was traced as the straight line between mitral annulus echo boundaries (i.e., at insertion of the mitral valve leaflets). The traces on the freeze-frame images (end-diastole and end-systole) were repeatedly evaluated against the moving endocardium and mitral annulus by use of the cineloop replay function. The endocardial edges from these three apical long-axis views of the left ventricle and their assumed rotation-angles made up input data to the surface reconstruction algorithm.

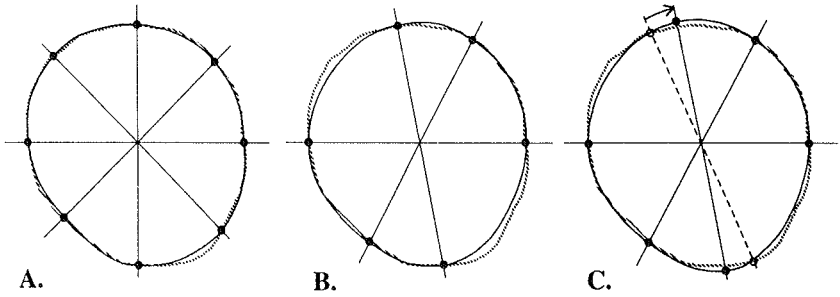

Figure 3 Reconstruction of left ventricular cross-sectional border. Closed cubic spline curve *(continuous line)* as compared with true endocardial border *(broken line)* in regionally diseased left ventricle at end-diastole imaged in cross-section from parasternal position. *A* and *B* show cubic spline curves interpolated on eight and six points *(closed circles)* corresponding to four (0, 45, 90, and 135 degrees) and three (0, 62, and 101 degrees) apical long-axis imaging planes *(straight lines)*. Difference between areas within true and interpolated cavity borders was −1.2% in *A* and −2.8% in *B*. *C* shows deviation of apical long axis 15 degrees *(dashed line)* from assumed angular position. Cubic spline interpolation was performed as if deviating endocardial point *(open circle)* was located at assumed imaging plane position *(closed circle)*. Difference between area within this curve and that obtained from correctly positioned imaging planes was 2.5%.

orithm for 3D Reconstruction of ity Surface

the cavity border traces and their measured or med spatial positions are entered into the spe- y designed software, the present 3D algorithm orms the following steps automatically. First 30 nts are equally distributed on each of the original der traces, which then are redefined to continuous oth curves by cubic spline interpolation on these nts. In each imaging plane the mitral plane mid- nt is defined as the midpoint of the straight line veen mitral annulus echo boundaries. The bor- s apex is defined as the border point furthest away n the mitral plane midpoint, and the major axis efined as the straight line between this apex and ral plane midpoint. To make the apex definition sensitive to inaccuracies of endocardial border ing, apex and major axis are automatically ad- ed so that the latter passes through the center of in the apical region of the border. Because the al probe position does not always correspond to cardiac apex, the imaging planes may occasionally oreshortened and lead to underestimation of vol- e. Assuming that the longest major axis is the most rect, the present algorithm compensates auto- ically for foreshortening by elongating the en- ardial border traces in major axes direction so that najor axes equal the longest. The border traces then reassembled in a xyz–space according to r measured or assumed input angles, with apex and the mitral midpoint of each border positioned in origo and at the y-axis, respectively, so that the common major axis coincides with the y-axis (Figure 2). The reconstruction of the cavity border surface is now performed as follows. A plane is found as best fit to the endpoints of the border traces (least squares method) and is defined to be the mitral plane. The endpoints are then projected into this plane, and the mitral valve annulus is approximated by a planar curve generated by cubic spline interpolation on these projected points. New equidistant planes parallel to the mitral plane are then positioned between apex and mitral midpoint. At each plane a cross-sectional closed curve is generated by cubic spline interpolation through the points of intersection between the plane and apical border traces. The number of reconstructed cross-sections corresponds to the selected axial resolution. With this procedure the cavity surface is reconstructed as a bicubic surface that interpolates the borders reassembled in the xyz–space. The cavity volume is calculated by disk summation (Simpson's rule). The area of each cross-sectional disk is obtained from the mathematic description of the cubic spline curve, and disk volume is calculated as the product of disk area and height where the latter is given as the major long axis length divided by the selected axial resolution. Stroke volume was calculated as end-diastolic minus end-systolic volume, and ejection fraction was calculated as stroke volume over end-diastolic volume.

Method	Shape	Imaging planes	Echo-TRUE (cm^3)	95% LA (cm^3)		CV (%)
				Lower	Upper	
D	Symmetric	4	0 ± 2 (−3, 6)	−4	3	1.3
D	Symmetric	3	−2 ± 3 (−6, 5)	−7	3	1.9
plane	Symmetric	2	−2 ± 3 (−8, 1)	−7	3	1.9
gle plane	Symmetric	1	−3 ± 4 (−13, 2)	−10	4	2.6
D	Asymmetric	4	−1 ± 3 (−7, 6)	−7	4	2.0
D	Asymmetric	3	−4 ± 4 (−9, 3)	−11	4	2.7
plane	Asymmetric	2	−5 ± 5 (−12, 3)	−15	5	3.8
gle plane	Asymmetric	1	−6 ± 6 (−24, 1)	−18	6	4.6

alues ± SD (range) from nine symmetric and nine asymmetric phantoms.
ie present three-dimensional method; *Echo-TRUE*, difference between echocardiographically determined and true phantom volume; *LA*, limits of nt; *CV*, coefficient of variation.

ity of Reconstructed Left Ventricular s-Sectional Area

resent algorithm reconstructs the borders of sectional disks from a limited number of apical ng planes and calculates cavity volume from nd height of these disks. The accuracy of the rea estimate depends on the agreement between nd reconstructed cavity border and the influ- of deviations from the assumed spatial position imaging planes. This accuracy was tested in bjects (eight men and two women) aged 24 to ars, with (n = 6, all with previous myocardial tion) or without (n = 4) left ventricular re- l wall motion abnormalities at rest. All were in rhythm. Cineloops of the midventricular short ere recorded by imaging from parasternal po- and were transferred to the computer. The ardial borders were traced in end-diastole and stole, excluding the papillary muscles. On borders we used the eight or six points corre- ing to the four (0, 45, 90, and 135 degrees) ee (0, 62, and 101 degrees) apical imaging , respectively, to generate a closed cubic spline (Figure 3). The end-diastolic and end-systolic within the true endocardial border trace and rresponding spline curves were obtained for all bjects, and the respective differences were cal- d in percent of the former.

apical four-chamber, long-axis (two-cham- and long-axis imaging planes may deviate up degrees from their assumed spatial position.[20] st how this deviation influences the disk area ites and thus volume estimates, we generated ubic spline curves corresponding to an angular ion of ± 15 degrees in any of the three imaging . We used the six points on the traced endo- cardial border corresponding to the assumed position of the three apical imaging planes (i.e., 0, 62, and 101 degrees). Each point's position is defined by its distance to the major axis (i.e., center of area within the border) and by the rotation angle of the corresponding imaging plane. The distance between point and major axis was identified along the deviating imaging plane. The reconstruction was performed with the point relocated to the correctly positioned plane with the identified distance to major axis (Figure 3, *C*). The difference between the areas within the new curve and that with correct position of the imaging planes was calculated in percent of the latter. In each patient this procedure was performed for end-diastolic and end-systolic borders according to 0, 15, and −15 degrees deviation in the three apical imaging planes (54 combinations).

Statistical Analysis

Values are presented as mean ± standard deviation (SD). Coefficient of variance and the 95% limits of agreement were obtained by standard methods.[21] Coefficient of repeatability was determined as 1.96 SD of the differences between the observers.[22] The relation between variables was also assessed by simple linear regression, where the squared correlation coefficient (R^2) and residual standard deviation (s_{res}) were used for assessing goodness of fit of the regression line.

RESULTS

In Vitro Accuracy

The estimated volumes agreed well with true volumes both in symmetric and deformed phantoms and when either four or three imaging planes were used

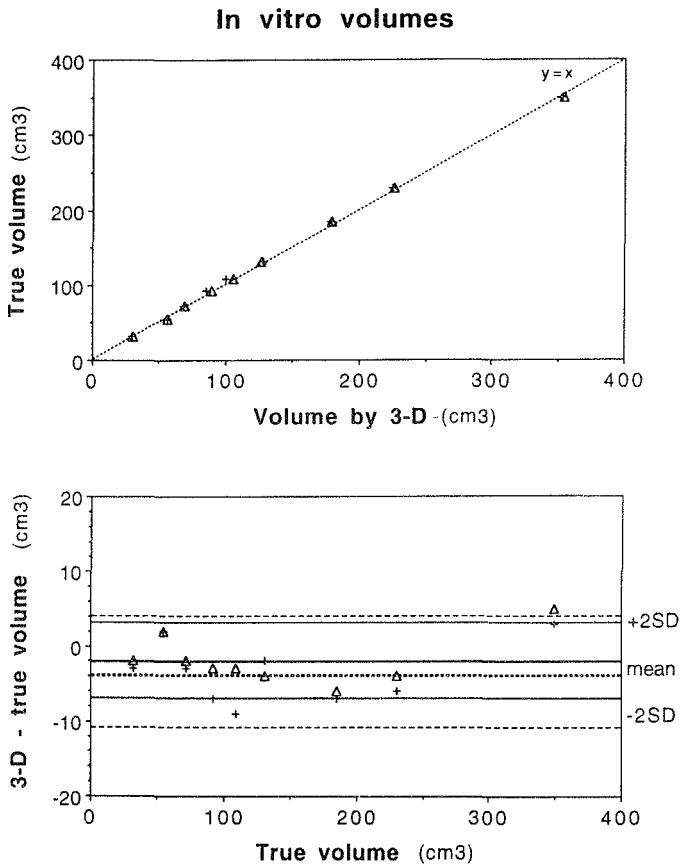

Figure 4 In vitro accuracy of volumes by three-dimensional method. Cavity surface of nine symmetric *(open triangles)* and nine asymmetric *(crosses)* fluid-filled latex phantoms were reconstructed by present algorithm from three long-axis imaging planes and volumes determined from this reconstruction (see text). *Upper panel,* plot of volumes by three-dimensional method, at abscissa, against true volumes, at ordinate. Line of identity (y = x) hides linear regression line for all phantoms (R^2 = 0.999, residual standard deviation 3.7 cm^3, $p < 0.001$). *Lower panel,* plot of difference between volumes by three-dimensional and true volumes, at ordinate, against true volumes, at abscissa. Mean ± 2 SD for symmetric phantoms is indicated by *continuous lines* and for asymmetric phantoms by *dashed lines.*

surface reconstruction (Table 2, Figure 4). The mated volumes tended to be slightly lower than volumes for all methods except when four imng planes were used on symmetric objects, and underestimation was greater on deformed obs. The regression lines between estimated and true umes were close to the line of identity when both r or three imaging planes were used. Although in vitro accuracy of volume estimation was best en four imaging planes were used, it was adequate en three were used as well, where 95% limits of eement indicates that any volume estimate in an asymmetric object would be less than 11 cm^3 less than and 4 cm^3 greater than true volume. Bias and variability were smallest with the 3D method, slightly greater for biplane method, and greatest for single plane method (Table 2). Intraobserver repeatability for analysis of phantom volumes by 3D method was good with coefficients of variation between 2.2% and 3.0% for both symmetric and deformed phantoms when reconstructed from either four or three imaging planes, whereas the repeatability was lower for biplane and single plane methods with coefficients of variation ranging from 3.3%

e 3 Interobserver variability for three-dimensional estimates of left ventricular volumes, analysis

	Analysis 1-2	CR	CV (%)
LV EDV (cm^3)	1 ± 4 (−10, 17)	8	3.5
LV ESV (cm^3)	−4 ± 4 (−15, 12)	8	6.2
LV SV (cm^3)	4 ± 4 (−7, 17)	8	7.5
LV EF (%)	4 ± 3 (−3, 10)	6	7.0

values (± SD), range in parentheses, of two independent observers' analysis of data from 15 subjects.
iations as in Table 1.

e 4 Intraobserver variability for three-dimensional estimates of left ventricular volumes, analysis

	Analysis 1-2	CR	CV (%)
LV EDV (cm^3)	3 ± 5 (−16, 16)	10	4.1
LV ESV (cm^3)	4 ± 4 (−9, 20)	8	6.1
LV SV (cm^3)	−2 ± 4 (−23, 11)	8	8.5
LV EF (%)	−2 ± 3 (−9, 9)	6	5.8

values (± SD), range in parentheses, of one observer's two independent analysis sessions on data from 15 subjects.
iations as in Table 1.

the biplane method) to 7.8% (with the single method).

ical Repeatability

observer repeatability for recording (Table 1) best for end-diastolic left ventricular volume with fficient of variation of 7.4% and was lower for ystolic volume and stroke volume. The coeffi- of repeatability indicates that any difference in ded end-diastolic or end-systolic volume less 18 or 16 cm^3, respectively, may be due to vari- in recording technique alone. The differences een the observers were, however, evenly dis- ted over the range of measurements. Interob- r repeatability for analysis (Table 3) was better that for recording, with coefficients of variation ng from 3.5% for end-diastolic volume to 7.5% troke volume. Variation in analysis technique xplain only a difference less than 8 cm^3 for serial entricular volumes analysis by 2 different ob- rs. The differences between the observers were y distributed over the range of measurements. observer repeatability for analysis (Table 4) was ilar level with coefficients of variation ranging 4.1% for end-diastolic volume to 8.5% for e volumes. The differences between the observ- ere evenly distributed over the range of mea- nents.

nstructed Left Ventricular s-Sectional Area

average difference between the area within the ventricular short axis endocardial border and that within the corresponding closed spline curve generated through eight or six border points (i.e., four or three apical imaging planes) were 0.8% ± 0.7% (95% limits of agreement: −0.3% to 1.9%) and 1.2% ± 1.6% (95% limits of agreement: −1.9% to 4.3%), respectively. The results were similar for end-systolic and end-diastolic area (Figure 5). The average difference between the reconstructed area generated from the six points that were allowed to deviate ±15 degrees from their assumed position on the endocardial border trace and that within the curve with correctly positioned points was 0.3% ± 3.2% (95% limits of agreement: −6.0% to 6.9%).

DISCUSSION

In this study we have presented a new algorithm for 3D surface reconstruction based on conventional 2D ultrasound apical imaging, and we have evaluated the accuracy in vitro and the repeatability of left ventricular volume determination in the clinical situation. The time needed for recording of three apical imaging planes depends on image quality and investigator experience, but it is usually less than 15 minutes. The endocardial borders of the three imaging planes can be traced in end-diastole and end-systole within 10 to 15 minutes. Once the traces are input to the special purpose software, surface reconstruction and volume calculation are completed within a few seconds with the described setup. We used the apical position for obtaining an image, because in

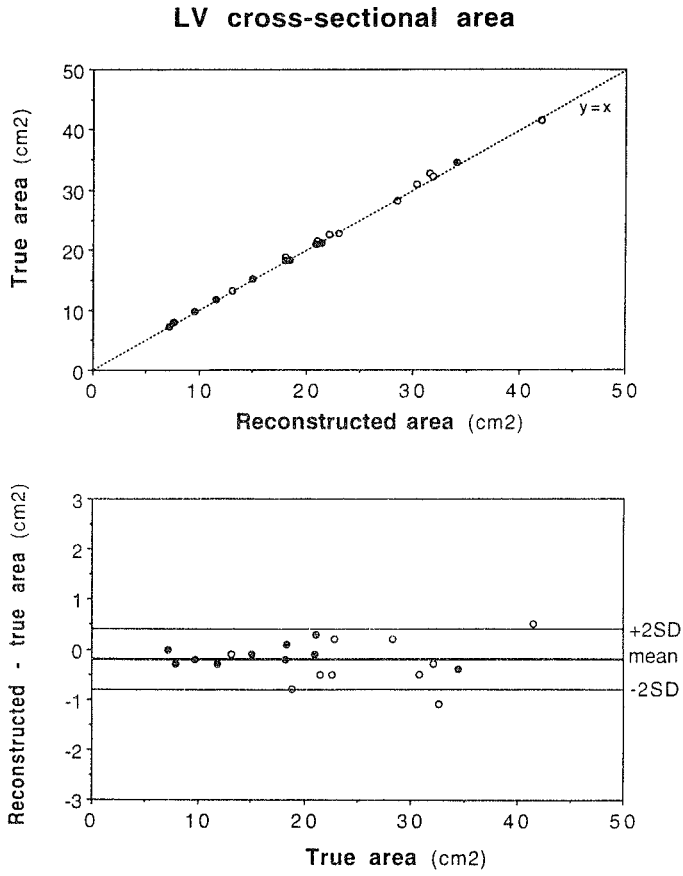

Figure 5 Validity of left ventricular *(LV)* reconstructed cross-sectional area. In vivo comparison (six subjects with and four without regional myocardial disease) of area within midventricular endocardial border (true area) as judged from parasternal short axis ultrasound image in end-diastole *(open circles)* and end-systole *(closed circles)*, and that reconstructed by cubic spline interpolation on six points on endocardial border corresponding to three apical imaging planes (0, 62, and 101 degrees). See also Figure 3. *Upper panel,* reconstructed areas, at abscissa, plotted against true areas, at ordinate. Line of identity (y = x) hides linear regression line ($R^2 = 0.999$, residual standard deviation 0.4 cm^2, $p < 0.001$). *Lower panel,* plot of difference between reconstructed and true areas, at ordinate, against true areas, at abscissa. Mean ± 2 SD indicated by continuous lines.

xperience it is less hampered by rib interference with the parasternal position. Moreover, in most nts an image of the entire left ventricle can be ined from this position by rotation of the probe. reas previous studies have used the rotational of the transducer as reference for 3D echocarraphy,[10,17] the present method uses the major axis ie left ventricle. This allows adjustment of each ging plane without changing the rotational an- and image quality can be optimized. Further- the reconstruction is not significantly influenced by movement of the heart and patient, and accessory mechanical devices are obviated.

The present study shows that the volumes of objects with a wide range of shapes and sizes can be accurately reproduced by 3D echocardiography based on three or four imaging planes. A volume estimate based on three or four imaging planes in an asymmetric object would be within 11 or 7 cm^3 less than and 4 cm^3 greater than the true volume (95% confidentiality), respectively. This is similar to results obtained with a more complex system for 3D echo-

graphy.[8] Hence we regard three apical imaging to be sufficient for volume estimates of sym- and asymmetric objects. This is important, e recording of four imaging planes requires a ocedure for echocardiographic imaging of left le, whereas the four-chamber, long-axis (two- er), and long-axis imaging planes are part of utine clinical echocardiographic examination. volumes of the asymmetrical objects were es- l from only two (biplane method) or one im- plane(s) (single plane method), the bias and ity were greater and repeatability was lower. in agreement with results of previous studies balloons[8] and excised hearts,[16] and is most due to the representation of object surface by 3D echocardiography than by the other ds. Moreover, in the present algorithm we plemented automatic elongation of the major that all equal the longest, and this feature rther improve the accuracy of volume esti- when the imaging planes occasionally are rtened. However, at least one imaging plane nake up the correct major axis for adequate reconstruction and volume estimation.

present algorithm produces a bicubic spline ntation of cavity surface from the input long es and their measured or assumed spatial po- The cubic spline curve maintains both direc- l curvature through the interpolation points. ne curves fulfilling this requirement, the cubic curve has minimum curvature variation and energy.[23] The present study shows that this well suited for reconstruction of the endo- border and produces areas within − 1.9% and 95% confidentiality) of true cross-sectional the endocardial border trace in left ventricles d without regional disease when generated x points (i.e., three apical imaging planes). more the disk area estimate is robust for ns from the assumed image plane positions, rs in disk area resulting from any 15 degrees n in the imaging planes would be within to 6.9% with 95% confidentiality. The vol- imate is calculated by disk summation and is e equally robust for angular deviations.

ave tested the algorithm with different levels resolution and have found that when the s of reconstructed cross-sections exceed 16, me estimate converges to be within 1% of ained when this number approaches infinity, ndicated by Figure 6. Thus to obtain volume es with high accuracy and a fast surface re- ction, we have chosen an axial resolution of

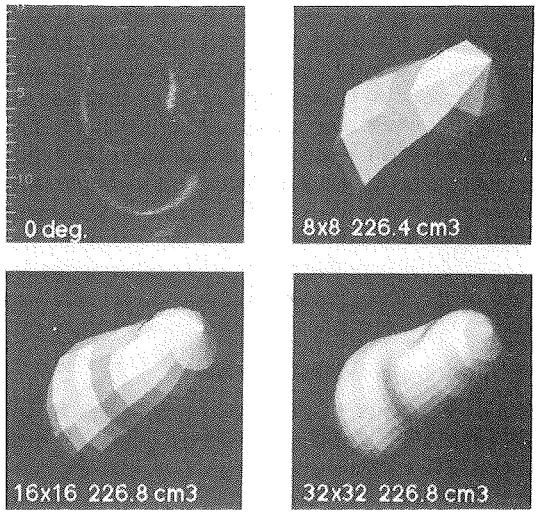

Figure 6 Examples of three-dimensional surface reconstructions with increasing axial resolution. Upper left panel shows two-dimensional long-axis ultrasound image (0 degree) of deformed latex phantom with true volume 230 cm^3. Subsequent panels show cavity surface reconstructions based on 0, 45, 90, and 135 degree images (latter three not shown) with increasing axial resolution (8, 16, and 32 points) and corresponding volume estimates. With increasing axial resolution, number of points displayed in circumferential direction is concordantly increased, and presented object surface approaches reconstructed smooth bicubic spline surface.

32. Higher resolution (i.e., 64 disks), adds computation time without increasing accuracy of volume determination.

The present study assessed repeatability of volumes in patients who were not specifically selected for their image quality, and the results should therefore be relevant for everyday clinical practice. In contrast to most other reports on repeatability of 3D echocardiography,[7-8,14,16,24] the present study discriminates between the variability caused by recording and that caused by analysis of the ultrasound images. The interobserver repeatability was better for analysis than for recording and was generally best for end-diastolic volume and lowest for stroke volume, which is in agreement with results from 2D echocardiographic studies.[25] The lower repeatability for image recording than for analysis indicates how two investigators tend to image the left ventricle slightly differently. In serial studies this problem can be eliminated by allowing only one investigator to obtain the images. Repeatability for analysis of left ventricular volumes was approximately equal between (interobserver vari-

lity) and within (intraobserver variability) the in-
tigators, indicating that the endocardial borders
defined similarly by different investigators and
t tracing can be performed by more than one in-
tigator when they are equally experienced. The
eatability for analysis of end-diastolic and end-
olic volumes was good with coefficients of vari-
n at or below 4% and 6%, which is in agreement
h a previous study involving a more complex sys-
for 3D echocardiography.[24] The repeatability for
lysis of stroke volume and ejection fraction was
ptable with coefficients of variation less than 9%.

thodologic Considerations

have assumed that the mitral annulus can be ap-
ximated by a planar curve, although it has been
nd to be saddle-shaped.[26] However, with the pres-
algorithm the mitral annulus is reconstructed
n the six or eight points on the true annulus iden-
d on the three or four apical imaging planes,
pectively, and represents in terms of volume an
rage of the spatial position of true annulus. Thus
reconstructed mitral annulus is not likely to pro-
e significant errors in the estimate of left ventric-
r cavity volume.

Endocardial border definition is important for ac-
ate 3D reconstruction and varies with image qual-
and heart rate. In our experience the precision of
locardial border tracing (on freeze frame) is mark-
y improved by use of the digital cineloop tech-
ogy. Because the acquired images are transferred
digital scanline data directly to the computer, im-
quality and the high frame rate are preserved from
ording to analysis with no need for video record-
. We think that this is important for the good
eatability of analysis in this study of nonselected
ients. Adequate reconstruction of left ventricular
ity requires regular cardiac rhythm, because data
sampled from different cardiac cycles. In this
dy all patients were in sinus rhythm.

We assessed clinical repeatability by sequential and
ded investigation of left ventricular volumes in
ients during rest. Although the second assessment
ach patient was performed immediately after the
and the total time for investigation of each sub-
was less than 1 hour, we cannot exclude small
ations in true cardiac volumes between the as-
ments. The randomized sequence of the investi-
ors should, however, ensure that this physiologic
ation contributed equally to the results of the two
stigators and did not influence repeatability
lts.

Conclusion

The present algorithm for 3D reconstruction of cavity surface is accurate over a wide range of shapes and volumes when both three or four image planes are used. Furthermore, volume estimates based on 3D reconstruction have less bias and are more repeatable than those of conventional biplane and single-plane methods. The algorithm performs well with standard ultrasound equipment without accessory devices and facilitates a feasible, repeatable, and relatively fast assessment of left ventricular volume in the clinical setting.

REFERENCES

1. Schiller NB, Acquatella H, Ports TA, et al. Left ventricular volume from paired biplane two-dimensional echocardiography. Circulation 1979;60:547-55.
2. Pearlman AS. Measurement of left ventricular volume by three-dimensional echocardiography—present promise and potential problems. J Am Coll Cardiol 1993;22:1538-40.
3. Nixon JV, Saffer SI, Lipscomb K, Blomqvist CG. Three-dimensional echoventriculography. Am Heart J 1983;106: 435-43.
4. Sawada H, Fujii J, Kato K, Onoe M, Kuno Y. Three dimensional reconstruction of the left ventricle from multiple cross sectional echocardiograms: value for measuring left ventricular volume. Br Heart J 1983;50:438-42.
5. Ariet M, Geiser EA, Lupkiewicz SM, Conetta DA, Conti CR. Evaluation of a three-dimensional reconstruction to compute left ventricular volume and mass. Am J Cardiol 1984;54:415-20.
6. Raichlen JS, Trivedi SS, Herman GT, St. John Sutton MG, Reichek N. Dynamic three-dimensional reconstruction of the left ventricle from two-dimensional echocardiograms. J Am Coll Cardiol 1986;8:364-70.
7. Zoghbi WA, Buckey JC, Massey MA, Blomqvist CG. Determination of left ventricular volumes with use of a new nongeometric echocardiographic method: clinical validation and potential application. J Am Coll Cardiol 1990;15: 610-7.
8. Schroeder KD, Sapin PM, King DL, Smith MD, DeMaria AN. Three-dimensional echocardiographic volume computation: in vitro comparison to standard two-dimensional echocardiography. J Am Soc Echocardiogr 1993;6:467-75.
9. Matsumoto M, Inoue M, Tamura S, Tanaka K, Abe H. Three-dimensional echocardiography for spatial visualization and volume calculation of cardiac structures. Journal of Clinical Ultrasound 1981;9:157-65.
10. Ghosh A, Nanda NC, Maurer G. Three-dimensional reconstruction of echocardiographic images using the rotation method. Ultrasound Med Biol 1982;8:655-61.
11. Fazzalari NL, Davidson JA, Mazumdar J, Mahar LJ, DeNardi E. Three dimensional reconstruction of the left ventricle from four anatomically defined apical two-dimensional echocardiographic views. Acta Cardiol 1984;39:409-36.
12. Geiser EA, Ariet M, Conetta DA, Lupkiewics SM, Christie LG, Conti CR. Dynamic three-dimensional echocardio-

raphic reconstruction of the intact human left ventricle: tech-ique and initial observations in patients. Am Heart J 982;103:1056-65.
Ioritz WE, Pearlman AS, McCabe DH, Medema DK, Ains-orth ME, Boles MS. An ultrasonic technique for imaging ie ventricle in three dimensions and calculating its volume. EEE Trans Biomed Eng 1983;BME-30:482-91.
ing DL, Harrison MR, King DL Jr, Gopal AS, Martin RP, eMaria AN. Improved reproducibility of left atrial and left entricular measurements by guided three-dimensional echo-ardiography. J Am Coll Cardiol 1992;20:1238-45.
opal AS, King DL, Katz J, Boxt LM, King DL Jr., Shao IY. Three-dimensional echocardiographic volume compu-tion by polyhedral surface reconstruction: in vitro validation nd comparison to magnetic resonance imaging. J AM SOC CHOCARDIOGR 1992;5:115-24.
apin PM, Schroeder KD, Smith MD, DeMaria AN, King L. Three-dimensional echocardiographic measurement of ft ventricular volume in vitro: comparison with two-di-ensional echocardiography and cineventriculography. J Am oll Cardiol 1993;22:1530-7.
IcCann HA, Sharp JC, Kinter TM, McEwan CN, Barillot , Greenleaf JF. Multidimensional ultrasonic imaging for car-iology. Proceedings of the Institute of Electrical and Elec-onic Engineers 1988;76:1063-73.
Iæhle J, Bjørnstad K, Aakhus S, Torp HG, Angelsen BAJ. hree-dimensional echocardiography for quantitative left entricular wall motion analysis: a method for reconstruction f endocardial surface and evaluation of regional dysfunction. chocardiography 1994;11:397-408.
19. Henry WL, DeMaria A, Gramiak R, et al. Report of the American Society of Echocardiography Committee on nomenclature and standards in two-dimensional echocardiography. Circulation 1980;62:212-7.
20. Henry WL, DeMaria A, Feigenbaum H, et al. Report of The American Society of Echocardiography Committee on Nomenclature and Standards: identification of myocardial wall segments. 1982.
21. Altman DG. Practical statistics for medical research. London: Chapman & Hall, 1991.
22. Bland JM, Altman DG. Statistical methods for assessing agreement between two methods of clinical measurement. Lancet 1986;ii:307-10.
23. Farin G. Curves and surfaces for computer aided geometric design. Boston: Academic Press, Inc., 1988.
24. Handschumacher MD, Lethor JP, Siu SC, et al. A new integrated system for three-dimensional echocardiographic reconstruction: development and validation for ventricular volume with application in human subjects. J Am Coll Cardiol 1993;21:743-53.
25. Wallerson DC, Devereux RB. Reproducibility of quantitative echocardiography: factors affecting variability of imaging and Doppler measurements. Echocardiography 1986;3:219-35.
26. Levine RA, Handschumacher MD, Sanfilippo AJ, et al. Three-dimensional echocardiographic reconstruction of the mitral valve, with implications for the diagnosis of mitral valve prolapse. Circulation 1989;80:589-98.

Paper V.

Aakhus S, Bjørnstad K, Hatle L. Noninvasive study of left ventricular function a
systemic haemodynamics during dipyridamole echocardiography stress test.
Clinical Physiology 1994;14:581-594.

Clinical Physiology (1994) **14**, 581–594

Noninvasive study of left ventricular function and systemic haemodynamics during dipyridamole echocardiography stress test

S. Aakhus, K. Bjørnstad and L. Hatle

Department of Medicine, Section of Cardiology, University Hospital, N-7006 Trondheim, Norway

(Received 22 October 1993; accepted 18 March 1994)

Summary. Left ventricular function and systemic haemodynamics were noninvasively assessed during cardiac stress testing with dipyridamole (0·84 mg kg^{-1} i.v.) in 10 subjects (44–61 years) with normal coronary arteries (group 1), and in 14 patients (46–77 years) with coronary artery disease either without (group 2, $n=6$) or with (group 3, $n=8$) echocardiographic evidence for myocardial ischaemia during test. Left ventricular wall motion and dimensions, and aortic root pressure and flow were obtained by Doppler echocardiography combined with an externally traced subclavian artery pulse calibrated with brachial artery pressures. Peripheral arterial resistance, total arterial compliance, and aortic characteristic impedance were estimated from aortic root pressure and flow, by use of a three-element windkessel model of the systemic circulation. Left ventricular ejection fraction improved from baseline to peak stress in group 1 (mean±SD: 62±6% vs. 65±6%, $P=0·05$), whereas it was not significantly changed in group 2 (58±10% vs. 56±6%) and decreased in group 3 (53±10% vs. 43±10%, $P<0·05$). Otherwise, the haemodynamic response was similar in the three groups: heart rate and cardiac index increased by at least 30% and 37%, respectively, whereas stroke index and arterial pressures were maintained at or slightly above baseline. Peripheral resistance decreased by at least 22%, and total arterial compliance and aortic characteristic impedance were not significantly altered during test. The worsening of wall motion abnormality at peak stress in group 3 was not significantly related to the change in systemic haemodynamics. Thus, dipyridamole acted predominantly on the arterioles without significantly influencing the large systemic arteries. Myocardial ischaemia during test impaired regional and global left ventricular function, but did not influence the systemic haemodynamic response.

Key words: cardiac stress test, dipyridamole, coronary artery disease, left ventricular function, windkessel model, echocardiography, non invasive method.

Correspondence: Svend Aakhus, Department of Medicine, Section of Cardiology, University Hospital, N-7006 Trondheim, Norway

Introduction

Dipyridamole reduces coronary resistance and increases coronary blood flow (Gould, 1978; Feldman *et al.*, 1981), presumably by elevating plasma adenosine levels (Sollevi *et al.*, 1984). Dipyridamole may provoke myocardial ischaemia in patients with coronary artery stenosis (Gould *et al.*, 1978), most likely by reduction of distal coronary perfusion pressure due to the increased coronary flow. Dipyridamole has therefore been extensively used with scintigraphic (Beller, 1989) and echocardiographic (Picano, 1989; Castello & Labowitz, 1992) imaging techniques for evaluation of the presence and severity of coronary artery disease, particularly in patients who cannot perform exercise tests adequately. In cardiac stress testing, dipyridamole 0·56 mg kg^{-1} body weight has routinely been used; however, the sensitivity for detection of coronary artery disease by echocardiography has been reported to improve by using 0·84 mg kg^{-1} (Picano *et al.*, 1986). Information on how this high dipyridamole dose influences systemic arterial properties, which are important determinants of left ventricular function (Urschel *et al.*, 1968), is, however, limited.

Thus, the purposes of this study were by noninvasive means: 1) to assess left ventricular function and systemic haemodynamics during a conventional stress test protocol with dipyridamole 0·84 mg kg^{-1}; and 2) to evaluate how myocardial ischaemia during the test influenced the cardiovascular response.

Subjects and methods

STUDY SUBJECTS

The 24 study subjects (13 men and 11 women) aged 44–77 years, underwent clinical examination, dipyridamole stress echocardiography, and cardiac catheterization for evaluation of the coronary arteries. Subjects with neck vessel bruit, aortic valvular disease, irregular cardiac rhythm, bundle branch block, severely impaired left ventricular function (echocardiographic ejection fraction below 35%), pulmonary congestion, unstable angina pectoris, baseline systolic blood pressure below 90 mmHg, obstructive pulmonary disease, or suboptimal echocardiograms or pulse tracings were excluded. Informed consent was given by the study subjects, and the investigation was approved by the regional ethical committee. In order to compare the cardiovascular response in apparently healthy subjects to that of patients with coronary artery disease with or without myocardial ischaemia, the study subjects were grouped according to results of coronary arteriography and stress test. Hence, group 1 comprised 10 subjects, aged 44–61 years, with normal baseline physical examination, 12 channel electrocardiograms, and coronary arteriograms, and no echocardiographic evidence of myocardial ischaemia during stress test. Nine were referred for atypical chest pain, and one was evaluated before renal donation. Left ventricular regional and global function were normal on echocardiography. Group 2, comprised six patients, aged 54–70 years, with

angiographically identified coronary artery disease, but without evidence for myocardial ischaemia during stress test. One-, two-, and three-vessel disease was present in three, one, and one patients, respectively, whereas one had diffusely narrowed coronary arteries without distinct stenosis. Five patients were referred for silent ischaemia on ergometer exercise testing, and one for atypical chest pain. Group 3 comprized eight patients, aged 46–77 years, with angiographically identified coronary artery disease and definite echocardiographic evidence for myocardial ischaemia during the test. All had multivessel coronary artery disease (i.e. four patients had two-, and four had three-vessel disease). Six patients were referred for silent ischaemia, and two for chest pain. Aorto-coronary bypass grafting had previously been performed in two patients in group 2, and in one in group 3. Two patients in group 2, and seven in group 3 had a history of previous myocardial infarction.

STUDY PROTOCOL

In order to perform the tests without influence from cardiovascular drugs, these were stopped at least four half-lives of each respective drug before the investigation. Coffee and tea were avoided on the date of study. Baseline recordings were obtained after at least 3 h fasting, and the stress test was performed with subjects resting in slight left lateral decubitus position. We followed the conventional procedure for high dose dipyridamole stress test (Picano *et al.,* 1986). Initially 0·56 mg dipyridamole per kg was infused over 4 min. If no obvious wall motion abnormality was observed during the next 4 min, a second bolus of 0·28 mg dipyridamole per kg was infused over the following 2 min (see also Fig. 4). Peak stress recordings were usually obtained at approximately 12 min of test time and aminophylline (90–150 mg), an adenosine receptor blocker, was thereafter infused over 2–5 min in order to reverse the dipyridamole effect promptly (Sollevi *et al.,* 1984). Echocardiographic imaging of the left ventricle was continuously performed during the test, and 12 channel electrocardiograms and brachial artery blood pressures were recorded every 2 min.

NONINVASIVE DATA RECORDING

The setup for data recording has been described previously (Aakhus *et al.,* 1993a). Briefly, an ultrasound scanner (CFM 750, Vingmed Sound, Horten, Norway) was used with a duplex probe for echocardiographic imaging (3·25 MHz) and Doppler velocity recordings (2·5 MHz), as well as for display of the external pulse tracing. The scanner was interfaced via a delta port (NB-Dio-24, National Instruments, Austin TX, USA) to a computer (Macintosh II series, Apple Computers, Cupertino, CA, USA) for transfer of digital ultrasound data.

Three conventional long axis image views of the left ventricle (i.e. four-chamber, two-chamber, and long axis) were obtained by echocardiography from the apical position, and transferred as cineloops to the computer. A cineloop comprises the sequential

ultrasound images recorded during one cardiac cycle. This technique allows replay of the cineloops on the computer for analysis without loss of image quality and with high temporal resolution (i.e. 47 frames s^{-1} with typical sector angle and depth). Aortic annulus diameter was measured on a parasteinal long axis echocardiogram at the base of the aortic valve leaflets with the trailing-to-leading-edge method. The average of 3 repeated diameter measurements at baseline was used in calculations of the aortic annulus cross-sectional area, assuming a circular and constant orifice during the test (Christie *et al.*, 1987). Aortic annulus blood flow velocities were recorded with pulsed Doppler from the apical position. The ultrasound beam was aligned with the central blood flow direction with sample volume positioned at the aortic annular level as defined by the valve closure click. The right subclavian arterial pressure pulse was recorded with an external transducer (120–0132, Irex Medical Systems, Ramsey, NJ, USA) with a capillary damped funnel (Siemens-Elema AB, Solna, Sweden) manually positioned over the artery in the right supraclavicular region. The echocardiographic imaging and Doppler velocity recordings were performed by one investigator and the external pulse tracing by another for all examinations. The analog signals were converted to digits at 200 Hz. At least five cardiac cycles with simultaneously recorded pulse tracing, Doppler velocities, and a lead III electrocardiogram were then transferred to the computer. In immediate succession, duplicate brachial artery blood pressures were obtained with an oscillometric manometer (UA 751, Takeda Medical Inc., Tokyo, Japan). The averaged pressure was used in subsequent calculations, however, the pressure measurements were repeated if they differed by more than 10 mmHg. All study subjects underwent left heart cardiac catheterization with selective coronary arteriography (Judkins' technique). A diameter reduction of at least 50% in one of the major coronary vessels was considered significant. The angiograms were examined without knowledge of the result of the dipyridamole echocardiography stress test.

ANALYSIS

The digital two-dimensional left ventricular images (cineloops) from baseline and peak stress, were interpreted more than 4 weeks after the day of study by one investigator who was blinded for results of coronary arteriography and patient data. A wall motion score index, based on movement and thickening of the myocardium (normal motion=1, reduced motion=2, no motion=3, systolic outward motion=4, and systolic and diastolic deformation=5), was calculated by use of a 16 segment model (Schiller *et al.*, 1989) of the left ventricle (Fig. 1). With this classification a normal left ventricle has wall motion score index 1·00, whereas one with severe wall motion abnormalities typically has an index above 2·00. The stress test was considered positive of myocardial ischaemia if new or worsened wall motion abnormality occurred on echocardiography in at least one segment during test. The inter-observer reproducibility for assessment of positive vs. negative tests is 94% at our laboratory (Bjoernstad *et al.*, 1993). Left ventricular volumes were determined in specially designed software using an algorithm for three-

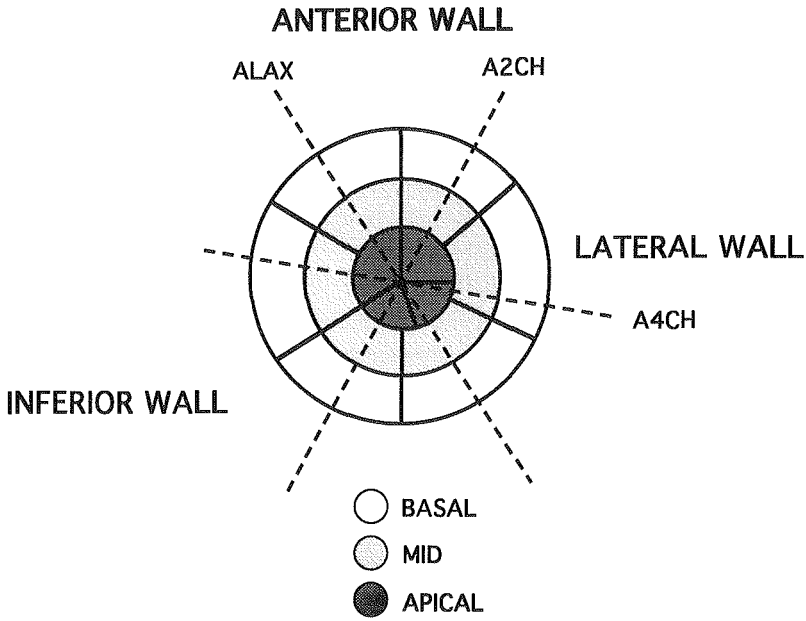

Fig. 1. Graphic representation of the left ventricle as divided into 16 myocardial segments for visual evaluation of regional wall motion. The dotted lines indicate the orientation of the three conventional long axis ultrasound image planes: apical long axis (ALAX), apical 2 chamber (A2CH), and apical 4 chamber (A4CH). Basal, mid, and apical refer to anatomical levels of the ventricle. Note that all segments can be assessed with these three image planes.

dimensional reconstruction of the endocardial surface (Aakhus *et al.*, 1994) on the manually traced endocardial contours of the three long axis apical image planes. End-diastole was defined at the peak of R-wave, and end-systole was defined as the last frame in the cineloop before first mitral valve opening. Ejection fraction was determined as end-diastolic minus end-systolic over end-diastolic volume.

At least three cardiac cycles with technically adequate pulse tracing and Doppler signals were selected for analysis. In order to provide noninvasive estimates of the aortic root pressure curve, the pulse tracing was calibrated with the oscillometrically determined systolic and diastolic brachial artery pressures (Colan *et al.*, 1985; Aakhus *et al.*, 1993b). The Doppler time-velocity integral was obtained by manual tracing of peak blood flow velocities during systole and at zero-line in diastole, with end-systole defined at the start of the aortic valve closure click. The Doppler velocity trace and the calibrated pulse tracing were then processed in a specially designed computer software operating under a general program for handling of digital ultrasound data (EchoDisp 3.0, Vingmed Sound). The pressure and flow traces from the selected cardiac cycles were low-pass filtered at 50 Hz, signal averaged, and corrected for pulse transmission-time from the aortic root to the subclavian artery by alignment of the pulse trace incisura with end-systole on the Doppler recording. Mean arterial pressure was determined as the integral of the averaged calibrated pulse curve over the average cardiac cycle length. The aortic root volume flow curve was obtained as the product of the averaged aortic

annular Doppler time-velocity integral and cross-sectional area (Skjærpe *et al.*, 1985), and stroke volume determined by integrating this curve over cardiac cycle length. Cardiac output was obtained as the product of stroke volume and heart rate, and corresponding indexes calculated by dividing with body surface area.

The properties of the systemic arteries were evaluated by use of an electric analog representation of the circulation with three parameters (Fig. 2): resistance, compliance, and characteristic impedance (Westerhof *et al.*, 1971). By use of this relatively simple model, equations can be derived that allows the parameters to be estimated from pressure and flow data recorded at the system inlet (i.e. aortic root). When translated to the human circulation, resistance represents the arteriolar resistance, compliance represents the total volume compliance of the systemic arterial tree, and characteristic impedance represents the proximal arterial (i.e. aortic) resistance. The sum of peripheral and proximal arterial resistance equals total peripheral resistance. The present parameter estimation scheme (Aakhus *et al.*, 1993a) produces first an estimate of inlet pressure based on inlet flow data and initial parameter guesses. Subsequently, the mean square difference between the measured and estimated pressure curve is minimized by a nonlinear optimization algorithm.

Left ventricular external total power was computed as the integrated product of instantaneous aortic root pressure and flow over the cardiac cycle. Steady power was obtained as the product of mean aortic root pressure and flow over the cardiac cycle, in order to calculate oscillatory power as the difference between total and mean power (Laskey *et al.*, 1985). Then, the ratio between oscillatory and total power was calculated.

STATISTICS

Continuous variables are presented with means and standard deviation (SD) or standard error of the mean, as indicated. The difference between baseline and peak dipyridamole was assessed with a two-sided *t*-test for paired data. Comparisons of group differences were made with one-factor analysis of variance with significance level set at 0·05 (Fisher PLSD test). Relation between variables was assessed with linear regression.

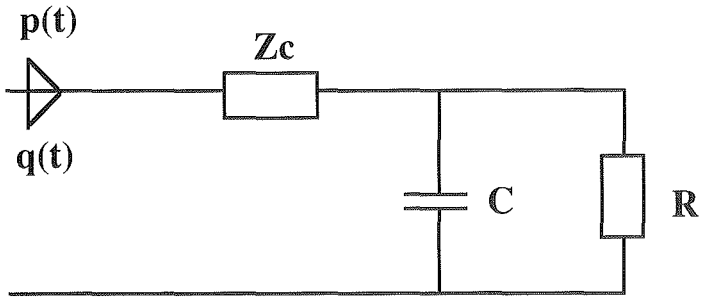

Fig. 2. Electric analog representation of the three-element windkessel model of the systemic circulation. Input variables are aortic root pressure (p) and flow (q) as functions of time (t). Systemic arterial parameters to be estimated are total arterial compliance (C), peripheral arterial resistance (R), and aortic characteristic impedance (Zc).

Results

No complications occurred during the tests and the protocol was completed in all patients, however, minor side effects were relatively common: light headache (seven subjects), shortness of breath (two subjects), flushing (one subject), and nausea (one subject).

BASELINE GROUP CHARACTERISTICS

At baseline, left ventricular end-diastolic and end-systolic volumes (Table 1) were significantly greater in group 3 than in group 1 (ANOVA $P<0{\cdot}05$), and ejection fraction trended to be lower (group 1 mean±SD: 62±6% vs. group 3: 53±10%, ANOVA $P=0{\cdot}10$). The per cent oscillatory power tended to be higher in group 2 than in 3 (ANOVA $P=0{\cdot}08$). Otherwise, the three groups had similar baseline haemodynamics. The inverse relationship between baseline left ventricular ejection fraction and severity of wall motion abnormality is shown in Fig. 3.

LEFT VENTRICULAR FUNCTION DURING STRESS TEST

During the first 6 min of the stress test, heart rate increased linearly from baseline, then remained constant until the second dipyridamole bolus was infused between 8 and 10 min, and raised heart rate further (Fig. 4). At peak stress, heart rate was increased by 35% in group 1, by 30% in group 2, and by 41% in group 3 (Table 1). Left ventricular regional wall motion, i.e. wall motion score index, was not changed during the test in

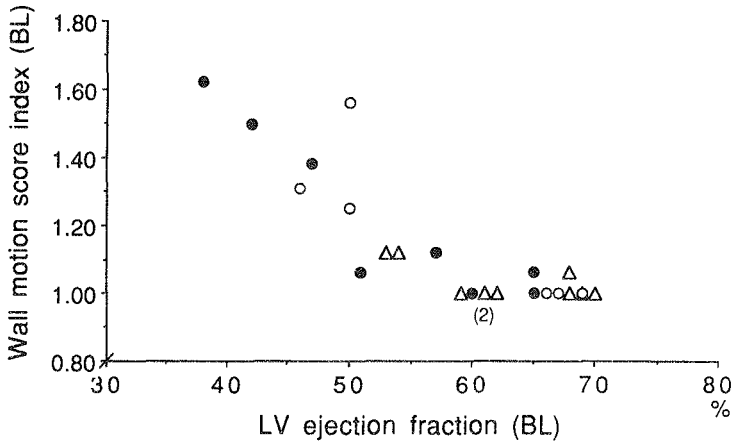

Fig. 3. Plot of baseline (BL) left ventricular (LV) ejection fraction, at abscissa, vs. BL wall motion score index, at ordinate, for all 24 study subjects. Triangles represent subjects with normal coronary arteries (group 1); open circles represent patients with coronary artery disease and no myocardial ischaemia during stress test (group 2); closed circles represent patients with coronary artery disease and myocardial ischaemia during stress test (group 3). Duplicate set of values is indicated by (2).

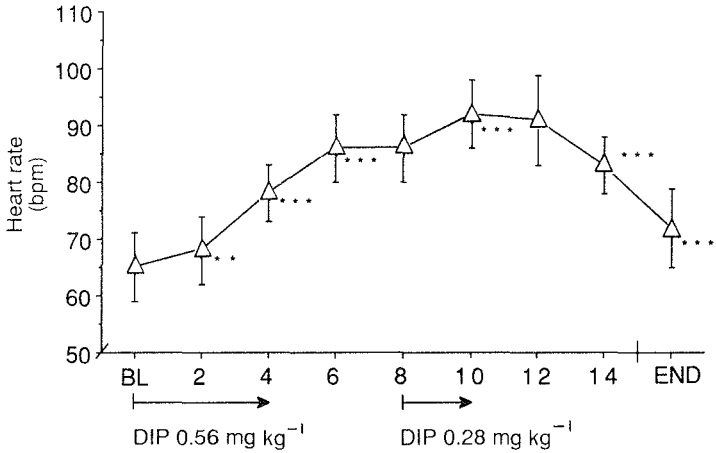

Fig. 4. Heart rate during dipyridamole (DIP) stress echocardiography in patients with normal coronary arteries (group 1). Numbers on abscissa represents minutes, and arrows indicate duration of DIP infusion. Aminophylline (90–150 mg) was infused over 2–5 min following peak stress, usually after 14 min. Triangles represent mean values, bars indicate 1 standard error. $^{**}P<0{\cdot}01$, $^{***}P<0{\cdot}01$ vs. previous value.

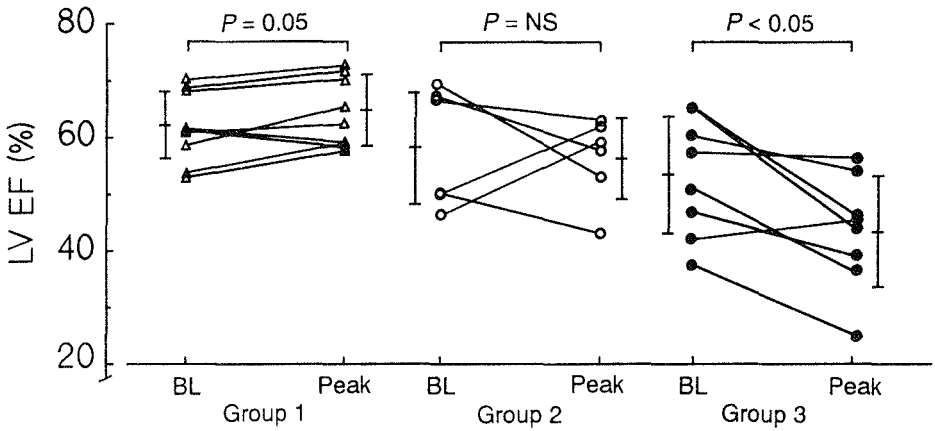

Fig. 5. Left ventricular ejection fraction (LV EF) at baseline (BL) and peak stress (PEAK) during dipyridamole echocardiography stress test in subjects with normal coronary arteries (group 1, triangles), in patients with coronary artery disease without myocardial ischaemia during test (group 2, open circles), and in patients with coronary artery disease and myocardial ischaemia during test (group 3, closed circles). Bars indicate mean ±1 SD.

group 1 or 2, whereas it deteriorated significantly in group 3. Left ventricular ejection fraction (Fig. 5) tended to improve from baseline to peak stress in group 1 (baseline: 62±6% vs. peak stress: 65±6%, $P=0{\cdot}05$), and was unchanged in group 2 (58±10% vs. 56±6%, $P=0{\cdot}72$), whereas it deteriorated significantly in group 3 (53±10% vs. 43±10%, $P<0{\cdot}05$). The impairment of left ventricular wall motion during peak stress (i.e. increase in wall motion score index) in this group, was not significantly related to the corresponding change in haemodynamic parameters or ejection fraction.

Table 1. Effects of dipyridamole on LV function

		Group 1 (n=10)	Group 2 (n=6)	Group 3 (n=8)
LV wall motion score index	BL	1·03±0·05	1·19±0·23	1·22±0·25
	PEAK	1·03±0·05	1·10±0·12	1·42±0·21**
End-diastolic volume index ($cm^3\ m^{-2}$)	BL	41±9	54±5	57±17
	PEAK	42±8	45±9	49±9
End-systolic volume index ($cm^3\ m^{-2}$)	BL	15±4	23±7	28±4
	PEAK	15±3	20±5	28±9
Heart rate ($b\ min^{-1}$)	BL	63±17	60±13	59±8
	PEAK	85±23***	78±21**	83±12***
Stroke index ($cm^3\ m^{-2}$)	BL	48±9	43±7	43±7
	PEAK	49±10	47±10	45±4
Cardiac index ($l\ min^{-1}\ m^{-2}$)	BL	3·0±0·9	2·5±0·3	2·5±0·6
	PEAK	4·1±1·2***	3·7±1·3*	3·7±0·7***
Total power (mW)	BL	1236±357	1078±352	1113±368
	PEAK	1802±512***	1735±950*	1629±413**
Steady power (mW)	BL	1018±326	849±306	925±308
	PEAK	1515±479***	1386±796*	1391±379**
Oscillatory power (mW)	BL	218±57	229±62	188±66
	PEAK	288±72**	349±157	238±52
% Oscillatory power	BL	18±5	21±4	17±2
	PEAK	16±4	19±4	15±3

Values are means±SD. Group 1 comprised subjects without coronary artery disease; Group 2 and 3 comprised patients with coronary artery disease with stress test negative (group 2) and positive (group 3) of myocardial ischaemia, respectively. LV, Left ventricular; BL, baseline; PEAK, peak dipyridamole; *P<0·05, **P<0·01, ***P<0·001 BL vs. PEAK.

Stroke index at peak stress was not different from baseline in any of the groups, however, cardiac index was increased by 37% in group 1, and by 48% in groups 2 and 3. Total external power at peak stress was increased by 46% in groups 1 and 3, and by 61% in group 2. Of similar magnitude were the changes in steady power (group 1: 49%, group 2: 63%, and group 3: 50%), whereas oscillatory power increased slightly less and was significant for group 1 (32%) only. The numerical decrease in percent oscillatory power at peak stress in all groups, was not statistically significant. The changes in these parameters were not significantly different between the groups. Ischaemic electrocardiographic abnormalities (i.e. at least 1 mm ST depression) during test were present in four patients in group 3, whereas it did not occur in group 1 or 2. Two patients in group 2, and three in group 3 experienced chest pain during test.

SYSTEMIC HAEMODYNAMICS DURING STRESS TEST

Systemic arterial pressures at peak stress were maintained at or slightly above baseline levels in all three groups (Table 2). Peripheral resistance was significantly lower at peak

Table 2. Effects of dipyridamole on systemic arterial parameters

		Group 1 (n=10)	Group 2 (n=6)	Group 3 (n=8)
Systolic pressure (mmHg)	BL	120±14	116±16	124±17
	PEAK	128±19*	121±14	121±13
End-systolic pressure (mmHg)	BL	98±11	93±13	106±16
	PEAK	100±15	91±11	100±12
End-diastolic pressure (mmHg)	BL	66±11	62±11	67±7
	PEAK	69±12	63±12	68±8
Mean arterial pressure (mmHg)	BL	89±13	83±13	91±11
	PEAK	97±16*	88±15	93±11
Peripheral resistance (dyn s cm^{-5})	BL	1337±321	1366±133	1562±329
	PEAK	1045±333**	1012±274*	1051±145***
Total arterial compliance (cm^3 $mmHg^{-1}$)	BL	1·49±0·45	1·72±0·64	1·50±0·67
	PEAK	1·32±0·45	1·83±0·84	1·42±0·52
Characteristic impedance (dyn s cm^{-5})	BL	130±53	151±59	115±53
	PEAK	127±64	147±47	103±43

Values are means±SD. Abbreviations as in Table 1.

ress (group 1: 22%, group 2: 26%, and group 3: 33%) than at baseline, whereas total rterial compliance and aortic characteristic impedance were not significantly altered, lthough the individual response varied. The change in these parameters were not gnificantly different between the groups.

Discussion

his noninvasive study shows that systemic arterial pressures were maintained at or ightly above baseline levels during stress test with infusion of dipyridamole 0·84 mg g^{-1}, irrespective of the absence or presence of coronary artery disease or myocardial chaemia. In all groups cardiac index was substantially augmented at peak stress due to ne raised heart rate. This tachycardia does not occur during intracoronary infusions of ipyridamole (Marchant *et al.,* 1986), and is therefore most likely due to reflex increase a sympathetic nervous system activity following the systemic vasodilatation. Heart rate creased linearly during the first 6 min of stress test but were thereafter constant until ne second dipyridamole bolus was infused between 8 and 10 min (Fig. 4). Thus, a more near cardiovascular response could potentially be obtained by infusing the second olus between 6 and 8 min, rather than between 8 and 10 min, as we did.

EFT VENTRICULAR FUNCTION

he normal left ventricular response at peak stress, was a slight improvement of ejection action (group 1). In patients with coronary artery disease without ischaemia during

test (group 2), the response was less consistent and the group mean for ejection fraction was not significantly changed by dipyridamole. In most patients with myocardial ischaemia at peak stress (group 3), ejection fraction was concordantly decreased. The change in regional wall motion and ejection fraction during test in group 3 were, however, not significantly related to the corresponding change in haemodynamic parameters. This may be explained first by the relatively moderate worsening of regional wall motion abnormality: the average increase in score index was 0·20, and represents for example new hypokinesia in 3 of the 16 myocardial wall segments, or new akinesia in two. This indicates that myocardial ischaemia was present in a relatively limited region of the ventricular wall. Second, left ventricular function improves during systemic vasodilatation, which occurred in all patients, and by the increased coronary blood flow (Abel & Reis, 1970) following dipyridamole infusion (Gould, 1978). In the present study, these factors balanced the ischaemic influence on the myocardium, and arterial pressure and stroke volume were maintained and cardiac output increased.

Left ventricular total external power represents the energy loss during transport of blood from the left ventricle to the tissues (O'Rourke, 1967) and is the sum of steady and oscillatory powers. The former is the energy loss related to steady blood flow, and the latter the energy lost in arterial pulsations. Infusion of dipyridamole 0·84 mg kg^{-1} increased left ventricular total power in all groups predominantly due to the augmentation of steady power which were related to the increased cardiac output while arterial blood pressure were maintained relatively constant. The increases in cardiac output and external power during dipyridamole test were not significantly different between the groups. This indicates that these parameters did not adequately reflect myocardial ischaemia during test, and that analysis of regional wall motion is the preferable method. This is consistent with the results of other investigators who used Doppler indexes of left ventricular function during dipyridamole stress testing to detect coronary artery disease (Grayburn *et al.*, 1989; Mazeika *et al.*, 1991). However, when Doppler indexes are combined with ultrasound image data, the sensitivity for coronary artery is better than that of image analysis alone (Labowitz *et al.*, 1988; Agati *et al.*, 1990). Myocardial ischaemia induces wall motion abnormalities before electrocardiographic abnormalities (Hauser *et al.*, 1985), as indicated by the four subjects in group 3 who had new wall motion abnormalities at peak stress, but no ST segment changes.

SYSTEMIC ARTERIAL PROPERTIES

The present study shows that dipyridamole did not significantly alter aortic characteristic impedance or total arterial compliance, but reduced peripheral resistance substantially. This implies that dipyridamole predominantly acts on the arteriolar level but little on large systemic arteries. A similar relation exists in the coronary circulation where dipyridamole dilates small resistance arteries more than conductive epicardial vessels (Fam & McGregor, 1968). In the systemic circulation, the vasodilators isoproterenol, nitroprusside, and nitroglycerine do not alter characteristic impedance significantly

(Gundel *et al.*, 1981; Yin *et al.*, 1983; Latson *et al.*, 1988). These results and ours, indicate that vasodilators in clinical doses do not influence aortic stiffness to any significant degree. Their main action is on the arterioles.

The percent oscillatory power, represents an inverse index of the efficiency of coupling between heart and arteries (O'Rourke, 1967). This efficiency increases (i.e. per cent oscillatory power decreases) with increasing aortic distensibility and heart rate, and decreases with increasing cardiac output and systemic vasodilatation. In the present study, percent oscillatory power was not changed significantly from baseline to peak stress in any group during dipyridamole, most likely because the substantial vasodilatation and augmented cardiac output balanced the effect of tachycardia.

METHODOLOGICAL CONSIDERATIONS

In the present study brachial artery pressures were measured by oscillometry. This method may be inaccurate during arrhythmias, however, all subjects were in sinus rhythm at baseline and during the test. The three-element windkessel model is a very simple representation of the systemic circulation. We have previously (Aakhus *et al.*, 1993a) shown that our parameter estimation scheme is appropriate in the sense that input pressure measurements can be predicted with acceptable precision.

Dipyridamole echocardiography stress test has a sensitivity for coronary artery disease that compares with exercise electrocardiography and is slightly below that of scintigraphic techniques (Picano, 1989). The sensitivity increases with the number of diseased coronary vessels, and has been reported to be 50, 81, and 100% in one-, two-, and three-vessel disease, respectively (Picano *et al.*, 1986). The end-point of echocardiography stress test is new wall motion abnormality (i.e. myocardial ischaemia) which may require a more severe vessel stenosis than one producing flow heterogeneities that are detectable on scintigrams. In the present study, group 2 patients had coronary artery disease but no evidence of myocardial ischaemia during test. This may thus be due to the generally mild coronary artery disease in most of these patients, so that regional wall motion abnormalities that could be identified on echocardiography did not occur.

CONCLUSION

This noninvasive study indicates that dipyridamole acts predominantly on the arterioles without significantly influencing the large systemic arteries. In spite of the substantial systemic vasodilatation during stress testing with dipyridamole 0·84 mg kg^{-1}, arterial pressures were maintained due to the heart rate driven augmentation of cardiac output. Left ventricular ejection fraction at peak stress was slightly increased in healthy subjects, whereas it decreased significantly in patients with myocardial ischaemia. Otherwise the haemodynamic response was similar in patients without and with coronary artery disease, and in those without and with myocardial ischaemia during test.

Acknowledgment

This investigation was supported by a grant from the Norwegian Council on Cardiovascular Diseases (Oslo, Norway).

References

AAKHUS S., SOERLI C., FAANES A., HAUGER S. O., BJOERNSTAD K., HATLE L. & ANGELSEN B. A. J. (1993a) Noninvasive computerized assessment of left ventricular performance and systemic haemodynamics by study of aortic root pressure and flow estimates in healthy men, and men with acute and healed myocardial infarction. *Am J Cardiol,* **72,** 260–267.

AAKHUS S., TORP H., HAUGLAND T. & HATLE L. (1993b) Noninvasive estimates of aortic root pressures: external subclavian arterial pulse tracing calibrated by oscillometrically determined brachial arterial pressures. *Clin Physiol,* **13,** 573–586.

AAKHUS S., MÆHLE J. & BJOERNSTAD K. (1994) A new method for echocardiographic computerized three-dimensional reconstruction of left ventricular endocardial surface: *in vitro* accuracy and clinical repeatability of volumes. *J Am Soc Endocardiogr* (in press).

ABEL R. M. & REIS R. L. (1970) Effects of coronary blood flow and perfusion pressure on left ventricular contractility in dogs. *Circ Res,* **27,** 961–971.

AGATI L., ARATA L., NEJA C. P., MANZARA C., VIZZA C. D., PENCO M., FEDELE F. & DAGIANTI A. (1990) Usefulness of the dipyridamole-Doppler test for diagnosis of coronary artery disease. *Am J Cardiol,* **65,** 829–834.

BELLER G. A. (1989) Dipyridamole thallium-201 scintigraphy: an excellent alternative to exercise scintigraphy. *J Am Coll Cardiol,* **14,** 1642–1643.

BJOERNSTAD K., AAKHUS S., LUNDBOM J., BOLZ K., ROKSETH R., SKJAERPE T. & HATLE L. (1993) Digital dipyridamole stress echocardiography in silent ischaemia after coronary artery bypass grafting and/or after healing of acute myocardial infarction. *Am J Cardiol,* **72,** 640–646.

CASTELLO R. & LABOWITZ A. J. (1992) Dipyridamole echocardiography. *Echocardiography,* **9,** 117–128.

CHRISTIE J., SHELDAHL L. M., TRISTANI F. E., SAGAR K. B., PTACIN M. J. & WANN S. (1987) Determination of stroke volume and cardiac output during exercise: comparison of two-dimensional and Doppler echocardiography, Fick oximetry, and thermodilution. *Circulation,* **76,** 539–547.

COLAN S. D., BOROW K. M. & NEUMANN A. (1985) Use of calibrated carotid pulse tracing for calculation of left ventricular pressure and wall stress throughout ejection. *Am Heart J,* **109,** 1306–1310.

FAM W. M. & MCGREGOR M. (1968) Effect of nitroglycerin and dipyridamole on regional coronary resistance. *Circ Res,* **12,** 649–659.

FELDMAN R. L., NICHOLS W. W., PEPINE C. J. & CONTI R. (1981) Acute effect of intravenous dipyridamole on regional coronary haemodynamics and metabolism. *Circulation,* **64,** 333–344.

GOULD K. L. (1978) Noninvasive assessment of coronary stenoses by myocardial perfusion imaging during pharmacologic coronary vasodilatation. I. Physiologic basis and experimental validation. *Am J Cardiol,* **41,** 267–278.

GOULD K. L., WESTCOTT R. J., ALBRO P. C. & HAMILTON G. W. (1978) Noninvasive assessment of coronary stenoses by myocardial imaging during pharmacologic coronary vasodilatation. II. Clinical methodology and feasiblity. *Am J Cardiol,* **41,** 279–287.

GRAYBURN P. A., POPMA J. J., PRYOR S. L., WALKER B. S., SIMON T. R. & SMITHERMAN T. C. (1989) Comparison of dipyridamole-Doppler echocardiography to thallium-201 imaging and quantitative coronary arteriography in the assessment of coronary artery disease. *Am J Cardiol,* **63,** 1315–1320.

GUNDEL W., CHERRY G., RAJAGOPALAN B., TAN L., LEE G. & SCHULTZ D. (1981) Aortic input impedance in man: acute response to vasodilator drugs. *Circulation,* **63,** 1305–1314.

HAUSER A. M., GANGADHARAN V., RAMOS R. G., GORDON S. & TIMMIS G. C. (1985) Sequence of mechanical, electrocardiographic and clinical effects of repeated coronary artery occlusion in human beings: echocardiographic observations during coronary angioplasty. *J Am Coll Cardiol,* **5,** 193–197.

LABOWITZ A. J., PEARSON A. C. & CHAITMAN B. R. (1988) Doppler and two-dimensional echocardiographic assessment of left ventricular function before and after intravenous dipyridamole stress testing for detection of coronary artery disease. *Am J Cardiol,* **62,** 1180–1185.

LASKEY W. K., KUSSMAUL W. G., MARTIN J. L., KLEAVELAND J. P., HIRSHFELD J. W. & SHROFF S. (1985) Characteristics of vascular hydraulic load in patients with heart failure. *Circulation,* **72,** 61–71.

LATSON T. W., HUNTER W. C., KATOH N. & SAGAWA K. (1988) Effect of nitroglycerine on aortic impedance, diameter, and pulse-wave velocity. *Circ Res,* **62,** 884–890.

MARCHANT E., PICHARD A., RODRIGUEZ J. A. & CASANEGRA P. (1986) Acute effect of systemic versus intracoronary dipyridamole on coronary circulation. *Am. J Cardiol,* **57,** 1401–1404.

MAZEIKA P., NIHOYANNOPOULOS P., JOSHI J. & OAKLEY C. M. (1991) Evaluation of dipyridamole-Doppler echocardiography for detection of myocardial ischaemia and coronary artery disease. *Am J Cardiol,* **68,** 478–484.

O'ROURKE M. F. (1967) Steady and pulsatile energy losses in the systemic circulation under normal conditions and in simulated arterial disease. *Cardiovasc Res,* **1,** 313–326.

PICANO E., LATTANZI F., MASINI M., DISTANTE A. & L'ABBATE A. (1986) High dose dipyridamole echocardiography test in effort angina pectoris. *J Am Coll Cardiol,* **8,** 848–854.

PICANO E. (1989) Dipyridamole-echocardiography test: historical background and physiological basis. *Eur Heart J,* **10,** 365–376.

SCHILLER N. B., SHAH P. M., CRAWFORD M., DEMARIA A., DEVEREUX R., FEIGENBAUM H., GUTGESELL H., REICHEK N., SAHN D., SCHNITTGER I., SILVERMAN N. H. & TAJIK A. J. (1989) Recommendations for quantitation of the left ventricle by two-dimensional echocardiography. *J Am Soc Echocardiogr,* **2,** 358–367.

SKJÆRPE T., HEGRENÆS L. & IHLEN H. (1985) Cardiac output. In *Doppler Ultrasound in Cardiology,* pp. 306–320. (eds Hatle L. & Angelsen B. A.), Lea & Febiger, Philadelphia.

SOLLEVI A., ØSTERGREN J., FAGRELL B. & HJEMDAHL P. (1984) Theophylline antagonizes cardiovascular responses to dipyridamole in man without affecting increases in plasma adenosine. *Acta Physiol Scand,* **121,** 165–171.

URSCHEL C. W., COVELL J. V., SONNENBLICK E. H., ROSS J. & BRAUNWALD E. (1968) Effects of decreased aortic compliance on performance of the left ventricle. *Am J Physiol,* **214,** 298–304.

WESTERHOF N., ELZINGA G. & SIPKEMA P. (1971) An artificial arterial system for pumping hearts. *J Appl Physiol,* **31,** 776–781.

YIN F. C. P., GUZMAN P. A., BRIN K. P., MAUGHAN W. L., BRINKER J. A., TRAILL T. A., WEISS J. L. & WEISFELDT M. L. (1983) Effect of nitroprusside on hydraulic vascular loads on the right and left ventricle of patients with heart failure. *Circulation,* **67,** 1330–1339.

Paper VI.

Aakhus S, Bjørnstad K, Hatle L. Cardiovascular response in patients with and without myocardial ischaemia during dobutamine echocardiography stress te for coronary artery disease. Clinical Physiology 1995;15:249-263.

Clinical Physiology (1995) **15**, 249–263

Cardiovascular response in patients with and without myocardial ischaemia during dobutamine echocardiography stress test for coronary artery disease

S. Aakhus, K. Bjørnstad and L. Hatle

Department of Medicine, Section of Cardiology, University Hospital, Trondheim, Norway

(Received 20 June 1994; accepted 16 November 1994)

Summary. Dobutamine is widely used in cardiac stress testing for coronary artery disease and myocardial viability. To assess the systemic cardiovascular response during dobutamine echocardiography stress testing, we investigated nine patients without myocardial ischaemia (group 1, aged 48 to 72 years) and nine patients with myocardial ischaemia during the test (group 2, aged 53 to 73 years), by use of Doppler/echocardiography and subclavian artery pulse trace calibrated with brachial artery pressures. Peripheral resistance, total arterial compliance, and aortic characteristic impedance were estimated using a 3-element windkessel model of the systemic circulation. During infusion of dobutamine up to 40 $\mu g\ kg^{-1}\ min^{-1}$, arterial pressure was maintained near baseline levels, whereas heart rate and cardiac index increased, more so in group 1 (mean: 89 and 79%) than in group 2 (58 and 52%; $P<0{\cdot}05$ vs. group 1). Peripheral resistance was decreased by $\geqslant$32% at peak stress, whereas characteristic impedance was maintained at or above baseline in both groups, and total arterial compliance was not significantly altered. The cardiovascular response in group 2 was not influenced by the wall motion abnormalities. Thus, in these patients the inotropic, chronotropic, and vasodilatory effects of dobutamine balanced the ischaemic impairment of left ventricular function during the stress test.

Key words: arteries, cardiac stress test, coronary artery disease, dobutamine, echocardiography, left ventricular function.

Introduction

The synthetic catecholamine dobutamine has routinely been used to enhance inotropy in patients with severe myocardial pump failure. More recently, dobutamine has been increasingly used in cardiac stress testing for evaluation of coronary artery disease

Correspondence: Svend Aakhus, MD, Medical Department, Section of Cardiology, Rikshospitalet, The National Hospital, N-0027 Oslo, Norway

(Berthe *et al.*, 1986; Salustri *et al.*, 1992) or myocardial viability (Pierard *et al.*, 1990). Dobutamine increases myocardial contractility and heart rate predominantly by stimulation of beta-1 adrenergic receptors (Ruffolo, 1987), and influences the arteries by stimulation of beta-2 and alpha-adrenoceptors (Ruffolo & Morgan, 1984). The haemodynamic response to low and medium infusion rates of dobutamine has been studied in patients with congestive heart failure (Leier *et al.*, 1979). During cardiac stress testing for coronary artery disease, high infusion rates of dobutamine (up to 40 $\mu g\ kg^{-1}\ min^{-1}$) are routinely used (Cohen *et al.*, 1991; Previtali *et al.*, 1991; Salustri *et al.*, 1992). The cardiovascular response during these routinely used tests has not been well defined.

The first aim of this study was therefore to assess by non-invasive means left ventricular function, systemic haemodynamics, and arterial properties during a conventional dobutamine echocardiography stress test in patients without congestive heart failure under evaluation for coronary artery disease. Systemic arterial properties were characterized by use of a 3-element windkessel model of the systemic circulation (Westerhof *et al.*, 1971). Secondly, we evaluated the relationship between dobutamine-induced myocardial ischaemia and the cardiovascular response.

Subjects and methods

SUBJECTS

The 18 study subjects (12 men and 6 women) were referred for routine dobutamine stress echocardiography testing in the evaluation of coronary artery disease. All patients gave their informed consent to participate in the study. Subjects with neck vessel bruit, baseline arterial blood pressure above 180/100 mmHg, aortic valvular disease, cardiac arrhythmias, bundle branch block, hypertrophic cardiomyopathy, unstable angina pectoris, recent myocardial infarction (within 2 months of stress test), severely impaired left ventricular function with echocardiographic ejection fraction below 40%, pulmonary congestion, or suboptimal echocardiograms and/or pulse tracings, were excluded from the study. All subjects were in sinus rhythm.

In order to assess the haemodynamic influence of myocardial ischaemia during the test, the patients were grouped according to the absence or presence of echocardiographic evidence of ischaemia at peak stress. Group 1 consisted of nine patients (aged 48 to 76 years) with stress tests providing negative evidence of myocardial ischaemia. Of these, seven were referred prior to non-cardiac vascular surgery, one was investigated because of chest pain, and one was referred because of silent ischaemia. Left ventricular wall motion abnormalities at baseline were present in seven patients, five of whom showed electrocardiographic evidence of previous myocardial infarction. Group 2 consisted of nine patients (aged 53 to 73 years) with stress tests providing positive evidence of ischaemia. Two of these patients were referred prior to non-cardiac vascular surgery, three were investigated because of angina pectoris, and four because of silent ischaemia. Wall motion abnormalities were present in eight patients at baseline, seven of whom showed electrocardiographic evidence of previous infarction. In group 2, coronary

arteriography demonstrated 1-, 2-, or 3-vessel coronary artery disease in two, one and six patients, respectively. Beta-adrenergic blockers, calcium channel antagonists, or nitrates were used by three, four, and two patients, respectively, in group 1, and by five, four, and six, respectively, in group 2. Medication was not taken on the day of the stress test.

METHODS

Stress test protocol. Baseline recordings were obtained after fasting for at least 3 h, and the stress test was performed with the patient in a slight left lateral decubitus position. Dobutamine was administered intravenously with incrementally increased infusion rates of 5, 10, 15, 20, 30, and finally 40 $\mu g\ kg^{-1}\ min^{-1}$, where each increment lasted for 4 min. The end-point of the test (peak stress) was defined as the occurrence of: (1) new or worsened left ventricular regional wall motion abnormality; and/or (2) heart rate $\geq$85% of age-determined maximum (ie 220−age in years); and/or (3) severe hypertension with either systolic or diastolic blood pressure above 200 and 110 mmHg, respectively; and/or (4) significant patient discomfort. Echocardiographic imaging of the left ventricle was performed continuously during the test, and a 12-channel electrocardiogram and brachial artery blood pressures were recorded at 2-min intervals.

Non-invasive data recording. The protocol has been described previously (Aakhus *et al.*, 1993a). Briefly, an ultrasound duplex scanner (CFM 750, Vingmed Sound, Horten, Norway) was used for echocardiographic imaging and Doppler flow recordings, as well as for display of the external subclavian artery pulse tracing. The latter was recorded with an external pulse transducer (Irex 120-0132, Irex Medical Systems, Ramsey, NJ, USA) with a capillary damped funnel (Siemens-Elema AB, Solna, Sweden) manually positioned in the medial right supraclavicular region. The scanner was interfaced via a data port (NB-DIO-24, National Instruments, Austin, TX, USA) to a computer (Macintosh II series, Apple Computers, Cupertino, CA, USA) for digital transfer of scanline ultrasound image and flow data, pulse trace data, and a single vector electrocardiogram (usually lead III). Analogue signals were converted to digits at 200 Hz.

Three conventional echocardiographic apical imaging views were obtained of the left ventricle (ie 4-chamber, long axis, and long-axis 2-chamber), and the systolic images recorded at baseline and during the last minute of peak stress were transferred as cineloops to the computer. A cineloop consists of sequentially recorded digital ultrasound images during the 450 ms following the R-wave peak.

Aortic annulus diameter was measured in triplicate at baseline, and the average diameter was used for calculation of annulus cross-sectional area, assuming a circular and constant orifice throughout the test (Christie *et al.*, 1987). Aortic annulus blood flow velocities were recorded with pulsed Doppler from the apical position with the ultrasound beam aligned with central blood flow direction and the sample volume positioned at aortic annular level. Doppler echocardiography was performed by one investigator and the external pulse tracing by another during all examinations. At baseline and during

the last minute of each increase in dobutamine infusion rate, data from at least five cardiac cycles consisting of pulse tracing, Doppler flow velocities, and a 1-lead electrocardiogram were transferred to the computer. Concordantly, right brachial artery blood pressures were recorded in duplicate using the oscillometric technique (UA 751, Takeda Medical Inc., Tokyo, Japan), and averaged for subsequent use in analysis.

On clinical indication, all patients in group 2 underwent left heart catheterization with selective coronary arteriography (Judkins' technique). The arteriograms were studied without knowledge of the result of the stress echocardiography test. A diameter reduction of at least 50% in one of the major coronary vessels was considered to be significant. Coronary arteriography was not performed in group 1 subjects.

Analysis. On the computer, the baseline and peak stress cineloops were compared side by side and replayed with maintained high temporal resolution (usually 47 frames s^{-1} with typical sector and depth settings) and image quality. Left ventricular wall motion at baseline and at peak stress was interpreted by one investigator who evaluated myocardial motion and thickening from the cineloops, and assigned a score to each of 16 left ventricular segments (Schiller *et al.*, 1989). The investigator was blinded with regard to patient data and the results of coronary arteriography and stress test. A normally contracting ventricle has a wall motion score index of 1·00, whereas a ventricle with severe wall motion abnormality typically has a score greater than 2·00. A test result was considered to be positive evidence of myocardial ischaemia if a new or progressing wall motion abnormality was observed during the test in at least one segment. We have an inter-observer agreement of 94% for evaluation of wall motion abnormality (ie positive vs. negative test) during stress echocardiography (Bjoernstad *et al.*, 1993).

An estimate of the aortic root pressure curve was obtained by calibrating the subclavian artery pulse tracing with the brachial artery pressures (Aakhus *et al.*, 1993b). Mean arterial pressure was obtained as the integral of this pressure curve over the cardiac cycle. The Doppler time-velocity curve was determined on the computer by tracing of aortic annular maximal flow velocities, which are more repeatable than mean velocities and less influenced by errors in sample volume positioning (Brubakk & Gisvold, 1982). End-systole was defined at aortic valve closure click. The aortic annular volume flow curve was obtained by multiplying the instantaneous flow velocities by the annular cross-sectional area. Stroke volume was then determined as the integral of the volume flow curve over cardiac cycle length, and cardiac output was calculated as the product of stroke volume and heart rate. Corresponding indexes were calculated by dividing by the body surface area. The properties of the systemic arteries were evaluated by use of an electric analogue representation of the systemic circulation with three parameters (Westerhof *et al.*, 1971). The non-invasive aortic root pressure and flow data were entered into the model and used to estimate resistance, compliance, and characteristic impedance (Aakhus *et al.*, 1993a). In the human systemic circulation, resistance represents peripheral arteriolar resistance, compliance represents the total volume compliance of the systemic arterial tree, and characteristic impedance represents the proximal arterial (ie aortic) resistance to left ventricular ejection of blood. The sum of

resistance and characteristic impedance equals total peripheral resistance which by convention is determined as mean arterial pressure divided by cardiac output.

Left ventricular total external power represents the energy lost in transport of blood from the left ventricle to tissues, and was determined as the integrated product of aortic root pressure and flow over one cardiac cycle. Steady power, ie the energy lost during non-pulsatile transport of blood, was obtained as the product of mean aortic root pressure and flow. Oscillatory power represents the energy lost in vascular pulsations, and was calculated as the difference between total and steady power (Laskey *et al.*, 1985), and percentage oscillatory power was determined as the ratio between oscillatory and total powers (O'Rourke, 1967).

Left ventricular endocardial contours of the three apical imaging views were traced on the computer using the end-diastolic frame, ie that corresponding to the R-wave peak on the electrocardiogram, and left ventricular end-diastolic volume was determined by use of an algorithm for 3-dimensional estimation of the endocardial surface (Aakhus *et al.*, 1994).

Statistical analysis. Continuous variables are presented as mean values±standard deviation (SD) or standard error of the mean, as indicated. A paired 2-sided *t*-test and a Wilcoxon matched-pairs test were used, as appropriate, for comparison of variables at baseline and peak stress and for comparison of each dobutamine infusion rate with the previous one. An unpaired 2-sided *t*-test was used for comparisons between groups of patients. For assessment of the independent effects of dobutamine and myocardial ischaemia at peak stress, a two-factor analysis of variance for repeated measurements (ANOVA) was used. Linear regression analysis was used to assess correlations between variables. Standard statistical software (STATVIEW 512 and SUPERANOVA, Abacus Concepts, Berkeley, CA, USA) was used for computations on a personal computer (Macintosh II series).

Results

Peak stress was attained at equivalent dobutamine infusion rates in group 1 (mean value±SD: 33±7 $\mu g\ kg^{-1}\ min^{-1}$) and group 2 (34±10 $\mu g\ kg^{-1}\ min^{-1}$). In group 1, four patients attained peak infusion rate (40 $\mu g\ kg^{-1}\ min^{-1}$), whereas four patients attained maximal heart rate and one had symptomatic hypotension at lower infusion rates. In group 2, all tests were terminated due to new wall motion abnormalities during testing. In this group, one subject had ventricular ectopic beats in bigemini at 10 and 20 μg dobutamine $kg^{-1}\ min^{-1}$, and one had moderate nausea at peak stress. No other adverse reactions occurred during testing. Electrocardiographic evidence of myocardial ischaemia (ST depression≥1 mm) or anginal pain at peak stress was present in five and four patients in group 2, respectively, whereas one had new wall motion abnormalities only. None of the patients had electrocardiographic changes or anginal pain during testing in group 1.

LEFT VENTRICULAR FUNCTION AND SYSTEMIC HAEMODYNAMICS (TABLE 1)

In group 1, regional wall motion at peak stress was improved from baseline in three patients, although the group average was not significantly changed. In group 2, the impaired left ventricular regional wall motion at peak stress was reflected in the wall motion score index, which increased by 0·39±0·19 from baseline. In this group, six patients had both new and worsened wall motion abnormalities at peak stress, whereas three had only new abnormalities. Left ventricular end-diastolic volume decreased by 37% in group 1 from baseline to peak stress, and by 26% in group 2.

Heart rate increased significantly (ANOVA; $P<0·001$) and linearly with increasing dobutamine infusion rates above 5 μg kg^{-1} min^{-1} for group 1 and above 10 μg kg^{-1} min^{-1} for group 2 (Fig. 1), and at peak stress was increased more in group 1 (89%) than

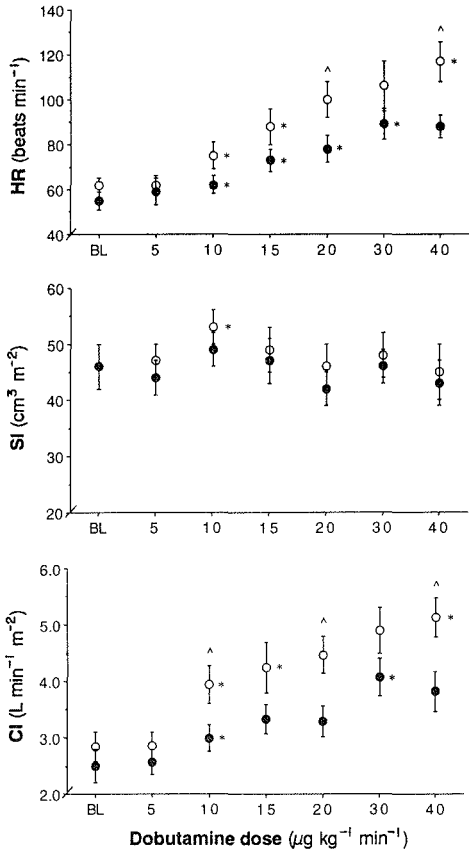

Fig. 1. Cardiac performance during dobutamine stress echocardiography. Heart rate (HR), top panel, stroke index (SI), middle panel, and cardiac index (CI), lower panel, for patients without (open circles) and with (closed circles) echocardiographic evidence of myocardial ischaemia during the test. Circles denote group means, and bars denote 1 standard error. Numbers at abscissa represent dobutamine infusion rate in μg kg^{-1} min^{-1}. BL, baseline. *$P<0·05$ vs. previous infusion rate within same group; ^$P<0·05$ for difference between the groups. The overall effect of dobutamine on HR and CI was significant at $P<0·001$ (analysis of variance), and the overall group difference for HR and CI showed borderline significance (ANOVA; $P=0·06$).

in group 2 (58%; $P<0{\cdot}05$). Stroke index increased by 15% from baseline to 10 μg dobutamine kg^{-1} min^{-1} (46±11 to 53±8 cm^3; $P<0{\cdot}05$) in group 1, whereas the change in group 2 (46±12 to 49±9 cm^3) was not significant (Fig. 1). With higher infusion rates, stroke index returned to baseline values in both groups. Cardiac index increased significantly (ANOVA; $P<0{\cdot}001$) with increasing dobutamine infusion rates above 5 μg kg^{-1} min^{-1} in both groups (Fig. 1), and was increased more in group 1 at peak stress (79%) than in group 2 (52%; $P<0{\cdot}05$), corresponding to the difference in heart rate response.

Left ventricular total power increased significantly (ANOVA; $P<0{\cdot}001$) with increasing dobutamine infusion rates above 5 μg kg^{-1} min^{-1} in both groups (Fig. 2), due to the increase in steady (ANOVA; $P<0{\cdot}001$) and oscillatory powers (ANOVA; $P<0{\cdot}001$), where the latter showed the greater relative increase. The increase in total power from baseline to stress was similar in groups 1 (88%) and 2 (75%). The % oscillatory power

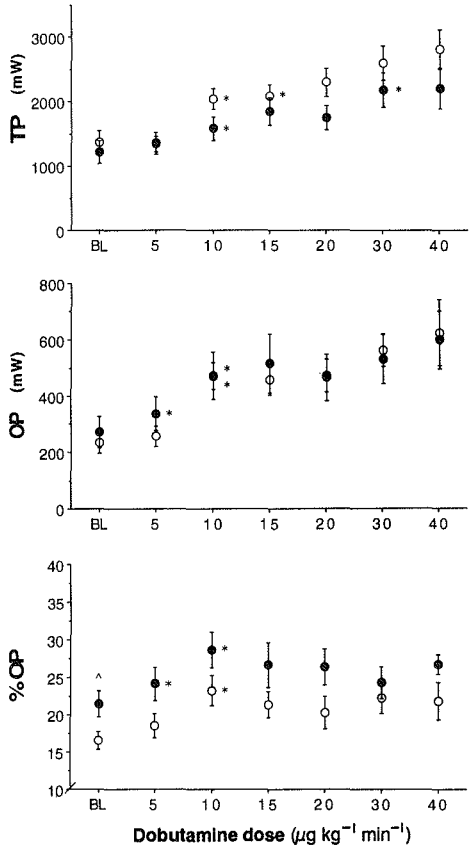

Fig. 2. External hydraulic power during dobutamine stress echocardiography. Total power (TP), top panel, oscillatory power (OP), middle panel, and % oscillatory power (the ratio between total and oscillatory powers), lower panel. Other symbols and abbreviations are as described in legend to Fig. 1. The overall effect of dobutamine on TP, OP, and %OP was significant at $P<0{\cdot}001$ (analysis of variance). Of these, only % OP was significantly different between the groups (ANOVA; $P<0{\cdot}05$).

Table 1. Effect of dobutamine on LV function and systemic haemodynamics in patients without (group 1) and with (group 2) myocardial ischaemia at peak stress

		Group 1 (n=9)	Group 2 (n=9)
Wall motion score index	BL	1·28±0·26	1·35±0·19
	PEAK	1·23±0·21	1·75±0·22**†
LV end-diastolic volume index ($cm^3\ m^{-2}$)	BL	59±20	57±13
	PEAK	37±12**	42±15**
Heart rate (beats min^{-1})	BL	62±10	55±13
	PEAK	117±23***	87±11***†
Stroke index ($cm^3\ m^{-2}$)	BL	46±11	46±12
	PEAK	44±11	44±10
Cardiac index ($l\ min^{-1}\ m^{-2}$)	BL	2·8±0·8	2·5±0·9
	PEAK	5·0±1·2***	3·8±0·7**†
Total power (mW)	BL	1374±519	1221±531
	PEAK	2583±859**	2133±608**
Oscillatory power (mW)	BL	234±111	273±166
	PEAK	521±225**	571±238**
% oscillatory power	BL	17±4	21±5
	PEAK	20±6	26±4*
Systolic arterial pressure (mmHg)	BL	128±24	128±22
	PEAK	136±19	146±28*
Diastolic arterial pressure (mmHg)	BL	73±12	64±8
	PEAK	71±11	66±11
Mean arterial pressure (mmHg)	BL	97±18	90±13
	PEAK	98±14	99±18

Mean values ± SD are shown. LV, left ventricular; BL, baseline; PEAK, peak stress; *P<0·05, **P<0·01, ***P<0·001 for difference between BL and PEAK; †P<0·05 for difference between the groups in change from BL to PEAK.

:aked at 10 μg dobutamine $kg^{-1}\ min^{-1}$, 41 and 34% above baseline for groups 1 and respectively (P<0·05 vs. baseline for both). At peak stress, % oscillatory power was gnificantly higher than baseline for group 2 only (24% increase; P<0·05). The % :cillatory power was significantly lower in group 1 than in group 2 at baseline and peak ress. Mean arterial pressure was maintained close to baseline levels in both groups ıring the test (Fig. 3), and was not significantly different from baseline at peak stress. 'stolic arterial pressure was at peak stress 14% above baseline in group 2, and was not gnificantly altered in group 1. Diastolic arterial pressures were not significantly al- red in either group.

Table 2. Effect of dobutamine on systemic arteries in patients without (group 1) and with (group 2) myocardial ischaemia at peak stress

		Group 1 (n=9)	Group 2 (n=9)
Peripheral resistance (dyn s cm^{-5})	BL	1449±390	1486±368
	PEAK	810±249***	1015±297**
Total arterial compliance (cm^3 mmHg^{-1})	BL	1·58±0·80	1·69±0·67
	PEAK	1·55±0·56	1·42±0·71
Characteristic impedance (dyn s cm^{-5})	BL	96±20	144±67
	PEAK	91±32	146±68

Mean values ± SD are shown. Abbreviations as in Table 1.

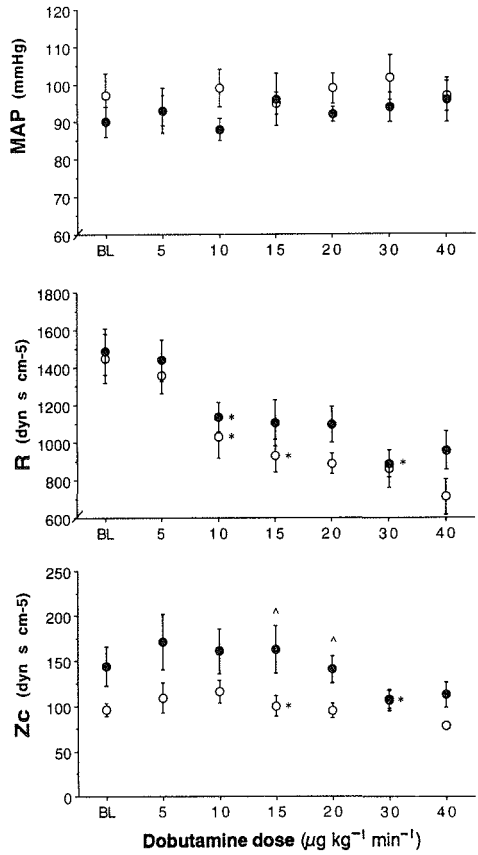

Fig 3. Systemic arterial parameters during dobutamine stress echocardiography. Mean arterial pressure (MAP), top panel, peripheral resistance (R), middle panel, and characteristic impedance (Zc), lower panel. R and Zc were estimated from aortic root pressure and flow data by use of a 3-element windkessel model of the systemic circulation. Other symbols and abbreviations are as described in legend to Fig. 1. The overall effect of dobutamine on R and Zc was significant at $P<0·001$ and $P<0·05$, respectively (analysis of variance). Of these, only Zc was significantly different between the groups (ANOVA; $P\subset 0·05$).

SYSTEMIC ARTERIAL PROPERTIES

Peripheral resistance was significantly decreased in both groups at 10 μg dobutamine kg^{-1} min^{-1} (Fig. 3), and was at peak stress 44 and 32% below baseline in groups 1 and 2, respectively (Table 2). In group 2, total arterial compliance was reduced at 15 μg dobutamine kg^{-1} min^{-1} (1·25±0·41 vs. baseline; 1·69±0·67 cm^3 $mmHg^{-1}$; $P<0·05$), and returned to baseline values with higher infusion rates. Total arterial compliance was not significantly altered in group 1, and the overall effect of dobutamine on compliance in these patients was not significant in either of the groups (ANOVA; $P=0·19$). Characteristic impedance was maintained at or above baseline values during infusion of 5 to 20 μg dobutamine kg^{-1} min^{-1} (ANOVA; $P<0·02$), and declined with higher infusion rates (Fig. 3). Characteristic impedance tended to be greater in group 2 than in group 1 at baseline ($P=0·055$) and at peak stress ($P<0·05$), and group 2 patients showed consistently greater characteristic impedance during testing than group 1 (ANOVA; $P<0·05$), although the difference declined with infusion rates above 20 μg kg^{-1} min^{-1} (Fig. 3).

The change in left ventricular wall motion score index from baseline to peak stress in group 2 (ie the severity of new wall motion abnormality) was not significantly correlated with the corresponding changes in left ventricular end-diastolic volume, heart rate, cardiac index, left ventricular external power estimates, or aortic root pressure estimates. There was no significant difference in baseline haemodynamics or cardiovascular response during testing between patients with ($n=8$) or without ($n=10$) beta-receptor blockers prior to the stress test.

Discussion

The present study assessed left ventricular function, systemic haemodynamics, and systemic arterial properties during a cardiac stress test with dobutamine up to 40 μg kg^{-1} min^{-1}. The study consisted of patients without (group 1) and with (group 2) evidence of myocardial ischaemia during the test. The groups had similar baseline standard haemodynamics and lined peak stress at equivalent dobutamine infusion rates. None of the patients had congestive heart failure or recent myocardial infarction.

In group 1, regional wall motion was improved or unchanged during testing. The three patients with improved wall motion demonstrate how dobutamine may activate regions of underperfused but viable myocardium (Pierard *et al.*, 1990). In group 2, all patients had new wall motion abnormalities during testing which accurately indicate the presence of myocardial ischaemia (Hauser *et al.*, 1985). The increase in wall motion score index in this group (mean: 0·39) is equivalent to new hypokinesia in six of the 16 left ventricular segments, or new akinesia in three of them. Although this impairment of regional left ventricular function may be considered substantial (ie impairment of 38% of the left ventricular wall), it did not significantly influence global left ventricular function or systemic haemodynamics. This is in agreement with previous studies on

dobutamine stress tests for coronary artery disease (Movahed *et al.*, 1990; Mazeika *et al.*, 1992), but differs from the observation in patients with recent myocardial infarction where stroke volume declined during dobutamine-induced ischaemia (Pierard *et al.*, 1989). In the present study, stroke index tended to increase at 10 μg dobutamine kg^{-1} min^{-1} in group 1 and remained unchanged in group 2, and the overall response was not significantly different between the groups, indicating that this level of ischaemia did not impair left ventricular global function. At peak stress, stroke index had returned to baseline values. One reason for this may be that in some patients the left ventricular cavity is partially obliterated during higher infusion rates of dobutamine (Pellikka *et al.*, 1992). Although late-peaking systolic velocities were occasionally observed during higher infusion rates of dobutamine, we did not recognize a significant intraventricular gradient in any of the study subjects. Thus, the declining stroke index during higher infusion rates in the present study was more likely to be due to tachycardia and the concordantly impaired diastolic filling (Miller *et al.*, 1962). This is also indicated by the significant decrease in end-diastolic left ventricular volumes at peak stress, which may have been accentuated by intravascular volume depletion and reduced venous return due to the fasting state.

Heart rate increased linearly with increasing dobutamine infusion rate. However, the response was attenuated in group 2 patients, where it also levelled off at the highest infusion rates. A similar impairment of the chronotropic response has been observed in patients with congestive heart failure due to a desensitization of the beta-adrenoceptor pathway (Colucci *et al.*, 1989). Although a similar mechanism may have been present in group 2 patients in the present study, where previous infarction was more prevalent than in group 1 patients, we cannot exclude the possibility that beta-blocking in some of the patients was still effective during the test. However, medication was not taken on the day of the test, baseline haemodynamics were similar in groups 1 and 2, and the haemodynamic response to the test was not significantly different in patients without and with beta-blockers, indicating that the drug effect was not a major one.

SYSTEMIC HAEMODYNAMICS AND ARTERIAL PROPERTIES

In the present study, mean arterial blood pressure was maintained near baseline levels during the test because the increased cardiac output was balanced by arteriolar vasodilatation. Dobutamine induces vasodilatation partly via a direct stimulation of arterial beta-2 adrenoceptors (Ruffolo & Morgan, 1987), and partly via an indirect activation of cardiovascular reflex pathways in response to increasing cardiac output and pulse pressure (Liang & Hood, 1979). Whereas the peripheral resistance decreased with increasing dobutamine infusion rates, the proximal resistance (ie characteristic impedance) was maintained at or above baseline levels during low to medium infusion rates, and declined during the high rates. This response was most accentuated in group 2, where total arterial compliance also tended to decrease during infusion of dobutamine. This conflicting response of peripheral and proximal arterial resistances during dobutamine

infusion is to our knowledge a new observation, and deviates from that reported in patients with congestive heart failure where 12 μg dobutamine kg^{-1} min^{-1} decreased peripheral resistance and characteristic impedance concordantly (Binkley *et al.*, 1990). Aortic stiffness is influenced by aortic blood pressure, dimensions, and wall properties. In our study, arterial pressures were essentially unchanged during test and cannot explain this observation. Alpha-adrenergic stimulation induces vasoconstriction, and since the mammalian thoracic aorta contains adrenoceptors (Fleisch *et al.*, 1970), such stimulation may have promoted the increase in aortic stiffness. Group 2 patients showed greater characteristic impedance than group 1. In this group, seven patients had multivessel disease, whereas the coronary artery disease in group 1 was, as judged from the clinical information and stress tests, likely to be less severe. Previous work has indicated that the aortic stiffness is related to the severity of coronary artery disease (Hirai *et al.*, 1989). However, the exact mechanism underlying the observed change in arterial properties in the present and other studies remains elusive.

The % oscillatory power has been proposed as an indicator of the efficiency of energy transfer from heart to tissues, and increases with increasing aortic stiffness, decreasing heart rate, and vasodilatation (O'Rourke, 1967; Cox, 1974). We found that % oscillatory power increased during dobutamine infusion in both groups, ie the efficiency of energy transfer was reduced. A similar response to dobutamine has been reported in patients with congestive heart failure (Binkley *et al.*, 1990), and during isoproterenol infusion in dogs (Cox, 1974). The effects on % oscillatory power of the increased heart rate were balanced by the reduced peripheral resistance. Thus, the increased aortic stiffness was most probably the reason for the increased % oscillatory power.

Coronary anatomy was arteriographically defined in group 2, whereas it was not explicitly known in group 1. Although the groups had similar wall motion abnormalities at baseline, the lack of new wall motion abnormalities during dobutamine infusion in group 1 provides strong evidence that these patients did not have clinically significant coronary stenoses (Cohen *et al.*, 1991; Previtali *et al.*, 1991; Salustri *et al.*, 1992), a view which is also supported by the general lack of angina pectoris (one patient had chest pain) in this group.

METHODOLOGICAL CONSIDERATIONS

Dobutamine has a half life of 2 min, and each infusion rate should last for at least 8 min in order to achieve a steady state (Goodman Gilman *et al.*, 1990). Then the stress test protocol would last for up to 48 min, which is clinically less feasible than the currently used protocol of 24 min. Our results are therefore not directly comparable with those obtained under steady-state conditions, but are relevant for patients who undergo the present or equivalent stress test protocols.

The inter-observer reproducibility for the Doppler-derived stroke index, cardiac index, and peripheral resistance is within 13% (coefficient of variation), whereas that for characteristic impedance and total arterial compliance obtained with this

methodology is within 20% (Aakhus *et al.*, 1993a), and that for left ventricular end-diastolic volume is 7% (Aakhus *et al.*, 1994). In the present study, repeated measurements were performed by the same investigator and the baseline aortic annulus diameter was used for calculation of stroke volume during the test, thus improving the reproducibility further.

The algorithm for 3-dimensional reconstruction of volumes used in this study provides very accurate estimates of object volumes (Aakhus *et al.*, 1994). However, determination of left ventricular volume *in vivo* requires optimal imaging conditions. During dobutamine stress testing, the tachycardia and cardiac translation and rotation may impair image quality and produce foreshortened images which lead to underestimation of left ventricular volume. However, since we were able to obtain standard apical images during the test, the relative change in left ventricular volume should be adequately characterized.

Conclusions

This non-invasive study shows that during a conventional cardiac stress test with dobutamine up to 40 $\mu g\ kg^{-1}\ min^{-1}$, systemic arterial blood pressures were maintained during a substantial increase in cardiac index due to decreased peripheral resistance. The efficiency of energy transfer from heart to tissues was reduced during the test, presumably due to increased proximal aortic resistance. Myocardial ischaemia during the test did not significantly impair global left ventricular function or systemic haemodynamics.

Acknowledgments

This work was supported by a grant from the Norwegian Council on Cardiovascular Diseases (Oslo, Norway). The authors appreciate the statistical advice provided by Lars Ødegaard, MSc, Section of Mathematical Sciences, Norwegian Institute of Technology.

References

AAKHUS S., SOERLI C., FAANES A., HAUGER S. O., BJOERNSTAD K., HATLE L. & ANGELSEN B. A. J. (1993a) Noninvasive computerized assessment of left ventricular performance and systemic hemodynamics by study of aortic root pressure and flow estimates in healthy men, and men with acute and healed myocardial infarction. *Am J Cardiol,* **72,** 260–267.

AAKHUS S., TORP H., HAUGLAND T. & HATLE L. (1993b) Noninvasive estimates of aortic root pressures: external subclavian arterial pulse tracing calibrated by oscillometrically determined brachial arterial pressures. *Clin Physiol,* **13,** 573–586.

AAKHUS S., MÆHLE J. & BJOERNSTAD K. (1994) A new method for echocardiographic computerized three-dimensional reconstruction of left ventricular endocardial surface: *in vitro* accuracy and clinical repeatability of volumes. *J Am Soc Echocardiogr* **7,** 571–581.

BERTHE C., PIERARD L. C., HIERNAUX M., TROTTEUR G., LEMPEREUR P., CARLIER J. & KULBERTUS H. E. (1986) Predicting the extent and location of coronary artery disease in acute myocardial infarction by echocardiography during dobutamine infusion. *Am J Cardiol*, **58,** 1167–1172.

BINKLEY P. F., VAN FOSSEN D. B., NUNZIATA E., UNVERFERTH D. V. & LEIER C. V. (1990) Influence of positive inotropic therapy on pulsatile hydraulic load and ventricular-vascular coupling in congestive heart failure. *J Am Coll Cardiol*, **15,** 1127–1135.

BJOERNSTAD K., AAKHUS S., LUNDBOM J., BOLZ K., ROKSETH R., SKJAERPE T. & HATLE L. (1993) Digital dipyridamole stress echocardiography in silent ischemia after coronary artery bypass grafting and/or after healing of acute myocardial infarction. *Am J Cardiol*, **72,** 640–646.

BRUBAKK A. O. & GISVOLD S. E. (1982) Pulsed Doppler ultrasound for measuring blood flow in the human aorta. In: *Doppler Ultrasound in Cardiology. Physical Principles and Clinical Applications* (eds Hatle, L. & Angelsen, B.), pp. 185–193. Lea & Febiger, Philadelphia.

CHRISTIE J., SHELDAHL L. M., TRISTANI F. E., SAGAR K. B., PTACIN M. J. & WANN S. (1987) Determination of stroke volume and cardiac output during exercise: comparison of two-dimensional and Doppler echocardiography, Fick oximetry, and thermodilution. *Circulation*, **76,** 539–547.

COHEN J. L., GREENE T. O., OTTENWELLER J., BINENBAUM S. Z., WILCHFORT S. D. & KIM C. S. (1991) Dobutamine digital echocardiography for detecting coronary artery disease. *Am J Cardiol*, **67,** 1311–1318.

COLUCCI W. W., RIBEIRO J. P., ROCCO M. B., QUIGG R. J., CREAGER M. A., MARSH J. D., GAUTHIER D. F. & HARTLEY L. H. (1989) Impaired chronotropic response to exercise in patients with congestive heart failure. *Circulation*, **80,** 314–323.

COX R. H. (1974) Determinants of systemic hydraulic power in unanesthetized dogs. *Am J Physiol*, **226,** 579–587.

FLEISCH J. H., MALING H. M. & BRODIE B. B. (1970) Beta-receptor activity in aorta. *Circ Res*, **26,** 151–162.

GOODMAN GILMAN A., RALL T. W., NIES A. S. & TAYLOR P. (1990) *The Pharmacological Basis of Therapeutics*, 8th edn. Pergamon Press, New York.

HAUSER A. M., GANGADHARAN V., RAMOS R. G., GORDON S. & TIMMIS G. C. (1985) Sequence of mechanical, electrocardiographic and clinical effects of repeated coronary artery occlusion in human beings: echocardiographic observations during coronary angioplasty. *J Am Coll Cardiol*, **5,** 193–197.

HIRAI T., SASAYAMA S., KAWASAKI T. & YAGI S. (1989) Stiffness of systemic arteries in patients with myocardial infarction. *Circulation*, **80,** 78–86.

LASKEY W. K., KUSSMAUL W. G., MARTIN J. L., KLEAVELAND J. P., HIRSHFELD J. W. & SHROFF S. (1985) Characteristics of vascular hydraulic load in patients with heart failure. *Circulation*, **72,** 61–71.

LEIER C. V., UNVERFERTH D. V. & KATES R. E. (1979) The relationship between plasma dobutamine concentrations and cardiovascular responses in cardiac failure. *Am J Med*, **66,** 238–242.

LIANG C. & HOOD W. B. (1979) Dobutamine infusion in conscious dogs with and without autonomic nervous system inhibition: effects on systemic hemodynamics, regional blood flow and cardiac metabolism. *J Pharmacol Exp Ther*, **211,** 698–705.

MAZEIKA P. K., NADAZDIN A. & OAKLEY C. M. (1992) Dobutamine stress echocardiography for detection and assessment of coronary artery disease. *J Am Coll Cardiol*, **19,** 1203–1211.

MILLER D. E., GLEASON W. L., WHALEN R. E., MORRIS J. J. & MCINTOSH H. D. (1962) Effect of ventricular rate on the cardiac ouput in the dog with chronic heart block. *Circ Res*, **10,** 658–663.

MOVAHED A., REEVES W. C., ROSE G. C., WHEELER W. S. & JOLLY S. R. (1990) Dobutamine and improvement of regional and global left ventricular function in coronary artery disease. *Am J Cardiol*, **66,** 375–377.

O'ROURKE M. F (1967) Steady and pulsatile energy losses in the systemic circulation under normal conditions and in simulated arterial disease. *Cardiovasc Res*, **1,** 313–326.

PELLIKKA P. A., OH J. K., BAILEY K. R., NICHOLS B. A. & MONAHAN K. H. (1992) Dynamic intraventricular obstruction during dobutamine stress echocardiography. *Circulation*, **86,** 1429–1432.

PIERARD L. A., BERTHE C., ALBERT A., CARLIER J. & KULBERTUS H.E. (1989) Haemodynamic alterations during ischaemia induced by dobutamine stress testing. *Eur Heart J*, **10,** 783–790.

PIERARD L. A., DE LANDSHEERE C. M., BERTHE C., RIGO P. & KULBERTUS H. E. (1990) Identification of viable myocardium by echocardiography during dobutamine infusion in patients with myocardial infarction after thrombolytic therapy: comparison with positron emission tomography. *J Am Coll Cardiol*, **15,** 1021–1031.

PREVITALI M., LANZARINI L., FERRARIO M., TORTORICI M., MUSSINI A. & MONTEMARTINI C. (1991) Dobutamine versus dipyridamole echocardiography in coronary artery disease. *Circulation*, **83** [Supp. III], III-27–III-31.

RUFFOLO R. R. & MORGAN E. L. (1984) Interaction of the novel inotropic agent, ASL-7022, with alpha and beta adrenoceptors in the cardiovascular system of the pitched rat: comparison with dobutamine and dopamine. *J Pharmacol Exp Ther*, **229**, 364–371.

RUFFOLO R. R. (1987) Review: the pharmacology of dobutamine. *Am J Med Sci*, **294**, 244–248.

SALUSTRI A., FIORETTI P. M., POZZOLI M. M. A., MCNEILL A. J. & ROELANDT J. R. T. C. (1992) Dobutamine stress echocardiography: its role in the diagnosis of coronary artery disease. *Eur Heart J*, **13**, 70–77.

SCHILLER N. B., SHAH P. M., CRAWFORD M., DEMARIA A., DEVEREUX R., FEIGENBAUM H., GUTGESELL H., REICHEK N., SAHN D., SCHNITTGER I., SILVERMANN N. H. & TAJIK A. J. (1989) Recommendations for quantitation of the left ventricle by two-dimensional echocardiography. *J Am Soc Echocardiogr*, **2**, 358–367.

WESTERHOF N., ELZINGA G. & SIPKEMA P. (1971) An artificial arterial system for pumping hearts. *J Appl Physiol*, **31**, 776–781.